The Detection and Fate of Enveloped Viruses in Water Environments

by

Yinyin Ye

A dissertation submitted in partial fulfillment
of the requirements for the degree of
Doctor of Philosophy
(Environmental Engineering)
in the University of Michigan
2018

Doctoral Committee:

Assistant Professor Krista R. Wigginton, Chair
Professor Glen T. Daigger
Associate Professor Adam Lauring
Professor Nancy G. Love

Yinyin Ye

yinyinye@umich.edu

ORCID iD: 0000-0003-0625-9657

Dedication

This dissertation is dedicated to my beloved grandfather, Linsen Ye.

Acknowledgements

This dissertation was funded by the U.S. National Science Foundation grant #1351188, the University of Michigan Jack A. Borchardt Fellowship, the University of Michigan Rackham International Student Fellowship, the University of Michigan Rackham Barbour Scholarship, the University of Michigan Rackham Graduate Student Research Grant, and the University of Michigan Rackham Conference Travel Grant.

This dissertation would not be possible without the support and help from many people. First, I would like to express my deep thanks to my advisor Dr. Krista R. Wigginton for her mentoring and guiding me towards a scientific researcher that I dream to be. She encourages me to think outside of box, open my minds to interdisciplinary ideas, and believe in MAKING A DIFFERENCE. I would like to thank my committee Dr. Glen T. Daigger, Dr. Adam Lauring, and Dr. Nancy G. Love for their technical support and career guidance. I would like to thank Dr. Rudy J. Richardson for his introducing me into the field of molecular modeling. I would like to thank Dr. Bethany Moore and her lab technician Carol Wilke, and Dr. Abimbola Kolawole for their initial help with cell culture and plaque assays. I would like to thank Dr. Machael J. Imperiale and his postdoctoral student Dr. Linbo Zhao for their thoughtful discussion on monkey and human cells. I would like to thank Dr. Michael Dodd for his help with the continuous quench flow system. In addition, I would like to thank Will Fitzsimmons, Dr. Julian Leibowitz's lab from Texas A&M College of Medicine, Dr. Linsey Marr's lab from Virginia Tech, and Dr. Lisa M. Casanova from Georgia State University for their kind sharing protocols, viruses, and host cells.

I would like to thank the graduate and the undergraduate students Robert M. Ellenberg, Katherine E. Graham, Pin Hsuan Chang, and John Hartert for their contributions to this dissertation. I would like to thank every member in the Biotech Research group. It was a fantastic experience to work in such a great research group. I would like to thank Dr. Jeseth Delgado Vela, Dr. Heather Goetsch, Dr. Zhong Qiao, Dr. Yun Shen, Andrea McFarland, Margaret Reuter, Chia-Chen Wu, Shilva Shrestha, Nicole Rockey, Kathryn Langenfeld, Emily Crossette for their support and friendship. I would like to thank Dr. Sarah Haig, Dr. William Tarpeh, and Dr. Xavier Fonoll Almansa for their advice and discussion on research.

In addition, I am grateful to the opportunities of teaching graduate and undergraduate courses as part of my Ph.D. training. I would like to thank Dr. Jeremy Semrau and Dr. Avery Demond for their patient guidance on teaching. I would like to thank Dr. Wenyu Gu and Ivan Jayawan for sharing their teaching experience.

I would like to express many thanks to staff members in the Department of Civil and Environmental Engineering. In particular, I would like to thank Tom Yavaraski for his timely help with mass spectrometry all the time. I am also grateful to the help from Jessica Randolph, Stephanie Ford, Tabitha Rohn, Ariane Smith, Stacey Stites, Ingra Stimach, Matt Blank, Rebi Varghese, and Levi Powis.

I would like to thank Dr. Christine A. Feak and Dr. John Swales for their inspiration on academic writing.

Last but not least, I would like to thank my families in China. Although we are over 10,000 kilometers apart, your love is always a strong support for me to pursue my dream fearlessly. I am also thankful to my dear husband, Chaozhe He, for teaching me the state-of-the-art control theories and cooking delicious meals.

Table of Contents

List of Tables

List of Figures

List of Appendices

Abstract

Removing and inactivating infectious viruses in water is critical in controlling waterborne diseases. Studies on the presence of viruses in wastewater and their fate through wastewater treatment plants have focused primarily on enteric viruses, which transmit gastrointestinal diseases via water. Most enteric viruses are nonenveloped, consisting only of proteins and nucleic acids. Enveloped viruses contain an outer lipid membrane in addition to proteins and nucleic acids. Certain enveloped viruses are responsible for high-profile diseases, such as severe acute respiratory syndrome (SARS), Middle East respiratory syndrome (MERS), and influenza. Enveloped viruses have often been assumed to be absent from wastewater and rapidly inactivated when they are released to water. However, recent studies suggest that certain enveloped viruses can enter wastewater, and may survive in water for long periods of time. Our current state of knowledge on enveloped viruses in aquatic environments has been limited due to a lack of appropriate methods for capturing and detecting infectious enveloped viruses in water. To address the knowledge gaps, this dissertation research aims to 1) evaluate the survival, partitioning, and recovery of model enveloped viruses in wastewater, 2) characterize the reactivity of enveloped viruses with common disinfectants, and 3) develop a new method for monitoring infectious human viruses in water samples.

To evaluate virus survival and partitioning, we applied four model viruses, two enveloped and two nonenveloped, and used plaque assays to track the infectivity and partitioning of the model viruses in untreated wastewater. We simulated our experimental data with virus sorption and

inactivation models to quantitatively characterize the fate of model enveloped viruses and model nonenveloped viruses. Our results suggest that model enveloped viruses can survive in wastewater, especially at cooler temperatures. We also demonstrated that a larger fraction of model enveloped viruses partitioned to the wastewater solids than nonenveloped viruses. As a result, we expect that enveloped viruses are removed to a greater extent than nonenveloped viruses during primary wastewater treatment. With the knowledge gained from the survival and partitioning experiments, we optimized an ultrafiltration method for recovering infectious enveloped viruses from wastewater. The second portion of this dissertation research characterized the reactivity of enveloped viruses in the disinfection process. The reactions in a model virus lipids, proteins, and genome were tracked as a model enveloped virus was treated with disinfectants using quantitative lipid and protein mass spectrometry, and molecular PCR techniques. We found that protein reactions drive the inactivation of the model enveloped virus by free chlorine, and genome reactions drive the inactivation of the model enveloped virus by UV_{254}. Furthermore, our results suggest that the model enveloped virus proteins were more susceptible to oxidant attack than the proteins of a model nonenveloped virus. The final portion of this dissertation research focused on the development of an integrated cell culture-mass spectrometry (ICC-MS) method for detecting infectious human viruses in wastewater. In proof of concept experiments, reoviruses were detected in samples collected throughout a wastewater treatment plant by applying the ultrafiltration concentration method developed in the first study and the ICC-MS detection method. These results suggest that ICC-MS is a promising tool for monitoring infectious enveloped or nonenveloped viruses in water samples.

Chapter 1 Background

1.1 Water environments and virus transmission

Water resources are essential for every aspect of human life. However, these resources are limited, and we are increasingly reusing our water in areas with high populations and limited water sources. Maintaining high water quality as water is circled through the urban water cycle is challenging due to the introduction of pollutants to the water, such as human viruses. Waterborne viruses are responsible for spreading a number of human diseases. Enteric viruses, for example, cause infections in human gastrointestinal system and are primarily transmitted via the fecal-oral route.[1-3] Enteric viruses such as norovirus, coxsackievirus, echovirus, and reovirus have been frequently detected in untreated municipal wastewater with infectious concentrations ranging from 10^0 to 10^8 gene copies/L.[1] If the wastewater is insufficiently treated, the infectious enteric viruses in the final effluent can contaminate surface waters that are used for recreation, agriculture irrigation, or serve as drinking water sources.[4-6] Enteric viruses are mostly nonenveloped and thus consist of nucleic acids and protein capsids (Figure 1.1). Their diameters range in size from 20-100 nanometers. Previous water treatment research and monitoring efforts have focused primarily on removing and inactivating nonenveloped enteric viruses.

Table 1.1 Example enveloped viruses detected in human specimens and/or wastewater.

Family/Genus	Virus	Diseases	Genome type	Levels in human specimens (ref.)	Levels in untreated wastewater (ref.)
Coronaviridae/ Torovirus	Torovirus	Gastroenteritis	ss RNA		Gene positive in winter municipal wastewater ([7])
Coronaviridae/ Coronavirus	SARS coronavirus	Respiratory illness, severe pneumonia, gastroenteritis,	ss RNA	30-70% gene positive last 10 days after disease onset ([8])	
	MERS coronavirus		ss RNA	10^3 gc/g stool ([9])	
	Human coronavirus	Pneumonia, bronchiolitis, gastroenteritis,	ss RNA	2.3% gene positive in stool samples ([10])	
Orthomyxoviridae/ Influenzavirus A	Avian influenza H5N1	Severe respiratory illness	ss RNA	8.6×10^2-1.5×10^6 gc/mL in rectal swab samples ([11])	
	Avian influenza H7N9	Severe respiratory illness	ss RNA	12/14 gene positive in stool samples ([12])	
	Seasonal influenza A virus	Respiratory illness	ss RNA	47% gene positive in stool samples, 10^4-10^6 gc/g stool ([13])	
Flaviviridae/ Flavivirus	Zika virus	Microcephaly, Guillain-Barre syndrome	ss RNA	Gene positive in urine samples. ([14,15]) Zika-carrying mosquito eggs detected in 49% of septic tank samples ([16])	
	Dengue virus	Severe bleeding, shock	ss RNA	20%-80% gene positive in urine, lasting for ~2 weeks ([17])	
	West Nile virus	Encephalitis, meningitis	ss RNA	44% gene positive in urine with acute infection ([18])	
Herpesviridae/ Cytomegalovirus	Cytomegalovirus	Hearing loss, pneumonia, microencephaly, liver disease	ds DNA	Prolonged excretion in urine from children with congenital infection ([19]) Infectious cytomegaloviruses in urine isolated in MRC-5 cell lines ([20])	

* gc, gene copies; IU, infectious units; MPNCU, maximum probable number culture unit; PFU, plaque-forming unit; FFU, focus-forming unit.
** Family and genus were based on the 2017 International Committee on Taxonomy of Viruses (ICTV), https://talk.ictvonline.org/taxonomy/

Unlike nonenveloped viruses, the presence and fate of enveloped viruses have not been broadly studied. Enveloped viruses contain a lipid membrane outside of their nucleic acids and protein capsids (Figure 1.1). Enveloped viruses are responsible for a number of high-profile diseases in humans, such as severe acute respiratory syndrome (SARS), Middle East respiratory syndrome

(MERS), and avian influenza. They are also responsible for less dangerous illnesses such as the common cold. Enveloped viruses have widely been assumed to be absent in water environments. In fact, some enveloped do enter wastewater, but methods for their detection and an understanding of their mechanistic fate is lacking. Some example enveloped viruses that can be released to wastewater are described below.

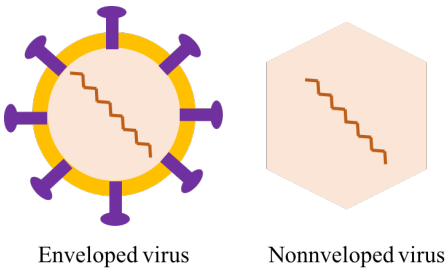

Figure 1.1 Structural illustrations of enveloped and nonenveloped viruses.

1.1.1 Coronavirus

Different coronaviruses can cause both respiratory and gastrointestinal illnesses.[21] Some strains of human coronaviruses, such as SARS coronavirus and MERS coronavirus, are the responsible agents for epidemics of deadly acute pneumonia diseases. The overall case-fatality rate for the SARS outbreak in 2003 was 10%,[22] and the accumulated case-fatality rate of MERS was 35%.[23] Infected individuals shed SARS and MERS coronavirus genes in their stool and urine samples with high frequency (Table 1.1), and infectious SARS coronaviruses were isolated from human stool samples.[24] In fact, a SARS outbreak in an apartment complex in Hong Kong was attributed to the SARS coronavirus in wastewater forming aerosols when toilets were flushed.[25] Genome shedding was reported for other low pathogenic strains of human coronaviruses (i.e., 229E, NL63, OC43, and HKU1),[10,26] and infectious coronavirus HKU1 was isolated from human

stool samples (Table 1.1).[21] These human coronaviruses are not deadly like SARS and MERS coronaviruses, and cause seasonal outbreaks of the common cold.

1.1.2 Influenza virus

Infectious avian influenza viruses (AIV) are shed in an extremely high concentrations in bird feces (10^9-10^{10} infectious units per day)[27] and are transmitted primarily via fecal-oral route in birds.[28] Occasionally, humans can acquire AIV, and the accumulated AIV H5N1 case fatality rate of human infection from 2003 to 2017 was 53% as estimated by WHO.[29] The transmission route of AIV from poultry to human is still elusive, but several transmission routes are hypothesized, including direct contact with the infected poultry, and contact with virus-laden fecal matter or water.[30,31] Despite that the human-to-human transmission has rarely been reported once humans acquired AIV, infected individuals can shed AIV genes in their stool samples with high frequency (Table 1.1).[11,12,32,33] The concentration of avian influenza virus H5N1 genes detected in rectal swab samples ranges from 8.6×10^2 to 1.5×10^6 gene copies/mL.[32,33] Like avian influenza viruses, seasonal human influenza virus strains were detected in feces, and the concentrations were 10^4 – 10^6 gene copies/g of stool samples.[34]

1.1.3 Other enveloped viruses

Zika virus is an emerging mosquito-borne human pathogenic virus, and Zika virus genes can be detected in urine specimens.[15] The genes of other mosquito-borne enveloped viruses such as dengue virus and West Nile virus were also widely detected in urine,[17,18,35] and infectious West Nile virus was isolated from the urine of infected individuals with acute infection (Table 1.1).[18]

Alternatively, wastewater is a habitat for mosquito larvae and adults that can carry and transmit those enveloped viruses.[36-38]

Cytomegalovirus is carried by people of all ages, in most cases, asymptomatically, but can be a threat to those who are immunodeficiency or immunocompromised. Infectious cytomegaloviruses can be shed in the urine from infants and children who are infected at birth (Table 1.1).[19,20] Contacting with urine is suspected as one of transmission routes of cytomegalovirus.

Ebola virus, causing deadly hemorrhagic fever, can enter wastewater when patients shed bodily fluids that contain high levels of infectious viruses;[39-41] however, the environmental transmission route for Ebola diseases has been observed.

Currently available clinical and epidemiological evidence therefore suggests that water environments can, in fact, be reservoirs for enveloped viruses. This highlights the importance to expand our knowledge on the presence and fate of viruses in water beyond nonenveloped viruses to include enveloped viruses. To do this, we must first develop reliable methods for capturing and monitoring infectious enveloped viruses from water. We must also evaluate the survivability of enveloped viruses that enter municipal wastewater.

1.2 Virus survival in wastewater

To cause infection, viruses in the environment must retain their infectivity until they come into contact with the next host. The survivability of viruses is often measured by the length of time to lose 90% of their original infectivity (i.e., T_{90} value). Enveloped viruses have often been assumed to be less stable in water, but this assumption is too simplistic. The T_{90} values available in the

literature suggest that enveloped viruses are not necessarily more susceptible to environmental conditions than nonenveloped viruses in various water environments[42] (Figure 1.2). Some strains of coronavirus and avian influenza virus retain their infectivity as long as nonenveloped viruses (Figure 1.2). SARS coronavirus and human coronavirus 229E, for example, had T_{90} greater than one day in urine and filtered wastewater samples, respectively.[42] For context, one day is the maximum retention time of wastewater in a common sewage system. However, the current survival studies of enveloped viruses have been less reported for raw wastewater.

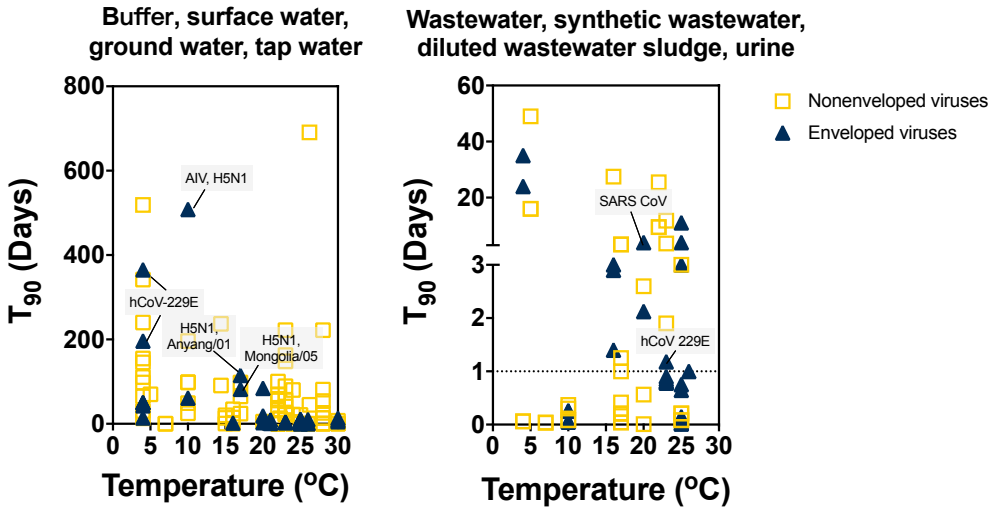

Figure 1.2 T_{90} values of viruses in different water matrices and temperatures. Data in this figure was replotted from previous research on virus survival.[42]

If the viruses are able to survive in raw wastewater and then enter the wastewater treatment plants, viruses need to be removed or inactivated effectively through the treatment processes. The removal efficiency and mechanisms of nonenveloped enteric viruses in wastewater treatment plants have been reviewed in previous publications.[43,44] For nonenveloped viruses, the removal efficiency from wastewater depends on virus partitioning with wastewater solids in primary

treatment and the adsorption to activated sludge in secondary treatment.[43] Corresponding studies have not been conducted for enveloped viruses. We therefore have a limited ability to predict the fate of infectious enveloped viruses in wastewater treatment plants.

Particle interaction theories have been applied for investigating the interactions between nonenveloped viruses and solids in water. The DLVO (Derjaguin-Landau-Verwey-Overbekk) theory and the extended DLVO (XDLVO) theory can be valid to describe the forces between virus particles and solids in water, depending on the solid materials.[45,46] In the DLVO and XDLVO theories, virus particles present in water are modelled as colloids that carry surface charges as a result of their protein and nucleic acid compositions.[47,48] To quantitatively characterize virus adsorption to solids, Langmuir and Freundlich isotherm adsorption models have been successfully applied for nonenveloped viruses in water at an equilibrium state.[47] Grant *et al.*[49] integrated the isotherm adsorption model with the first-order inactivation kinetics model to describe nonenveloped virus inactivation in liquid and on solid surface. We hypothesize that the adsorption and inactivation models are still applicable for enveloped viruses, but enveloped viruses would behave differently due to their structural differences. Models of enveloped virus partitioning with wastewater solids could help in predicting enveloped virus survivability and removal efficiency through wastewater treatment processes.

1.3 Virus inactivation by disinfection treatment

Disinfection is used in both drinking water and wastewater treatment plants, and is intended to inactivate pathogenic viruses and other microorganisms. The disinfection efficacy of a number of disinfection methods has been widely reported for nonenveloped viruses,[50-53] whereas limited data is available for enveloped viruses. Here, we focus on reviewing virus inactivation mechanisms by

ultraviolet 254 (UV_{254}) and free chlorine, as representative UV light disinfection and chemical oxidant disinfection, respectively.

1.3.1 UV disinfection

UV is one of the most commonly applied disinfection methods. UV light can be subdivided into three regions according to wavelength, namely UVA (320-400 nm), UVB (290-320 nm), and UVC (100-290 nm). Viruses are most sensitive to UVC due to the high photoreactivity of nucleic acids in the UVC region. Low-pressure mercury lamps emit the highest UVC intensity around 254 nm; therefore, most studies on virus inactivation by UVC focus on this specific region (i.e., UV_{254}).

Our current knowledge on virus inactivation mechanisms was established primarily with nonenveloped model viruses. A study of bacteriophage MS2, for example, suggests that the inactivation of a nonenveloped virus by UV_{254} is majorly attributed to damage in the viral genome.[54] Follow-up studies on nonenveloped viruses underscore the findings that the UV_{254} reactivity of viral genomes correlate to virus susceptibility to UV_{254}.[55-59] Two main factors determine the UV_{254} reactivity of viral genomes, namely genome size and genome types (single-stranded DNA (ssDNA), double-stranded DNA (dsDNA), single-stranded RNA (ssRNA), and double-stranded RNA (dsRNA)). Other mechanisms of virus particle damage by UV_{254} can also lead to nonenvelopd virus inactivation. In the MS2 model, protein damage sensitized by adjacent viral RNA sequences contributes to 20% of the observed virus inactivation,[54] whereas in nonenveloped dsDNA viruses, the damaged genome can be repaired in the host cell and this results in higher resistance to UV_{254}.[60] Compared to nonenveloped viruses, the mechanisms of enveloped virus inactivation by UV_{254} have not been investigated and deserves further investigation.

1.3.2 Free chlorine disinfection

Free chlorine is a strong oxidant that readily inactivates microorganisms. Free chlorine is an aqueous solution of the following chlorine species: HOCl, OCl^-, $Cl_2(aq)$, and $Cl_2O(aq)$.[61] The primary oxidant species is the neutral molecule hypochlorous acid (HOCl). Based on the nonenveloped MS2 model, the reactions of free chlorine with virus proteins and genomes impact the ability of viruses to bind, enter, and replicate in the host cell.[54] The inactivation of enveloped viruses with free chlorine have only been compared to nonenveloped viruses in one study. There, the enveloped bacteriophage Phi6 and Ebola virus experienced higher levels of inactivation than nonenveloped bacteriophages MS2 and M13 in 0.5% sodium hypochlorite solution.[62] However, that report provided limited information on the chlorine demand of samples and other important experimental conditions; consequently, it is impossible to draw general conclusions about whether enveloped viruses are more or less susceptible to inactivation by free chlorine than nonenveloped viruses.

A bottom-up characterization of enveloped virus inactivation could help identify molecular features that drive inactivation. With this information, we would be better equipped to select and improve disinfection methods for treating enveloped viruses. This is particularly important during outbreak events, when culturing viruses to see how well disinfection are working is often not possible.

1.4 Virus concentration and detection

Monitoring infectious human viruses in water is important for environmental surveillance and water quality control. Due to the low concentrations of human viruses in wastewater and drinking

water samples, concentration steps are often necessary prior to virus detection. Published virus concentration methods have nearly all been developed and optimized for nonenveloped viruses and therefore may not be effective for recovering infectious enveloped viruses from water samples. In the limited studies that attempted to recover enveloped viruses, low recoveries of infectious enveloped viruses were reported. For example, a method employing glass wool and ceramic membrane filtration combined with PEG precipitation only recovered of 0.01% to 7.89% of infectious enveloped influenza A viruses from lake water and 3.63% to 13.79% from rainwater.[63] A positively charged membrane filtration method recovered 1% of infectious enveloped SARS coronaviruses from sewage samples.[64] A reliable concentration method is therefore needed for recovering infectious enveloped viruses from water.

Once the infectious viruses have been concentrated, viruses must be detected. The traditional culture-based methods detect infectious viruses using host cell lines that are susceptible to virus infection. One major drawback of this technique is that it requires long periods of time for clear cytopathic effects to appear in the host cells, which is a sign of virus infection. Another drawback is that it is usually impossible to discern the virus strain or species responsible for the cytopathic effects observed in the cells without further testing.

To decrease this detection period, virus culturing has been integrated with polymerase chain reaction (ICC-PCR) to detect viral genomes that are formed in the culture system before cytopathic effects appear.[65-68] The success of ICC-PCR, however, depends on the effectiveness of primers, and PCR assay optimization can be time-consuming. Moreover, unpredictable genetic variations in viruses may result in the failure of PCR methods.[69] In recent years, mass spectrometry (MS) techniques have been developed to identify viruses in clinical samples.[70,71] In those studies, infectious viruses in clinical samples were first cultured in cells. Proteins were then extracted from

the culturing system, digested into peptide sequences, and sent to mass spectrometry for peptide detection.[70,71] Mass spectrometry detects the masses and sequences of peptides that are compared to those available in viral protein database. The obtained protein sequences are likely to distinguish viruses at strain levels. Integrated cell culture-MS (ICC-MS) methods hold promise for detecting infectious human viruses in water samples as they can screen for large groups of viruses at once and may help avoid tedious method optimization.

1.5 Overview of dissertation chapters

This dissertation aims to expand our current state of knowledge on the fate and detection of nonenveloped enteric viruses in wastewater and drinking water. To evaluate enveloped virus survival in wastewater and removal in treatment processes, the inactivation kinetics and solid partitioning kinetics were characterized for model viruses (Chapter 2). The initial results guided the optimization of a concentration method designed for recovering infectious enveloped viruses from wastewater (Chapter 2). To investigate enveloped virus inactivation through disinfection processes, the biomolecule reactions in a model enveloped virus were characterized following the exposure to free chlorine and UV_{254} (Chapter 3). Molecular features that contributed to the model enveloped virus inactivation by free chlorine and UV_{254} were identified and compared with a model nonenveloped virus (Chapter 3). In the final chapter, a new virus detection method using integrated cell culture-mass spectrometry (ICC-MS) was developed for monitoring infective viruses in water. A proof-of-concept application of the ICC-MS method was successfully applied to detect human viruses in wastewater (Chapter 4).

1.6 References

(1) Fong, T. -T.; Lipp, E. K. Enteric viruses of humans and animals in aquatic environments: Health risks, detection, and potential water quality assessment tools. *Microbiol. Mol. Biol. Rev.* **2005**, *69* (2), 357–371.

(2) Boone, S. A.; Gerba, C. P. Significance of fomites in the spread of respiratory and enteric viral disease. *Appl. Environ. Microbiol.* **2007**, *73* (6), 1687–1696.

(3) Fannin, K. F.; Vana, S. C.; Jakubowski, W. Effect of an activated sludge wastewater treatment plant on ambient air densities of aerosols containing bacteria and viruses. *Appl. Environ. Microbiol.* **1985**, *49* (5), 1191–1196.

(4) Okoh, A. I.; Sibanda, T.; Gusha, S. S. Inadequately treated wastewater as a source of human enteric viruses in the environment. *Int. J. Environ. Res. Public Health* **2010**, *7* (6), 2620–2637.

(5) Borchardt, M. A.; Haas, N. L.; Hunt, R. J. Vulnerability of drinking-water wells in La Crosse, Wisconsin, to enteric-virus contamination from surface water contributions. *Appl. Environ. Microbiol.* **2004**, *70* (10), 5937–5946.

(6) Gallimore, C. I.; Pipkin, C.; Shrimpton, H.; Green, A. D.; Pickford, Y.; McCartney, C.; Sutherland, G.; Brown, D. W. G.; Gray, J. J. Detection of multiple enteric virus strains within a foodborne outbreak of gastroenteritis: an indication of the source of contamination. *Epidemiol. Infect.* **2005**, *133* (1), 41–47.

(7) Wong, M. V. M.; Hashsham, S. A.; Gulari, E.; Rouillard, J.-M.; Aw, T. G.; Rose, J. B. Detection and characterization of human pathogenic viruses circulating in community wastewater using multi target microarrays and polymerase chain reaction. *J. Water Health* **2013**, *11* (4), 659–670.

(8) Poon, L. L. M.; Chan, K. H.; Wong, O. K.; Cheung, T. K. W.; Ng, I.; Zheng, B.; Seto, W. H.; Yuen, K. Y.; Guan, Y.; Peiris, J. S. M. Detection of SARS coronavirus in patients with severe acute respiratory syndrome by conventional and real-time quantitative reverse transcription-PCR assays. *Clin. Chem.* **2004**, *50* (1), 67–72.

(9) Drosten, C.; Seilmaier, M.; Corman, V. M.; Hartmann, W.; Scheible, G.; Sack, S.; Guggemos, W.; Kallies, R.; Muth, D.; Junglen, S.; et al. Clinical features and virological analysis of a case of Middle East respiratory syndrome coronavirus infection. *Lancet Infect Dis* **2013**, *13* (9), 745–751.

(10) Jevšnik, M.; Steyer, A.; Zrim, T.; Pokorn, M. Detection of human coronaviruses in simultaneously collected stool samples and nasopharyngeal swabs from hospitalized children with acute gastroenteritis. *Virol. J.* **2013**, *10*, 46–52.

(11) de Jong, M. D.; Cam, B. V.; Qui, P. T.; Hien, V. M.; Thanh, T. T.; Hue, N. B.; Beld, M.; Phuong, L. T.; Khanh, T. H.; Chau, N. V. V.; et al. Fatal avian influenza A (H5N1) in a child presenting with diarrhea followed by coma. *N. Engl. J. Med.* **2009**, *352* (7), 686–691.

(12) Hu, Y.; Lu, S.; Song, Z.; Wang, W.; Hao, P.; Li, J.; Zhang, X.; Yen, H. L.; Shi, B.; Li, T.; et al. Association between adverse clinical outcome in human disease caused by novel influenza A H7N9 virus and sustained viral shedding and emergence of antiviral resistance. *Lancet* **2013**, *381* (9885), 2273–2279.

(13) Chan, M. C. W.; Lee, N.; Chan, P. K. S.; To, K. F.; Wong, R. Y. K.; Ho, W. S.; Ngai, K. L. K.; Sung, J. J. Y. Seasonal influenza A virus in feces of hospitalized adults. *Emerg. Infect. Dis.* **2011**, *17* (11), 2038–2042.

(14) Rozé, B.; Najioullah, F.; Fergé, J.-L.; Apetse, K.; Brouste, Y.; Cesaire, R.; Fagour, C.; Fagour, L.; Hochedez, P.; Jeannin, S.; et al. Zika virus detection in urine from patients with Guillain-Barré syndrome on Martinique, January 2016. *Euro Surveill.* **2016**, *21* (9), 1–4.
(15) Gourinat, A.-C.; O'Connor, O.; Calvez, E.; Goarant, C.; Dupont-Rouzeyrol, M. Detection of Zika virus in urine. *Emerg. Infect. Dis.* **2015**, *21* (1), 84–86.
(16) Burke, R.; Barrera, R.; Lewis, M.; Kluchinsky, T.; Claborn, D. Septic tanks as larval habitats for the mosquitoes Aedes aegypti and Culex quinquefasciatus in Playa-Playita, Puerto Rico. *Med. Vet. Entomol.* **2010**, *24* (2), 117–123.
(17) Hirayama, T.; Mizuno, Y.; Takeshita, N.; Kotaki, A.; Tajima, S.; Omatsu, T.; Sano, K.; Kurane, I.; Takasaki, T. Detection of dengue virus genome in urine by real-time RT-PCR: A laboratory diagnostic method useful after disappearance of the genome in serum. *J Clin. Microbiol.* **2012**, *50* (6), JCM.06557–11.
(18) Barzon, L.; Pacenti, M.; Franchin, E.; Pagni, S.; Martello, T.; Cattai, M.; Cusinato, R.; Palù, G. Excretion of West Nile virus in urine during acute infection. *J. Infect. Dis.* **2013**, *208* (7), 1086–1092.
(19) Noyola, D. E.; Demmler, G. J.; Williamson, D. W.; Griesser, C.; Sellers, S.; Llorente, A.; Littman, T.; Williams, S.; Jarrett, L.; Yow, M. D.; et al. Cytomegalovirus urinary excretion and long term outcome in children with congenital cytomegalovirus infection. *Pediatr. Infect. Dis. J.* **2000**, *19* (6), 505.
(20) Alpert, G.; Mazeron, M. C.; Colimon, R.; Plotkin, S. Rapid detection of human cytomegalovirus in the urine of humans. *J. Infect. Dis.* **1985**, *152*, 631–633.
(21) Vabret, A.; Dina, J.; Gouarin, S.; Petitjean, J.; Corbet, S.; Freymuth, F. Detection of the new human coronavirus HKU1: a report of 6 cases. *Clin. Infect. Dis.* **2006**, *42* (5), 634–639.
(22) Who Website; http://www.who.int/csr/sars/country/table2004_04_21/en/.
(23) Alsolamy, S.; Arabi, Y. M. Infection with Middle East respiratory syndrome coronavirus. *Can. J. Respir. Ther.* **2015**, *51* (4), 102.
(24) Chan, K. H.; Poon, L. L. L. M.; Cheng, V. C. C.; Guan, Y.; Hung, I. F. N.; Kong, J.; Yam, L. Y. C.; Seto, W. H.; Yuen, K. Y.; Peiris, J. S. M. Detection of SARS coronavirus in patients with suspected SARS. *Emerg. Infect. Dis.* **2004**, *10* (2), 294–299.
(25) Yu, I. T. S.; Li, Y.; Wong, T. W.; Tam, W.; Chan, A. T.; Lee, J. H. W.; Leung, D. Y. C.; Ho, T. Evidence of airborne transmission of the severe acute respiratory syndrome virus. *N. Engl. J. Med.* **2009**, *350* (17), 1731–1739.
(26) Risku, M.; Lappalainen, S.; Rasanen, S.; Vesikari, T. Detection of human coronaviruses in children with acute gastroenteritis. *J. Clin. Virol.* **2010**, *48* (1), 27–30.
(27) Webster, R. G.; Yakhno, M.; Hinshaw, V. S.; Bean, W. J.; Copal Murti, K. Intestinal influenza: Replication and characterization of influenza viruses in ducks. *Virology* **1978**, *84* (2), 268–278.
(28) Watanabe, T.; Watanabe, S.; Maher, E. A.; Neumann, G.; Kawaoka, Y. Pandemic potential of avian influenza A (H7N9) viruses. *Trends Microbiol.* **2014**, *22* (11), 623–631.
(29) Who Website; http://www.wpro.who.int/emerging_diseases/AvianInfluenza/en/.
(30) Markwell, D. D.; Shortridge, K. F. Possible waterborne transmission and maintenance of influenza viruses in domestic ducks. *Appl. Environ. Microbiol.* **1982**, *43* (1), 110–115.
(31) Peiris, J. S. M.; de Jong, M. D.; Guan, Y. Avian influenza virus (H5N1): A threat to human health. *Clin. Microbiol. Rev.* **2007**, *20* (2), 243–267.

(32) de Jong, M. D.; Simmons, C. P.; Thanh, T. T.; Hien, V. M.; Smith, G. J. D.; Chau, T. N. B.; Hoang, D. M.; Van Vinh Chau, N.; Khanh, T. H.; Dong, V. C.; et al. Fatal outcome of human influenza A (H5N1) is associated with high viral load and hypercytokinemia. *Nat. Med.* **2006**, *12* (10), 1203–1207.

(33) Buchy, P.; Mardy, S.; Vong, S.; Toyoda, T.; Aubin, J.-T.; Miller, M.; Touch, S.; Sovann, L.; Dufourcq, J.-B.; Richner, B.; et al. Influenza A/H5N1 virus infection in humans in Cambodia. *J. Clin. Virol.* **2007**, *39* (3), 164–168.

(34) Chan, M.; Lee, N.; Chan, P.; To, K. F.; Wong, R.; Ho, W. S.; Ngai, K.; Sung, J. Seasonal Influenza A Virus in Feces of Hospitalized Adults. *Emerg. Infect. Dis.* **2011**, *17* (11), 1–5.

(35) Poloni, T. R.; Oliveira, A. S.; Alfonso, H. L.; Galvão, L. R.; Amarilla, A. A.; Poloni, D. F.; Figueiredo, L. T.; Aquino, V. H. Detection of dengue virus in saliva and urine by real time RT-PCR. *Virol. J.* **2010**, *7* (1), 22.

(36) Hossini, H.; Pirsaheb, M.; Hossaini, H.; Limoee, M. Zika virus (ZIKV) and wastewater treatment plants. *health scope* **2017**, *6*, e39789.

(37) Duffy, M. R.; Chen, T.-H.; Hancock, W. T.; Powers, A. M.; Kool, J. L.; Lanciotti, R. S.; Pretrick, M.; Marfel, M.; Holzbauer, S.; Dubray, C.; et al. Zika virus outbreak on Yap Island, federated states of Micronesia. *N. Engl. J. Med.* **2009**, *360* (24), 2536–2543.

(38) Ponnusamy, L.; Böröczky, K.; Wesson, D. M.; Schal, C.; Apperson, C. S. Bacteria stimulate hatching of yellow fever mosquito eggs. *PLoS ONE* **2011**, *6* (9), e24409.

(39) Bibby, K.; de Carvalho, N. A.; Wigginton, K. Research needs for wastewater handling in virus outbreak response. *Environ. Sci. Technol.* **2017**, *51*, 2534–2535.

(40) Bausch, D. G.; Towner, J. S.; Dowell, S. F.; Kaducu, F.; Lukwiya, M.; Sanchez, A.; Nichol, S. T.; Ksiazek, T. G.; Rollin, P. E. Assessment of the risk of Ebola virus transmission from bodily fluids and fomites. *J. Infect. Dis.* **2007**, *196* (Suppl 2), S142–S147.

(41) Mora-Rillo, M.; Arsuaga, M.; Ramírez-Olivencia, G.; la Calle, de, F.; Borobia, A. M.; Sánchez-Seco, P.; Lago, M.; Figueira, J. C.; Fernández-Puntero, B.; Viejo, A.; et al. Acute respiratory distress syndrome after convalescent plasma use: treatment of a patient with Ebola virus disease contracted in Madrid, Spain. *Lancet Respir. Med.* **2015**, *3*, 554–562.

(42) Brainard, J.; Pond, K.; Hunter, P. R. Censored regression modeling to predict virus inactivation in wastewaters. *Environ. Sci. Technol.* **2017**, *51* (3), 1795–1801.

(43) Gerba, C. P. Virus survival in wastewater treatment. In *Viruses and Wastewater Treatment*; Pergamon, 1981; pp 39–48.

(44) Hurst, C. J.; Gerba, C. P. Fate of viruses during wastewater sludge treatment processes. *Crit. Rev. Env. Sci. Technol.* **2009**, *18* (4), 317–343.

(45) Hermansson, M. The DLVO theory in microbial adhesion. *Colloids and Surf. B: Biointerfaces* **1999**, *14* (1-4), 105–119.

(46) Chrysikopoulos, C. V.; Syngouna, V. I. Attachment of bacteriophages MS2 and ΦX174 onto kaolinite and montmorillonite: Extended-DLVO interactions. *Colloids and Surf. B: Biointerfaces* **2012**, *92*, 74–83.

(47) Gerba, C. P. Applied and theoretical aspects of virus adsorption to surfaces. *Advan. Appl. Microbiol.* **1984**, *30*, 133–168.

(48) Schaldach, C. M.; Bourcier, W. L.; Shaw, H. F.; Viani, B. E.; Wilson, W. D. The influence of ionic strength on the interaction of viruses with charged surfaces under environmental conditions. *J. Colloid. Interface Sci.* **2006**, *294* (1), 1–10.

(49) Grant, S. B.; List, E. J.; Lidstrom, M. E. Kinetic analysis of virus adsorption and inactivation in batch experiments. *Water Resour. Res.* **1993**, *29* (7), 2067–2085.
(50) Hijnen, W. A. M.; Beerendonk, E. F.; Medema, G. J. Inactivation credit of UV radiation for viruses, bacteria and protozoan (oo)cysts in water: A review. *Water Res.* **2006**, *40* (1), 3–22.
(51) Aieta, E. M.; Berg, J. D. A review of chlorine dioxide in drinking water treatment. *J. AWWA* **1986**, *78* (6), 62–72.
(52) Kim, J. G.; Yousef, A. E.; Dave, S. Application of ozone for enhancing the microbiological safety and quality of foods: A review. *J. Food Prot.* **1999**, *62* (9), 1071–1087.
(53) Kitis, M. Disinfection of wastewater with peracetic acid: A review. *Environ. Inte.* **2004**, *30* (1), 47–55.
(54) Wigginton, K. R.; Pecson, B. M.; Sigstam, T.; Bosshard, F.; Kohn, T. Virus Inactivation Mechanisms: Impact of Disinfectants on Virus Function and Structural Integrity. *Environ. Sci. Technol.* **2012**, *46* (21), 12069–12078.
(55) Qiao, Z.; Ye, Y.; Chang, P. H.; Thirunarayanan, D.; Wigginton, K. R. Nucleic acid photolysis by UV_{254} and the impact of virus encapsidation. *Environ. Sci. Technol.* **2018**, *52* (18), 10408–10415.
(56) Beck, S. E.; Rodríguez, R. A.; Linden, K. G.; Hargy, T. M.; Larason, T. C.; Wright, H. B. Wavelength dependent UV inactivation and DNA damage of adenovirus as measured by cell culture infectivity and long range quantitative PCR. *Environ. Sci. Technol.* **2013**, *48* (1), 591–598.
(57) Beck, S. E.; Rodríguez, R. A.; Hawkins, M. A.; Hargy, T. M.; Larason, T. C.; Linden, K. G.; Dozois, C. M. Comparison of UV-induced inactivation and RNA damage in MS2 phage across the germicidal UV spectrum. *Appl. Environ. Microbiol.* **2016**, *82* (5), 1468–1474.
(58) Sigstam, T.; Gannon, G.; Cascella, M.; Pecson, B. M.; Wigginton, K. R.; Kohn, T. Subtle differences in virus composition affect disinfection kinetics and mechanisms. *Appl. Environ. Microbiol.* **2013**, *79* (11), 3455–3467.
(59) Ho, J.; Seidel, M.; Niessner, R.; Eggers, J.; Tiehm, A. Long amplicon (LA)-qPCR for the discrimination of infectious and noninfectious phix174 bacteriophages after UV inactivation. *Water Res.* **2016**, *103*, 141–148.
(60) Sinha, R. P.; Häder, D.-P. UV-induced DNA damage and repair: a review. *Photochem. Photobiol. Sci.* **2002**, *1* (4), 225–236.
(61) Sivey, J. D.; McCullough, C. E.; Roberts, A. L. Chlorine monoxide (Cl_2O) and molecular chlorine (Cl_2) as active chlorinating agents in reaction of dimethenamid with aqueous free chlorine. *Environ. Sci. Technol.* **2010**, *44* (9), 3357–3362.
(62) Gallandat, K.; Lantagne, D. Selection of a Biosafety Level 1 (BSL-1) surrogate to evaluate surface disinfection efficacy in Ebola outbreaks: Comparison of four bacteriophages. *PLoS ONE* **2017**, *12* (5), 1–10.
(63) Deboosere, N.; Horm, S. V.; Pinon, A.; Gachet, J.; Coldefy, C.; Buchy, P.; Vialette, M. Development and validation of a concentration method for the detection of influenza A viruses from large volumes of surface water. *Appl. Environ. Microbiol.* **2011**, *77* (11), 3802–3808.
(64) Wang, X.; Li, J.; Guo, T.; Zhen, B.; Kong, Q.; Yi, B.; Li, Z.; Song, N.; Jin, M.; Xiao, W. Concentration and detection of SARS coronavirus in sewage from Xiao Tang Shan

Hospital and the 309th Hospital of the Chinese Peoples Liberation Army. *Water Sci. Technol.* **2005**, *52* (8), 213–221.

(65) Lee, H. K.; Jeong, Y. S. Comparison of total culturable virus assay and multiplex integrated cell culture-PCR for reliability of waterborne virus detection. *Appl. Environ. Microbiol.* **2004**, *70* (6), 3632–3636.

(66) Reynolds, K. A.; Gerba, C. P.; Abbaszadegan, M.; Pepper, I. L. ICC/PCR detection of enteroviruses and hepatitis A virus in environmental samples. *Canadian Journal of Microbiology* **2001**, *47*, 153–157.

(67) Reynolds, K. A.; Gerba, C. P.; Pepper, I. L. Detection of infectious enteroviruses by an integrated cell culture-PCR procedure. *Appl. Environ. Microbiol.* **1996**, *62* (4), 1424–1427.

(68) Greening, G. E.; Hewitt, J.; Lewis, G. D. Evaluation of integrated cell culture-PCR (C-PCR) for virological analysis of environmental samples. *J. Appl. Microbiol.* **2002**, *93* (5), 745–750.

(69) Kojima, S.; Kageyama, T.; Fukushi, S.; Hoshino, F. B.; Shinohara, M.; Uchida, K.; Natori, K.; Takeda, N.; Katayama, K. Genogroup-specific PCR primers for detection of Norwalk-like viruses. *J. Virol. Methods* **2002**, *100* (1-2), 107–114.

(70) Nguyen, A. P.; Downard, K. M. Proteotyping of the parainfluenza virus with high-resolution mass spectrometry. *Anal. Chem.* **2013**, *85*, 1097–1105.

(71) Majchrzykiewicz-Koehorst, J. A.; Heikens, E.; Trip, H.; Hulst, A. G.; de Jong, A. L.; Viveen, M. C.; Sedee, N. J. A.; van der Plas, J.; Coenjaerts, F. E. J.; Paauw, A. Rapid and generic identification of influenza A and other respiratory viruses with mass spectrometry. *J. Virol. Methods* **2015**, *213*, 75–83.

Chapter 2 Survivability, partitioning, and recovery of enveloped viruses in untreated municipal wastewater

Reprinted with permission from Yinyin Ye, Robert M. Ellenberg, Katherine E. Graham, and Krista R. Wigginton, Survivability, Partitioning, and Recovery of Enveloped Viruses in Untreated Municipal Wastewater, *Environmental Science & Technology*, **2016**, *50*, 5077– 5085, © 2016 American Chemical Society.

2.1 Introduction

Recent severe disease outbreaks caused by enveloped viruses, such as Ebola, severe acute respiratory syndrome (SARS), Middle East respiratory syndrome (MERS), and avian influenza H5N1 have heightened fears of an imminent deadly viral pandemic. The major transmission routes of these viruses involved direct person-to-person contact or indirect contact with contaminated objects.[1,2] Human enveloped viruses are often presumed to exist in low concentrations in human excrement and undergo rapid inactivation in aqueous environments; however, several lines of evidence suggest these assumptions are not always correct. The genes of coronaviruses and avian influenzas have been detected in the feces of infected individuals,[3-9] and some enveloped viruses were measured in wastewater biosolid residuals.[10] Likewise, some enveloped viruses can survive for days to weeks in pasteurized wastewater.[11-13] A review of virus T_{90} values (*i.e.* time to reach 90% inactivation) suggests that avian influenza viruses survive just as long, if not longer, than nonenveloped enteric viruses in some aqueous environments.[14] Based on this information, it is therefore feasible that sewage and fecal-contaminated water could serve as vectors for certain

enveloped viruses. Indeed, a SARS coronavirus outbreak in an apartment complex in Hong Kong was attributed to the transport of viruses in wastewater to the air ducts.[15]

The vast majority of studies on the presence and fate of viruses in human waste and municipal wastewater have focused on nonenveloped enteric viruses (e.g., adenoviruses, polioviruses, enteroviruses, noroviruses and rotaviruses).[16-21] These viruses replicate in human gut tissues and transmit diseases primarily via the fecal-oral route. Due to the major role of water and food in the transmission of enteric viruses, there are a number of established methods for nonenveloped enteric virus detection in complex environmental matrices. Enveloped viruses differ structurally from nonenveloped viruses due to the presence of a lipid bilayer membrane outside the viral protein capsid, which contains proteins or glycoproteins. The different functional groups on the outer surface of enveloped viruses compared to nonenveloped viruses likely impact their survival and partitioning behavior in aqueous environments.[22-24] Likewise, methods to concentrate and recover nonenveloped enteric viruses from wastewater and other environmental matrices may not be suitable for enveloped viruses. For example, lipid layers are sensitive to the detergents and organic solvents[25,26] that are commonly used to extract and purify nonenveloped enteric viruses.

To address the paucity of data on the fate and recovery of enveloped viruses in wastewater matrices, we studied the survival and partitioning behavior of the human enveloped virus surrogates, murine hepatitis virus (MHV) and *Pseudomonas* phage Phi6, in pasteurized and unpasteurized wastewater. We compared the inactivation kinetics and liquid-solid partitioning of the two enveloped viruses with two nonenveloped virus surrogates, *Enterobacteria* phage MS2 and T3. Furthermore, we systematically tested the effectiveness of three virus recovery methods—initially developed for using on enteric viruses—for extracting and concentrating enveloped

viruses from both liquid and solid fractions in wastewater. Finally, we proposed an optimized ultrafiltration method for detecting both enveloped and nonenveloped viruses.

2.2 Materials and methods

2.2.1 Wastewater samples

Wastewater samples were collected from the Ann Arbor Wastewater Treatment plant, an activated sludge treatment plant serving roughly 115,000 people with an average flow rate of 19 million gallons per day (MGD). Grab samples were collected after wastewater equalization, screening, and grit removal chambers, and just before the primary settling tanks. All samples were collected and sealed in sterile plastic bottles and then immediately transported on ice to laboratories at the University of Michigan where they were stored at 4 °C and analyzed within 24 hours. Wastewater pH, total suspended solids (TSS), volatile suspended solids (VSS), and total chemical oxygen demand (COD) were measured with standard methods.[27]

2.2.2 Virus strains and methods

We chose to study MHV strain A59 and *Pseudomonas* phage Phi6 because they are common surrogates for human enveloped viruses (Table 2.1).[11,13,28] We also studied two nonenveloped *Enterobacteria* phages MS2 and T3 to allow for direct comparisons between enveloped and nonenveloped virus inactivation, partitioning, and recovery.[29-31]

Table 2.1 Characteristics of tested viruses.

Virus	Structure	Family/Genus	Genome Type	Genome Size (Kb)	Particle Size (nm)
MHV	Enveloped	*Coronaviridae/Coronavirus*	(+) ssRNA	32	100
Phi6	Enveloped	*Cystoviridae/Cystovirus*	Segmented dsRNA	13.5	80
MS2	Nonenveloped	*Leviviridae/Levivirus*	(+) ssRNA	3.6	25
T3	Nonenveloped	*Podoviridae/T7-like viruses*	dsDNA	38.2	50 × 20 (tail)

MHV strain A59, and its supporting cell lines L2 and DBT, were kindly provided by Dr. Leibowitz's lab at Texas A&M Health Science Center College of Medicine. L2 and DBT cells were grown in Dulbecco's Modified Eagle Medium (DMEM) with 10% newborn calf serum, 1% L-glutamine, and 1% penicillin/streptomycin, and incubated at 37 °C with 5% CO_2. MHV stocks were propagated in DBT and titered by plaque assay on L2 according to a published protocol.[32] After amplification, MHV stocks were centrifuged at 3,000 × g for 10 min, and then filtered through a 0.22 μm polyethersulfone (PES) membrane (Millipore, USA), in order to remove cell debris and aggregated viruses. The MHV stocks (~10^6 PFU mL^{-1}) were stored at -80 °C.

Phi6 and its bacterial host *Pseudomonas syringae* were kindly provided by Dr. Linsey Marr's lab at Virginia Tech. *P. syringae* was grown in Luria-Bertani (LB) medium containing 5 g L^{-1} NaCl at 26 °C. To propagate Phi6 stocks, soft LB-agar (0.7% agar) layers were removed from the double-layer plates, and dissolved in 3 mL of LB medium.[33] The recovered viruses were purified with centrifugation at 3,000 × g for 10 min at 4 °C and filtration through 0.22 μm PES membranes. The Phi6 stocks (~10^{10} PFU mL^{-1}) were stored at 4 °C.

MS2 (ATCC 15597-B1) and T3 (recovered from ATCC 11303-B4), and their corresponding *Escherichia coli* hosts ATCC 15597 and ATCC 11303, respectively, were purchased from American Type Culture Collection (ATCC). The MS2 and T3 were propagated and assayed in their *E. coli* hosts based on published methods.[34,35] The viruses were purified with an Econo Fast

Protein Liquid Chromatography system (Bio-Rad, USA) equipped with a HiPrep Sephacryl S-400 HR column (GE, USA). The collected viral fraction was concentrated with 100 kDa Amicon ultracentrifugal filters (Millipore, USA), and filtered through a 0.22 μm PES membrane filter. The final MS2 and T3 stocks (~10^{11} PFU mL^{-1}) were stored in phosphate buffer (5 mM NaH_2PO_4 and 10 mM NaCl, pH 7.5) at 4 °C.

2.2.3 Survivability experiments

Virus surrogates were spiked into 30 mL samples of unpasteurized and pasteurized wastewater to final concentrations of 3×10^4 PFU mL^{-1} for MHV and $5—8 \times 10^5$ PFU mL^{-1} for Phi6, MS2 and T3; the lower MHV concentrations were due to the lower MHV stock concentrations. Wastewater was pasteurized by heating to 70 °C for 3 h; this treatment is consistent with previous studies involving enveloped virus survival in pasteurized wastewater.[11,13] Wastewater samples were quickly mixed after viruses were added, titered for the initial virus concentrations, and then incubated at 25 °C or 10 °C to mimic typical summer and winter wastewater temperatures. Aliquots of wastewater were removed at specific incubation times and infective virus concentrations were enumerated with plaque assays. The wastewater samples were diluted at least 10-fold to minimize wastewater effects on the host cells. Replicate experiments (n = 3) were conducted in wastewater samples collected on different days to incorporate potential impacts of wastewater variation on virus survivability.

2.2.4 Partitioning experiments

To evaluate the kinetics and extent of virus sorption to wastewater solids, the virus surrogates were spiked into 30 mL samples of untreated wastewater and wastewater with solids removed via

centrifugation at 30,000 × g for 10 min. (i.e., solids-removed samples). This centrifugation treatment, which was previously shown to remove solids less than 0.3 μm in diameter,[36] consistently removed 85—95% of the TSS in our wastewater samples (Table S2). Samples were spiked to achieve final virus concentrations of 5×10^4 PFU mL^{-1} for MHV, and $6—8 \times 10^5$ PFU mL^{-1} for Phi6, MS2, and T3—these were low enough to be feasible concentrations present in wastewater (< 10^6 PFU mL^{-1}) and high enough that more than 99% loss could be quantified with plaque assays. The spiked samples were stirred and then incubated at 4 °C; this temperature is at the low-end of mean municipal wastewater temperatures in the U.S. (3 °C—27 °C)[37] and was selected to minimize virus inactivation through the duration of the experiment. At various incubation times, aliquots of the untreated and solids-removed samples were centrifuged at 30,000 × g for 10 min, and the centrates were assayed for infective viruses.

Virus inactivation and sorption kinetics in wastewater batch reactors were analyzed with an approach proposed by Grant *et al*. that accounts for virus sorption and desorption from sorbents, as well as inactivation in the liquid and solid fractions.[38] In our system, the solids-containing samples were the untreated wastewater influent and the solids-free samples were wastewater samples with solids removed via centrifugation. Virus inactivation in the wastewater liquid was assumed to be equal to virus inactivation in the solids-removed sample, and to follow first-order kinetics:

$$\ln C_l^* = -k_1 \mathrm{t} \qquad (1)$$

where, C_l^* is the nondimensional concentration of infective viruses measured in the solids-removed wastewater samples ($C_l/C_{l,0}$), t is the incubation time in hours, and k_1 (h^{-1}) is the first-order virus inactivation constant in the solids-removed wastewater.

In a wastewater sample spiked with viruses, the nondimensional concentration of infective viruses in the wastewater liquid $C^*_{l,ww}$is related to the fraction of viruses inactivated in the liquid phase (ξ^*_1), and the fraction reversibly adsorbed to wastewater solids (ξ^*_2):

$$C^*_{l,ww} = 1 - \xi^*_1 - \xi^*_2 \quad (2)$$

The change of the viral fraction in the liquid and solid phases with time can be described with the following set of differential equations:

$$\frac{d\xi^*_1}{d\tau} = 1 - \xi^*_1 - \xi^*_2 \quad (3a)$$

$$\frac{d\xi^*_2}{d\tau} = N_b\left[1 - \frac{n^*_{sro}}{N_f - 1} - \xi^*_1 - \xi^*_2\left(\frac{N_f}{N_f - 1}\right) + \xi^*_3\left(\frac{N_s}{N_f - 1}\right)\right] \quad (3b)$$

$$\frac{d\xi^*_3}{d\tau} = N_i[n^*_{sro} + \xi^*_2 - N_s\xi^*_3] \quad (3c)$$

where, ξ^*_3 is the fraction of viruses inactivated on the solid surface; τ is the nondimensional time, equal to $k_1 t$; n^*_{sro} is the initial amount of viruses reversibly adsorbed to solids (assumed zero in the study); $N_b = k_2/k_1$, where k_2 (h^{-1}) is the rate constant for reversible virus adsorption; $N_s = (k_3 + k_4)/k_3$, where k_3 (h^{-1}) is the rate constant for virus inactivation at the solid surface and k_4 (h^{-1}) is the rate constant for the conversion of reversibly adsorbed viruses to an irreversibly adsorbed state; $N_i = k_3/k_1$; $N_f = [(k_2 W/k_{-2} V) + 1]$, where k_{-2} (g L^{-1} h^{-1}) is the rate constant for virus desorption from solid phase to liquid phase, W (g) is the mass of solids, and V (L) is the liquid volume. At time zero ($\tau = 0$), $\xi^*_1 = \xi^*_2 = \xi^*_3 = 0$.

The relationship between $C^*_{l,ww}$ and incubation time t was solved from numerical simulations of the above differential equation system with the 4th order Runge-Kutta algorithm in MATLAB2015. An extensive description of the equation derivations, simplifications, and parameter calculations can be found in 38.

2.2.5 Virus recovery methods

Virus recovery methods were tested with wastewater that had been spiked with one enveloped virus (MHV) and one nonenveloped virus (MS2). Three approaches for separating and concentrating viruses from the liquid fraction of municipal wastewater, including polyethylene glycol (PEG) precipitation,[39,40] ultracentrifugation,[19] and ultrafiltration,[18,41] were selected based on their previous application in recovering viruses from wastewater. Published enteric virus methods that involved steps likely to inactivate the enveloped viruses (e.g., pH adjustment outside 6-8 range,[42-44] organic solvent extractions,[25,26] etc.) were avoided. The best-performing method for MHV and MS2 was then further validated with the enveloped virus Phi6 and nonenveloped virus T3. In the first set of experiments, MHV and MS2 were spiked in wastewater samples to final concentrations of 8×10^3 PFU mL^{-1} and 5×10^5 PFU mL^{-1}, respectively. Samples were then briefly mixed and incubated at 4 °C for one hour before they were treated with the extraction/concentration techniques; the one-hour incubation time was selected based on the results from the partitioning experiments. In each experiment, samples were concentrated 100 ×, and infective viruses in the concentrates were measured with plaque assays. Virus recovery was calculated based on the following relationship:

$$Virus\ recovery\ (\%) = \frac{C_{con} \cdot V_{con}}{C_s \cdot V_s} \times 100\% \qquad (4)$$

where $(C_s \cdot V_s)$ equals the number of infective viruses spiked in, and $(C_{con} \cdot V_{con})$ is the number of infective viruses measured in the concentrate.

Polyethylene glycol (PEG) precipitation method. Following incubation with the spiked viruses, wastewater samples (250 mL) were centrifuged at 2,500 × g for 5 min at 4 °C to remove large solids. The centrate was collected and mixed with 8% (w/v) of PEG 8000 and 0.5 M of NaCl. The mixture was incubated for 2 h at 4 °C, and then centrifuged at 10,000 g for 30 min at 4 °C. The

PEG pellet was resuspended in 2.5 mL phosphate buffered saline (PBS, pH 7.4; Life Technologies, USA) and assayed for infective viruses.

Ultracentrifugation method. Following incubation with the viruses, wastewater samples (60 mL) were centrifuged at 100,000 × g for 1 h at 4 °C using a Sorvall WX Ultra centrifuge (Thermo Scientific, Germany; SureSpin 630 (36 mL) rotor, P/N 79368; SureSpin swinging bucket, P/N 79388). The pellet was resuspened in 8 mL of 0.25 M glycine buffer (pH 9.5) and allowed to sit on ice for 30 minutes. After neutralizing the solution pH with 16 mL PBS, the solids were removed by centrifugation at 10,000 × g for 15 min at 4 °C. The supernatant was collected and centrifuged again at 100,000 × g for 1 h at 4 °C to pellet the viruses. The final virus pellet was dissolved in 600 μL PBS.

Ultrafiltration method. Following incubation with the spiked viruses, solids in the wastewater samples (250 mL) were removed by either centrifuging at 30,000 × g for 10 min at 4 °C, or by centrifugation at 2,500 × g for 5 min at 4 °C followed by filtration through 0.22 μm PES membrane filters. After the large solids had been removed, the samples were concentrated with Centricon centrifugal filters (Millipore, USA) to a final volume of 2.5 mL. Recoveries from centrifugal filters with 10 kDa and 100 kDa cut-offs were compared. Centrifugal filter reuse was tested by first washing used filters with 100 mL of 0.5 M NaOH and then storing the regenerated filters in 70% ethanol. The reused filters were rinsed with 100 mL of Milli-Q water prior to use.

In an attempt to recover viruses associated with wastewater solids, the solids collected in the centrifugation step prior to ultrafiltration were mixed with different elution buffers, including PBS, 0.05 M glycine buffer (pH 8.5), 0.05 M glycine buffer (pH 9.5), 0.05 M glycine buffer (pH 10.5), 3% beef extract (pH 7.5), 3% beef extract (pH 9.5), and 3% beef extract with 0.5 M sodium chloride (pH 9.5). Suspensions were set on ice for 30 min. and gently shaken every 10 min. The

solutions were centrifuged at 10,000 × g for 15 min at 4 °C and the resulting centrate was neutralized with PBS (pH 7.4), and then titered for infective viruses.

2.2.6 Statistical analyses

Non-parametric t-tests were applied to two groups of experimental data to assess statistical significance. Two-tailed *P* values were calculated, and $P < 0.05$ was considered statistically significant.

2.3 Results and discussion

2.3.1 Comparison of virus survival in wastewater

Inactivation of the two enveloped viruses (MHV and Phi6) and nonenveloped virus MS2 in unpasteurized and pasteurized wastewater at 10 °C and 25 °C followed first-order kinetics (Figure 2.1; Table A-3), with inactivation proceeding faster for the enveloped viruses. In unpasteurized wastewater at 25 °C, the T_{90} (±s.d.) values for MHV and Phi6 were 13 (±1) and 7 (±0.4) hours, respectively, and 121 (±36) hours for MS2 (Table A-3). The nonenveloped T3 virus survived much longer than the other virus surrogates with no significant decrease in infectivity observed within the 48-hour experiments for both temperatures (Figure 2.1). This is consistent with long survival times reported for tailed phages in adverse conditions.[45] The inactivation kinetics of the enveloped viruses were significantly ($P < 0.0001$) slower in wastewater at 10 °C compared to 25 °C (Figure S4), with T_{90} (±SD) values of 36 (±5) and 28 (±2) hours for MHV and Phi6 at 10 °C, respectively (Table A-3). Like T3, MS2 inactivation was not statistically different at the two temperatures ($P = 0.1813$) within the tested timescale (Figure A-4).

Inactivation kinetics of the enveloped viruses MHV, Phi6, and Ebolavirus in pasteurized or gamma-irradiated wastewater have been reported previously.[11-13] In our experiments, the two enveloped viruses lost infectivity at a significantly slower rate in pasteurized wastewater compared to unpasteurized wastewater, except for the case of MHV at 25 °C (Figure 2.1; Table A-3). The most pronounced effect occurred with Phi6, which had a first-order inactivation rate constant (±s.d.) of 0.317 (±0.022) h^{-1} in unpasteurized wastewater and 0.044 (±0.004) h^{-1} in pasteurized wastewater at 25 °C. A statistically significant difference in the inactivation kinetics of the nonenveloped viruses was not observed in pasteurized wastewater and unpasteurized wastewater; this may be due to the fact that our experiments were stopped before 90% of the nonenveloped viruses were inactivated. Discrepancies in inactivation kinetics in sterilized and non-sterilized wastewater have been reported previously for nonenveloped viruses,[46] and may be due to bacterial extracellular enzyme activity and protozoan or metazoan predation.[47,48] Overall, the results suggest that unpasteurized wastewater samples should be employed for survivability tests when feasible.

Wastewater residence times in sewage systems are typically less than 24 hours. Although Phi6 and MHV had T_{90} values of 7—13 hours in unpasteurized wastewater at 25 °C, the T_{90} values increase to 28—36 hours at 10 °C. Human enveloped viruses excreted in feces may therefore reach wastewater treatment plants in an infective state, especially in cool climates. Local outbreaks and global pandemics of enveloped viruses excreted in feces or urine are therefore relevant for wastewater utilities.

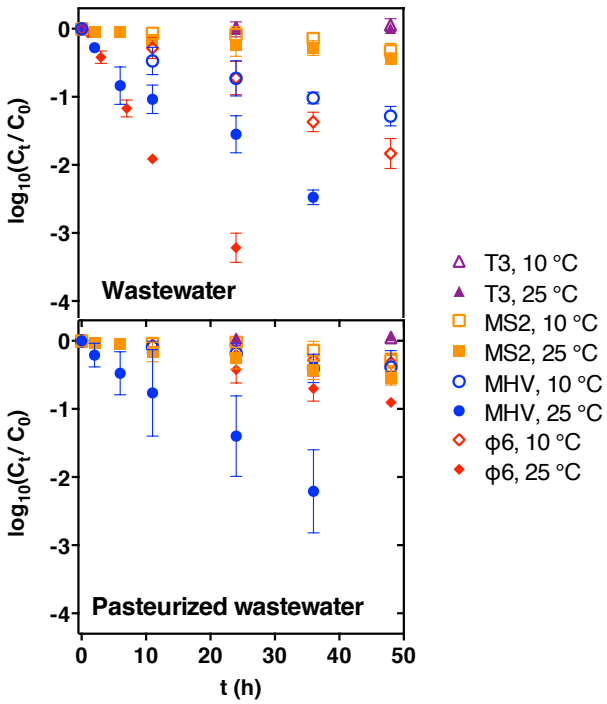

Figure 2.1 Virus survival in wastewater and pasteurized wastewater at 10 and 25 °C. Viruses were spiked into wastewater to final concentrations of 3×10^4 PFU mL^{-1} for MHV and 5—8×10^5 PFU mL^{-1} for MS2, T3 and Phi6. Error bars represent the standard deviations of replicates from wastewater samples collected on different days (n = 3). Table S3 summarizes corresponding rate constants and estimated T_{90} values.

2.3.2 Comparison of virus partitioning in wastewater.

The measured concentrations of infective MHV and Phi6 in the solids-removed wastewater samples immediately after spiking, mixing, and centrifuging, were consistently lower than the theoretical concentrations based on the amount of viruses spiked into the sample (Figure S1). Approximately 47% of the spiked MHV and 77% of the spiked Phi6 were recovered in the centrate of the solids-removed wastewater. This is compared to a nearly 100% recovery of the nonenveloped viruses MS2 and T3. Nearly all of the MHV was recovered when it was spiked into PBS and centrifuged in the same manner (Figure S1). This suggests that a fraction of the enveloped

viruses (53% MHV and 23% Phi6) were rapidly inactivated in the solids-removed wastewater. A pronounced initial decrease in infective virus concentration was previously observed when Ebola virus was added to pasteurized wastewater.[12] In those experiments, the number of infective Ebola viruses decreased rapidly over the first 24 hours (~2-log loss) and then stabilized at a much slower inactivation rate over the subsequent seven days. Similar biphasic inactivation kinetics have also been observed with nonenveloped viruses, which were attributed to subpopulations of viruses with varied susceptibilities to solution chemistry or temperature.[38] In our partitioning experiments, we chose to normalize measured concentrations in the wastewater and solids-removed wastewater samples over time to concentrations measured in solids-removed samples immediately after they were spiked with viruses, mixed, and centrifuged. We felt this approach was justified because the behaviors of the persistent subpopulations are of most interest for real wastewater systems.

MHV, Phi6, and MS2 concentrations decreased significantly over a three-day period in the solids-removed wastewater samples (Figure 2.2) and the resulting rate constants were assumed to equal virus inactivation rates in the liquid fraction of wastewater (Eq. 1, k_1).[38] When the viruses were spiked in wastewater samples containing solids, the normalized MHV and Phi6 concentrations in the wastewater liquid phase (in centrate after centrifugation) decreased rapidly in the first hour, and then eventually decreased at the same rate as virus inactivation in the solids-removed sample (Figure 2.2). The MS2 concentration in the wastewater liquid phase decreased rapidly at first, and then slowed to a rate that was faster than MS2 inactivation in the solids-removed sample (Figure 2.2). No significant decay of T3 was observed in the solids-removed wastewater samples or the liquid phase of wastewater samples.

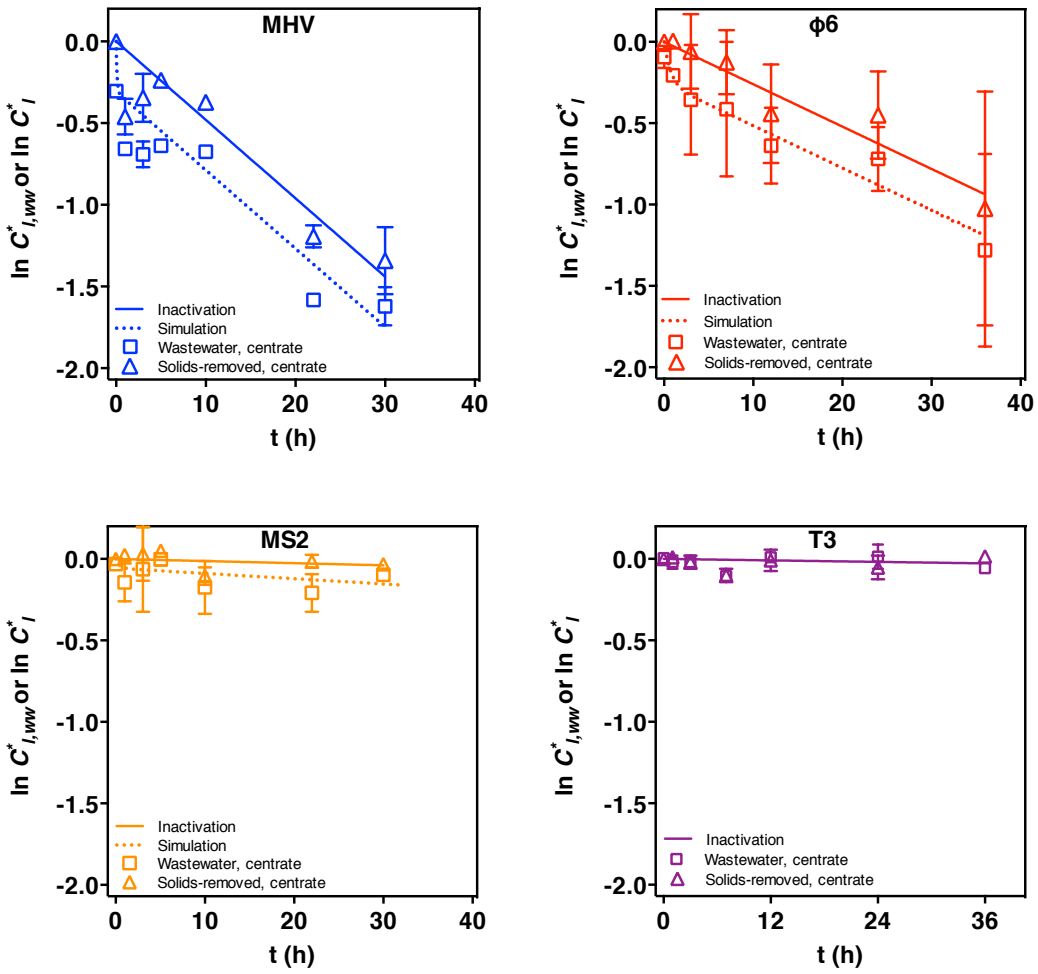

Figure 2.2 Adsorption and inactivation kinetics and model simulations for enveloped viruses (MHV and Phi6) and nonenveloped viruses (MS2 and T3) in 4 °C wastewater. Viruses were spiked into wastewater and solids-removed wastewater samples to final concentrations of 5 × 10^4 PFU mL^{-1} for MHV, and 6—8 × 10^5 PFU mL^{-1} for MS2, T3 and Phi6. $\boldsymbol{C_l^*}$ and $\boldsymbol{C_{l,ww}^*}$ are nondimensional concentrations of infective viruses in the solids-removed sample centrates and wastewater sample centrates, respectively. Both values were normalized to the initial measured virus concentration in the solids-removed sample centrates. No significant decline in T3 infectivity was observed within 36 hours. Error bars represent the range of data from duplicate experiments conducted in wastewater samples collected on different days (n = 2).

Based on these results, the MHV and Phi6 sorption kinetics can be best described by a non-instantaneous quasi-equilibrium adsorption model in which the virus sorption to wastewater solids does not occur instantaneously and the inactivation rates in the wastewater solid and liquid phases are equal (Table A-4). A similar model was used to describe bacteriophage λ sorption kinetics with sand.[38] In comparison, MS2 behavior is best described by the non-instantaneous quasi-equilibrium adsorption and surface sink model. In this model, virus inactivation is faster in the solid phase than in the liquid phase (Table A-4); a similar model was proposed for the interaction of bacteriophage MS2 and PRD1 with sediments.[49] Bacteriophage T3 could not be modeled due to the non-significant decreases in infective viruses measured over the experiment timescale.

These models predict that 26% of MHV, 22% of Phi6, and 6% of MS2 adsorbed to wastewater solids at equilibrium (Figure 2.3; Table A-4). Although the T3 virus kinetics could not be modeled, < 5% of the spiked T3 had partitioned to the wastewater solids at the end of the 36-hour experiment; this suggests that like MS2, T3 partitions overwhelmingly to the liquid fraction of wastewater (Figure 2.2). The equilibrium percentages reported here are not representative for all wastewaters because wastewater solids concentrations vary widely. It should be noted that our wastewater solid concentrations were typical for medium-strength municipal wastewaters[37] (Table A-1) with an average TSS value of 235 mg L^{-1}.

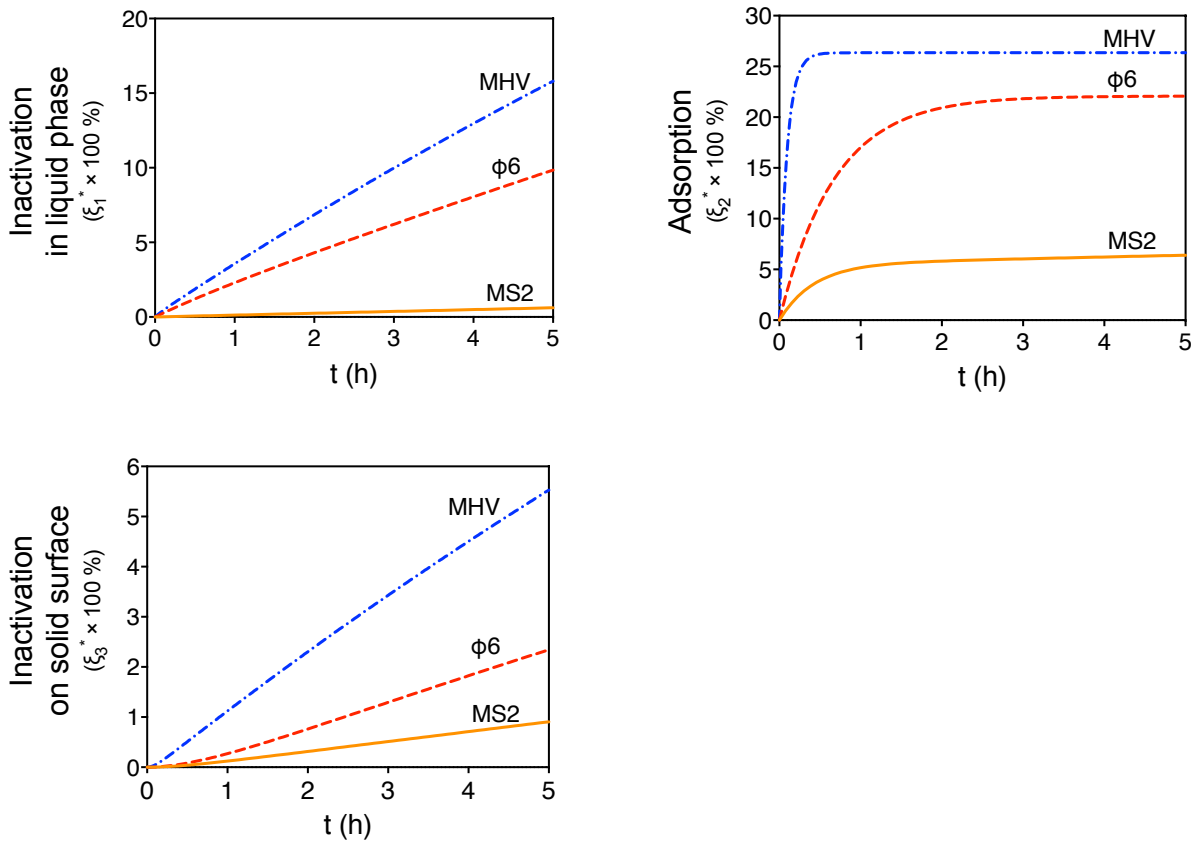

Figure 2.3 Models for adsorption and inactivation kinetics of enveloped viruses (MHV and Phi6) and nonenveloped viruses (MS2) in 4 °C wastewater. $\boldsymbol{\xi_1^*}$ represents the fraction of viruses inactivated in liquid fraction of wastewater; $\boldsymbol{\xi_2^*}$ represents the fraction of viruses reversibly adsorbed to wastewater solids; $\boldsymbol{\xi_3^*}$ represents the fraction of viruses inactivated on the solid surface.

The partitioning results for MS2 and T3 are consistent with an early observation that wastewater solids are poor at absorbing enteric viruses.[50] Wastewater solids tend to be negatively charged, as is MS2 (isoelectric point = 3.9). The isoelectric point for T3 has not been reported, but the similar T2 and T4 viruses have isoelectric points < 6.[51] A study on the adsorption of four nonenveloped viruses to various solid surfaces demonstrated that long-ranged electrostatic interactions and hydrophobic effects between the virus capsid proteins and the sorbent surfaces dictated adsorption, with short-ranged van der Waals and steric interactions playing less important

roles.[52] Similar work has not been conducted for enveloped viruses, and the impact that the surface phospholipids and various membrane proteins have on partitioning remains elusive.

Despite the poor sorption of nonenveloped enteric viruses to wastewater solids, some enteric viruses have been observed in primary settled solids in high concentrations.[36,53] In such cases, the viruses were likely released into wastewater within or strongly associated with fecal solids and never reached equilibrium between the liquid and solid fractions. When excreted in watery diarrhea or urine, the viruses would more likely reach equilibrium. Our results suggest that if allowed to reach equilibrium, enveloped viruses more strongly associate with wastewater solids than nonenveloped viruses. Consequently, enveloped viruses would be removed to a greater extent than nonenveloped viruses in primary wastewater treatment. More enveloped and nonenveloped viruses will need to be tested to confirm the results obtained with the two enveloped and two nonenveloped model viruses.

In addition to relaying information on virus partitioning between solid and liquid phases at equilibrium, the models also predicted the amount of time it takes for the viruses to reach equilibrium. This information is important for virus recovery experiments, where viruses are spiked into an environmental sample and then extracted and quantified with various techniques. If the spiked viruses are extracted too soon, results may be biased due to the spiked viruses in liquid phase. In water with soils and clays, nonenveloped virus adsorption is assumed to reach equilibrium within an hour.[54] Our models estimated that the viruses in wastewater reached 90% of equilibrium concentrations after 0.3—1.5 hours, and 99% of equilibrium concentrations after 0.4—2.9 hours (Figure 2.3; Table A-4). Based on these results, we allowed samples to equilibrate for at least one hour before extraction methods were tested.

2.3.3 Virus recovery from wastewater.

According to the simulation results of virus partitioning, greater than 70% of the infective model enveloped viruses were associated with wastewater liquids at equilibrium. We therefore focused primarily on the wastewater liquid fraction in our virus recovery experiments. Of the three methods we tested, the ultrafiltration method and the PEG precipitation methods involved an initial step to remove wastewater solids and then focused on recovering the viruses in the liquid phase. The ultracentrifugation method, on the other hand, involved pelleting all of the wastewater solids and colloids and then extracting the viruses from the pellet.

The enveloped MHV recoveries were consistently lower than the nonenveloped MS2 recoveries when the PEG precipitation and ultrafiltration methods were applied (Figure 2.4); this was not unexpected given that MHV partitioned to solids to a greater extent than the MS2. Low mean recoveries (< 6%) were achieved for both MS2 and MHV with the ultracentrifugation method (Figure 2.4). The ultrafiltration method resulted in significantly higher MHV recoveries than the PEG precipitation ($P = 0.0065$) and the ultracentrifugation ($P = 0.0084$) methods. MS2 recoveries with the ultrafiltration method were significantly higher than ultracentrifugation ($p=0.0074$), but not significantly different than PEG precipitation ($P = 0.4137$) method (Figure 2.4).

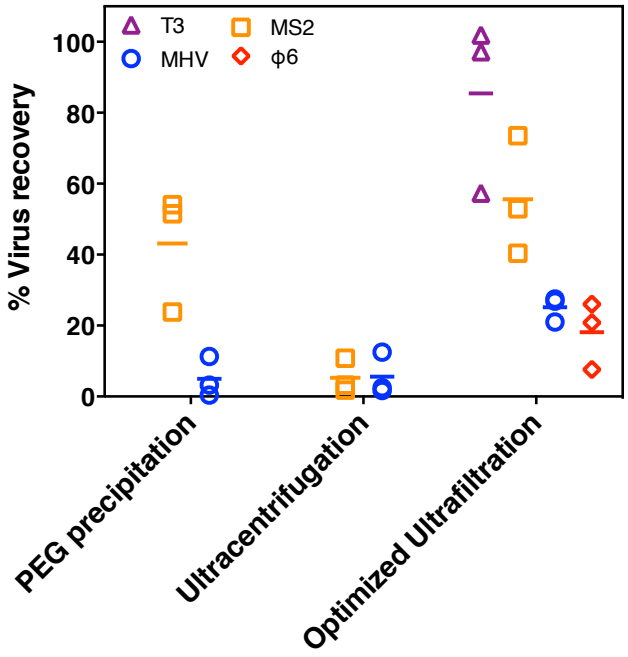

Figure 2.4 Recoveries for enveloped and nonenveloped viruses from wastewater with PEG precipitation, ultracentrifugation, and optimized ultrafiltration method. Viruses were spiked into wastewater samples to final concentrations of 8×10^3 PFU mL^{-1} for MHV, and $2—5 \times 10^5$ PFU mL^{-1} for MS2, T3 and Phi6.

Additional experiments suggested that incubation with PEG caused a major drop in infective MHV. The T_{90} for MHV in wastewater with PEG was 16 hours compared to 40 hours in wastewater without PEG (Figure A-2). The enveloped influenza viruses were previously recovered from surface waters with the PEG method,[55] but recoveries were very low (0.2%—0.6%). The low recoveries for MHV and influenza with PEG may be due to disruption of their lipid bilayers.[56] Meanwhile, the MS2 recovery obtained here with the PEG method (43.1 ± 16.8%) was comparable to the recovery of nonenveloped *Echovirus* 7 from raw wastewater (78.5 ± 11.0%).[57] These results suggest that PEG precipitation method, which is effective at recovering infective nonenveloped viruses from water samples, is not optimal for recovering infective enveloped viruses.

In the ultracentrifugation method, the initial centrifugation (100,000 × g for 1 h) step did not effectively pellet bacteriophage MS2, and 63% of the spiked MS2 was detected in the centrate. Comparatively, only 1% of the spiked MHV was detected in the centrate. Previously, the ultracentrifugation method was successful at recovering rotavirus genes from raw wastewater (47% mean recovery), but the infectivity state of the recovered viruses was not tested.[19] Our low recovery of infective MHV viruses in the pellet may be due to virus inactivation by the large ultracentrifuge forces.[58] Taken together, this suggests that pelleting wastewater solids with ultracentrifugation may be effective at recovering enveloped viruses genes for qPCR detection, but not appropriate when infective viruses are desired.

Additional experiments were conducted to optimize recoveries with the ultrafiltration method (description in Appendix A; Figure A-3). The optimized method involves pre-filtering 250 mL of wastewater through a 0.22 μm PES membrane to remove solids, followed by concentration of the filtrate with 10 kDa centrifugal filters to a final volume of 2.5 mL. Using this method, we achieved mean virus recoveries of 25.1% for MHV, 18.2% for Phi6, 55.6% for MS2, and 85.5% for T3 (Figure 2.4). Ultrafiltration methods have been successfully applied for recovering nonenveloped enteric viruses from wastewater, such as polioviruses, adenoviruses, noroviruses, and enteroviruses.[18,41] Here, we have demonstrated that the method can also be optimized for recovering enveloped viruses. In future work, we will test hollow fiber ultrafilters and tangential flow ultrafiltration to potentially increase wastewater sample volumes that can be processed, and thus decrease the detection limits of infective enveloped viruses in wastewater.

2.3.4 Environmental Implications.

Our results shed light on the behavior of enveloped viruses in wastewater and provide guidance on how to recover infective enveloped viruses from raw wastewater. Although the two model enveloped viruses were more rapidly inactivated in wastewater, they did survive long enough to be of concern for wastewater treatment facilities, stormwater overflow events, and wastewater intrusion in drinking water. The results presented here will be particularly important during potential future avian influenza or coronavirus outbreaks in humans, as some strains of these viruses can be excreted in feces. Future work should examine additional enveloped viruses to elucidate the specific virus characteristics that contribute to their survival times and enhanced partitioning to solids.

2.4 References

(1) Bausch, D. G.; Towner, J. S.; Dowell, S. F.; Kaducu, F.; Lukwiya, M.; Sanchez, A.; Nichol, S. T.; Ksiazek, T. G.; Rollin, P. E. Assessment of the risk of Ebola virus transmission from bodily fluids and fomites. *J. Infect. Dis.* **2007**, *196*, 142–147.

(2) Couch, R. B.; Cate, T. R.; Douglas, R. G., Jr; Gerone, P. J.; Knight, V. Effect of route of inoculation on experimental respiratory viral disease in volunteers and evidence for airborne transmission. *Bacteriol. Rev.* **1966**, *30* (3), 517–529.

(3) Jevšnik, M.; Steyer, A.; Zrim, T.; Pokorn, M. Detection of human coronaviruses in simultaneously collected stool samples and nasopharyngeal swabs from hospitalized children with acute gastroenteritis. *Virol. J.* **2013**, *10*, 46–52.

(4) Poon, L. L. M.; Chan, K. H.; Wong, O. K.; Cheung, T. K. W.; Ng, I.; Zheng, B.; Seto, W. H.; Yuen, K. Y.; Guan, Y.; Peiris, J. S. M. Detection of SARS coronavirus in patients with severe acute respiratory syndrome by conventional and real-time quantitative reverse transcription-PCR assays. *Clin. Chem.* **2004**, *50* (1), 67–72.

(5) To, K. K. W.; Chan, K. H.; Li, I. W. S.; Tsang, T. Y.; Tse, H.; Chan, J. F. W.; Hung, I. F. N.; Lai, S. T.; Leung, C. W.; Kwan, Y. W.; et al. Viral load in patients infected with pandemic H1N1 2009 influenza A virus. *J. Med. Virol.* **2010**, *82* (1), 1–7.

(6) Esper, F.; Ou, Z.; Huang, Y. T. Human coronaviruses are uncommon in patients with gastrointestinal illness. *J. Clin. Virol.* **2010**, *48*, 131–133.

(7) Arena, C.; Amoros, J. P.; Vaillant, V.; Balay, K.; Chikhi-Brachet, R.; Varesi, L.; Arrighi, J.; Blanchon, T.; Carrat, F.; Hanslik, T.; et al. Simutaneous investigation of influenza and enteric viruses in the stools of adult patients consulting in general practice for acute diarrhea. *Virology* **2012**, *116* (9), 1–8.

(8) Chan, K. H.; Poon, L. L. L. M.; Cheng, V. C. C.; Guan, Y.; Hung, I. F. N.; Kong, J.; Yam, L. Y. C.; Seto, W. H.; Yuen, K. Y.; Peiris, J. S. M. Detection of SARS coronavirus in patients with suspected SARS. *Emerg. Infect. Dis.* **2004**, *10* (2), 294–299.

(9) Metcalf, T. G.; Metcalf, T. G.; Melnick, J. L.; Melnick, J. L.; Estes, M. K.; Estes, M. K. Environmental virology: from detection of virus in sewage and water by isolation to identification by molecular biology-A trip of over 50 years. *Annu Rev Microbiol* **1995**, *49* (1), 461–487.

(10) Bibby, K.; Peccia, J. Identification of viral pathogen diversity in sewage sludge by metagenome analysis. *Environ. Sci. Technol.* **2013**, *47* (4), 1945–1951.

(11) Casanova, L.; Casanova, L.; Rutala, W. A.; Rutala, W. A.; Weber, D. J.; Weber, D. J.; Sobsey, M. D.; Sobsey, M. D. Survival of surrogate coronaviruses in water. *Water Res.* **2009**, *43* (7), 1893–1898.

(12) Bibby, K.; Bibby, K.; Fischer, R.; Fischer, R.; Casson, L.; Casson, L.; Stachler, E.; Stachler, E. Persistence of Ebola virus in sterilized wastewater. *Environ. Sci. Technol. Lett.* **2015**, *2*, 245–249.

(13) Casanova, L. M.; Weaver, S. R. Inactivation of an enveloped surrogate virus in human sewage. *Environ. Sci. Technol. Lett.* **2015**, *2*, 76–78.

(14) Wigginton, K. R.; Ye, Y.; Ellenberg, R. M. Emerging investigators series: the source and fate of pandemic viruses in the urban water cycle. *Environ. Sci.: Water Res. Technol.* **2015**, *1*, 735–746.

(15) Yu, I. T. S.; Li, Y.; Wong, T. W.; Tam, W.; Chan, A. T.; Lee, J. H. W.; Leung, D. Y. C.; Ho, T. Evidence of airborne transmission of the severe acute respiratory syndrome virus. *N. Engl. J. Med.* **2004**, *350*, 1731–1739.

(16) Puig, M.; Jofre, J.; Lucena, F.; Allard, A. Detection of adenoviruses and enteroviruses in polluted waters by nested PCR amplification. *Appl. Environ. Microbiol.* **1994**, *60* (8), 2963–2970.

(17) Girones, R.; Puig, M.; Allard, A.; Lucena, F.; Wadell, G.; Jofre, J. Detection of adenovirus and enterovirus by PCR amplification in polluted waters. *Water Sci. Technol.* **1995**, *31* (5), 351–357.

(18) Katayama, H.; Haramoto, E.; Oguma, K.; Yamashita, H.; Tajima, A.; Nakajima, H.; Ohgaki, S. One-year monthly quantitative survey of noroviruses, enteroviruses, and adenoviruses in wastewater collected from six plants in Japan. *Water Res.* **2008**, *42*, 1441–1448.

(19) Fumian, T. M.; Leite, J. P. G.; Castello, A. A.; Gaggero, A.; Caillou, M. S. L. de; Miagostovich, M. P. Detection of rotavirus A in sewage samples using multiplex qPCR and an evaluation of the ultracentrifugation and adsorption-elution methods for virus concentration. *J. Virol. Methods* **2010**, *170*, 42–46.

(20) Tambini, G.; Andrus, J. K.; Marques, E. Direct detection of wild poliovirus circulation by stool surveys of healthy children and analysis of community wastewater. *Journal of Infection* **1993**, *168* (6), 1510–1514.

(21) Lago, P. M.; Gary, H. E., Jr; Perez, L. S.; Caceres, V.; Olivera, J. B.; Puentes, R. P.; Corredor, M. B.; Jimenez, P.; Pallansch, M. A.; Cruz, R. G. Poliovirus detection in wastewater and stools following an immunization campaign in Havana, Cuba. *Int. J. Epidemiol.* **2003**, *32* (5), 772–777.

(22) Arbely, E.; Granot, Z.; Kass, I.; Orly, J.; Arkin, I. T. A trimerizing GxxxG motif is uniquely inserted in the severe acute respiratory syndrome (SARS) coronavirus spike

protein transmembrane domain. *Biochemistry* **2006**, *45* (38), 11349–11356.
(23) Shigematsu, S.; Dublineau, A.; Sawoo, O.; Batéjat, C.; Matsuyama, T.; Leclercq, I.; Manuguerra, J. Influenza A virus survival in water is influenced by the origin species of the host cell. *Influenza Other Respi Viruses* **2013**, *8* (1), 123–130.
(24) Gundy, P. M.; Gerba, C. P.; Pepper, I. L. Survival of coronaviruses in water and wastewater. *Food Environ Virol* **2009**, *1*, 10–14.
(25) van der Hoek, L.; Pyrc, K.; Jebbink, M. F.; Vermeulen-Oost, W.; Berkhout, R. J. M.; Wolthers, K. C.; Wertheim-van Dillen, P. M. E.; Kaandorp, J.; Spaargaren, J.; Berkhout, B. Identification of a new human coronavirus. *Nat. Med.* **2004**, *10* (4), 368–373.
(26) Vidaver, A. K.; Koski, R. K.; Van Etten, J. L. Bacteriophage ϕ6: A lipid-containing virus of Pseudomonas phaseolicola. *J. Virol.* **1973**, *11* (5), 799–805.
(27) Clescerl, L. S., Greenberg, A. E., Eaton, A. D., Eds. *Standard Methods for Examination of Water & Wastewater*, 20th, ed.; American Public Health Assocaition: Washington, DC, 1998.
(28) Turgeon, N.; Toulouse, M.-J.; Martel, B.; Moineau, S.; Duchaine, C. Comparison of five bacteriophages as models for viral aerosol studies. *Appl. Environ. Microbiol.* **2014**, *80*, 4242–4250.
(29) Periasamy, D.; Sundaram, A. A novel approach for pathogen reduction in wastewater treatment. *J. Environ. Health Sci. Eng.* **2013**, *11*, 1–9.
(30) Blaise-Boisseau, S.; Hennechart-Collette, C.; Guillier, L.; Perelle, S. Duplex real-time qRT-PCR for the detection of hepatitis A virus in water and raspberries using the MS2 bacteriophage as a process control. *J. Virol. Methods* **2010**, *166*, 48–53.
(31) Hill, V. R.; Kahler, A. M.; Jothikumar, N.; Johnson, T. B.; Hahn, D.; Cromeans, T. L. Multistate evaluation of an ultrafiltration-based procedure for simultaneous recovery of enteric microbes in 100-Liter tap water samples. *Appl. Environ. Microbiol.* **2007**, *73*, 4218–4225.
(32) Leibowitz, J.; Kaufman, G.; Liu, P. Coronaviruses: propagation, quantification, storage, and construction of recombinant mouse hepatitis virus. *Curr. Protoc. Microbiol* **2011**, *21* (15E.1), 1–52.
(33) Daugelavicius, R.; Cvirkaite, V.; Gaidelyte, A.; Bakiene, E.; Gabrenaite-Verkhovskaya, R.; Bamford, D. H. Penetration of enveloped double-stranded RNA bacteriophages φ13 and φ6 into Pseudomonas syringae cells. *J. Virol.* **2005**, *79*, 5017–5026.
(34) Pecson, B. M.; Martin, L. V.; Kohn, T. Quantitative PCR for determining the infectivity of bacteriophage MS2 upon inactivation by heat, UV-B radiation, and singlet oxygen: Advantages and limitations of an enzymatic treatment to reduce false-positive results. *Appl. Environ. Microbiol.* **2009**, *75*, 5544–5554.
(35) *Environmental protection agency method 1601: male-specific (f+) and somatic coliphage in water by two-step*; United States Environmental Protection Agency: Washington, DC, 2001; http://www.epa.gov/sites/production/files/2015-12/documents/method_1601_2001.pdf.
(36) Hejkal, T. W.; Wellings, F. M.; Lewis, A. L.; Larock, P. A. Distribution of viruses associated with particles in wastewater. *Appl. Environ. Microbiol.* **1981**, *41* (3), 628–634.
(37) Tchobanoglous, G.; Burton, F. L.; Stensel, H. D. *Wastewater Engineering: Treatment and Reuse*, 4th ed.; McGraw-Hill Higher Education, 2003.
(38) Grant, S. B.; List, E. J.; Lidstrom, M. E. Kinetic analysis of virus adsorption and inactivation in batch experiments. *Water Resour. Res.* **1993**, *29* (7), 2067–2085.

(39) Lewis, G. D.; Metcalf, T. G. Polyethylene glycol precipitation for recovery of pathogenic viruses, including hepatitis A virus and human rotavirus, from oyster, water, and sediment samples. *Appl. Environ. Microbiol.* **1988**, *54* (8), 1983–1988.
(40) Masclaux, F. G.; Masclaux, F. G.; Hotz, P.; Hotz, P.; Friedli, D.; Friedli, D.; Savova-Bianchi, D.; Savova-Bianchi, D.; Oppliger, A.; Oppliger, A. High occurrence of hepatitis E virus in samples from wastewater treatment plants in Switzerland and comparison with other enteric viruses. *Water Res.* **2013**, *47* (14), 5101–5109.
(41) Haramoto, E.; Katayama, H.; Oguma, K.; Yamashita, H.; Nakajima, E.; Ohgaki, S. One-year monthly monitoring of Torque teno virus (TTV) in wastewater treatment plants in Japan. *Water Res.* **2005**, *39*, 2008–2013.
(42) Sturman, L. S.; Ricard, C. S.; Holmes, K. V. Conformational change of the coronavirus peplomer glycoprotein at pH 8.0 and 37 degrees C correlates with virus aggregation and virus-induced cell fusion. *J. Virol.* **1990**, *64* (6), 3042–3050.
(43) Pocock, D. H.; Garwes, D. J. The influence of pH on the growth and stability of transmissible gastroenteritis virusin vitro. *Arch Virol* **1975**, *49* (2-3), 239–247.
(44) Lamarre, A.; Talbot, P. J. Effect of pH and temperature on the infectivity of human coronavirus 229E. *Can. J. Microbiol.* **1989**, *35*, 972–974.
(45) Jończyk, E.; Kłak, M.; Międzybrodzki, R.; Górski, A. The influence of external factors on bacteriophages—review. *Folia Microbiol* **2011**, *56* (3), 191–200.
(46) Hurst, C. J.; Gerba, C. P.; Cech, I. Effects of environmental variables and soil characteristics on virus survival in soil. *Appl. Environ. Microbiol.* **1980**, *40* (6), 1067–1079.
(47) Ward, R. L.; Knowlton, D. R.; Winston, P. E. Mechanism of inactivation of enteric viruses in fresh water. *Appl. Environ. Microbiol.* **1986**, *52* (3), 450–459.
(48) Kim, T.-D.; Unno, H. The roles of microbes in the removal and inactivation of viruses in a biological wastewater treatment system. *Water Sci. Technol.* **1996**, *33*, 243–250.
(49) Ryan, J. N.; Harvey, R. W.; Metge, D.; Elimelech, M.; Navigato, T.; Pieper, A. P. Field and laboratory investigations of inactivation of viruses (PRD1 and MS2) attached to iron oxide-coated quartz sand. *Environ. Sci. Technol.* **2002**, *36* (11), 2403–2413.
(50) Clarke, N. A.; Stevenson, R. E.; Chang, S. L.; Kabler, P. W. Removal of enteric viruses from sewage by activated sludge treatment. *Am. J. Public Health* **1961**, *51*, 1118–1129.
(51) Michen, B.; Graule, T. Isoelectric points of viruses. *J Appl Microbiol* **2010**, *109*, 388–397.
(52) Armanious, A.; Aeppli, M.; Jacak, R.; Refardt, D.; Sigstam, T.; Kohn, T.; Sander, M. Viruses at solid–water interfaces: A systematic assessment of interactions driving adsorption. *Environ. Sci. Technol.* **2016**, *50* (2), 732–743.
(53) Wellings, F. M.; Lewis, A. L.; Mountain, C. W. Demonstration of solids-associated virus in wastewater and sludge. *Appl. Environ. Microbiol.* **1976**, *31* (3), 354–358.
(54) Moore, R. S.; Taylor, D. H.; Sturman, L. S. Poliovirus adsorption by 34 minerals and soils. *Appl. Environ. Microbiol.* **1981**, *42* (6), 963–975.
(55) Deboosere, N.; Horm, S. V.; Pinon, A.; Gachet, J.; Coldefy, C.; Buchy, P.; Vialette, M. Development and validation of a concentration method for the detection of influenza A viruses from large volumes of surface water. *Appl. Environ. Microbiol.* **2011**, *77* (11), 3802–3808.
(56) Boni, L. T.; Stewart, T. P.; Alderfer, J. L.; Hui, S. W. Lipid-polyethylene glycol interactions: II. Formation of defects in bilayers. *J. Membrane Biol.* **1981**, *62*, 71–77.
(57) Amdiouni, H.; Maunula, L.; Hajjami, K.; Faouzi, A.; Soukri, A.; Nourlil, J. Recovery

comparison of two virus concentration methods from wastewater using cell culture and real-time PCR. *Curr. Microbiol.* **2012**, *65* (4), 432–437.

(58) Lawrence, J. E.; Steward, G. F. Purification of viruses by centrifugation. In *Manual of Aquatic viral ecology*; Wilhelm, S. W., Weinbauer M. G., Suttle, C. A., Eds.; American Society of Limnology and Oceanography: Waco 2010; pp 166–181.

Chapter 3 Reactivity of enveloped virus genome, proteins, and lipids with free chlorine and UV_{254}

Reprinted with permission from Yinyin Ye, Pin Hsuan Chang, John Hartert, and Krista R. Wigginton, Reactivity of Enveloped Virus Genome, Proteins, and Lipids with Free Chlorine and UV_{254}, *Environmental Science & Technology*, **2018**, *52*, 7698– 7708, © 2018 American Chemical Society.

3.1 Introduction

Viruses that are transmitted through direct person-to-person contact or in large respiratory droplets do not typically survive for very long outside of their host in the environment.[1] On the other hand, viruses that are transmitted through aerosols or by contact with water, food, and solid surfaces tend to survive longer in order to come into contact with their next host.[2,3] Survivability, often reported as the time necessary for 90% of a population to lose infectivity (T_{90}), can therefore vary widely amongst different viruses, and depends on environmental conditions including temperature,[4-6] relative humidity,[4-9] UV radiation,[10-12] and oxidants.[13-15] Survivability is also impacted by virus structures. Nonenveloped viruses are generally considered more stable than enveloped viruses in the environment. For example, the T_{90} values for nonenveloped viruses in wastewater range from days to months, whereas the T_{90} values for enveloped viruses range from several hours to days.[16-18] In terms of susceptibility to chemical disinfectants, the enveloped Ebola and Phi6 viruses experience higher levels of inactivation than the nonenveloped MS2 and M13 viruses when exposed to 0.5% NaOCl.[19] Even closely related enveloped viruses can have varied

survivabilities. For example, the T_{90} of severe acute respiratory syndrome (SARS) coronavirus in serum-free culture media is 9 days, whereas the T_{90} of human coronavirus 229E is less than 1 day under the same conditions.[20] The mechanistic reasons for the higher susceptibility of enveloped viruses to inactivation in aqueous environments are mostly unknown.

Despite their greater susceptibility to environmental conditions, many enveloped viruses do undergo environmental transmission. SARS coronaviruses were transmitted through airflow and virus-laden fecal aerosols.[21,22] Human influenza viruses retain their infectivity on the nonporous surfaces, increasing their chances to infect.[23,24] Avian influenza viruses are shed into water, where they can survive months before being consumed by their next host.[25,26] Porcine reproductive and respiratory syndrome viruses can travel several kilometers via aerosols, spreading swine diseases from farm to farm.[27] Infectious Ebola viruses persist in patient blood, feces and urine, and can survive in liquid for several days; however, an environmental transmission route has been observed.[3,28]

Research on what makes enveloped viruses more or less persistent in the environment and through disinfection processes could help with predicting risks posed by newly emerging viruses that are difficult or dangerous to culture. For example, in the recent Ebola outbreak, a mechanistic understanding of enveloped virus inactivation would have helped scientists predict how long Ebola virus remained infective in wastewater, blood, and vomit.[29] Comprehensive inactivation mechanisms have been published for a limited number of nonenveloped viruses with disinfectants,[12,15,30,31] but are lacking for enveloped viruses. In general, UV radiation targets nonenveloped virus genomes, whereas chemical oxidants inactivate nonenveloped viruses by genome or protein reactions, depending on the virus and oxidant.

Recent fate and survival studies of enveloped viruses in the environment have adopted *Pseudomonas* virus Phi6 as a model enveloped virus.[17,32-36] Phi6 is a double stranded RNA virus. The Phi6 particle is 85 nm in diameter[37] and contains 11 different viral proteins.[38] Like influenza viruses, Phi6 is enveloped, has a segmented genome, and contains glycerophospholipids in its envelope.[39,40] In addition, it is the best studied virus in the family *Cystoviridae*, which includes the only bacteriophages that have a lipid outer layer. Moreover, Phi6 is easier to work with than other enveloped viruses and can be propagated to high titers.

To develop a better mechanistic understanding of enveloped virus inactivation, we employed Phi6 in an initial investigation of enveloped virus reactivity with chemical oxidants and UV radiation. We characterized the biomolecule reactions in Phi6 following exposure to free chlorine and UV_{254}. Phi6 inactivation, genome reactions, and protein and lipid reactions were quantified with plaque assays, real-time reverse transcription polymerase chain reactions (RT-qPCR), and liquid chromatography-tandem mass spectrometry (LC-MS/MS), respectively. We compared the reaction rate constants of the Phi6 genome and proteins to those of nonenveloped viruses reported in earlier studies and measured under similar experimental conditions to elucidate the molecular features that may impact enveloped virus persistence in aqueous environments.

3.2 Materials and methods

3.2.1 Virus propagation and purification

Phi6 and its bacterial host *Pseudomonas syringae* pv. phaseolicola were kindly provided by Dr. Linsey Marr's lab at Virginia Tech. To propagate Phi6, *P. syringae* was grown in Luria-Bertani (LB) medium containing 5 g L^{-1} NaCl at 26 °C and 180 rpm to an optical density of 0.10 at 640 nm (i.e., when the cell density was approximately 1.8×10^8 cells mL^{-1}). At that point, Phi6 was

added to the bacteria at a multiplicity of infection equal to 2 (i.e., ratio of Phi6 plaque-forming units (PFU) to *P. syringae* colony forming units (CFU)), and then incubated under the same conditions for 7 to 9 hours. Cells and debris were removed from the virus suspension by filtering it through 0.22 μm polyethersulfone (PES, Millipore) membranes.

The filtered virus suspensions (~1 L) were concentrated to approximately 20 mL (i.e., ~50× concentration) in a lab-scale tangential flow filtration system (Millipore) outfitted with a 30 kDa cellulous filter. The concentrate was purified in a 10-40% (w/v) step sucrose gradient (average 65,700 × g, 1.5 h, 4 °C), then in a 40-60% (w/v) linear sucrose gradient (average 65,700 × g, 15 h, 4 °C). The phage band was collected with a needle and the buffer was exchanged for 5 mM phosphate buffer (PBS; 10 mM NaCl, pH 7.4) with a 100 kDa Amicon Ultra-15 centrifugal filter (Millipore). Virus purity was confirmed by SDS-PAGE with 8-16% TGX™ precast protein gels (Bio-Rad), according to the manufacturer's instructions (Figure B-1). The final Phi6 stocks (10^{12} PFU mL^{-1}) were filter-sterilized with 0.22 μm PES membranes, aliquoted, and stored at -80 °C until use.

3.2.2 Free chlorine and UV_{254} experiments

Experimental virus solutions were prepared by diluting Phi6 in PBS. All free chlorine and UV_{254} experiments were conducted at room temperature. Infectious virus concentrations (PFU mL^{-1}) were measured immediately before and after the viruses were exposed to chlorine and UV_{254} via plaque assays on LB agar plates.[41] Samples were stored on ice during the plaque assays. Following free chlorine and UV treatment, samples were immediately stored at -80 °C prior to nucleic acid, protein, and lipid analyses.

Free chlorine experiments. Free chlorine was prepared by diluting NaClO stock solution (Sigma-Aldrich) in PBS. At pH 7.4, HOCl and OCl^- are equal in molar concentrations. Free chlorine disinfection was conducted in a modified continuous quench-flow system that was described previously for ozone reactions (Figure B-2).[42] In brief, free chlorine and Phi6 solutions were continuously mixed in a PEEK micro static mixing tee (IDEX Health & Science) at flow rates of 0.125 mL min^{-1} each to reach initial reaction conditions of 2 mg L^{-1} free chlorine as Cl_2 and 4-5 × 10^{10} PFU mL^{-1} Phi6. The reacting mixture then passed through sample loops with varied volumes to reach contact times of 0.3, 0.6, 2, 4, 8 and 11 s. The reactions were quenched with 550 mM Tris-HCl (pH 7.4) at a flow rate of 0.025 mL min^{-1}. Control experiments demonstrated that the addition of Tris-HCl as a quenching agent for free chlorine effectively halted Phi6 inactivation (Figure B-3). Approximately 2.4 mL of the quenched samples were collected for nucleic acid, protein, and lipid analyses. After each experiment, the quench-flow system was thoroughly rinsed with chlorine-demand-free water. Free chlorine concentrations in reaction solutions were measured with the *N*,*N*-diethyl-*p*-phenylenediamine (DPD) ferrous titrimetric method and the DPD colorimetric method according to the standard method.[43] The percentage of free chlorine consumed through the experiments was kept below 20% in order to maintain pseudo-first order conditions. Negative controls for the free chlorine experiments were run in the continuous quench-flow system in the same manner as the free chlorine samples, but with PBS rather than free chlorine.

UV_{254} experiments. The UV_{254} experimental solutions consisted of 2.4 mL of Phi6 (4-5 × 10^{10} PFU mL^{-1}) in PBS continuously stirred in 10 mL glass beakers. Samples were exposed to UV_{254} in a collimated beam reactor[44] with 0.16 mW cm^{-2} lamps (model G15T8, Philips) that were regularly measured with chemical actinometry.[45] The average UV_{254} intensity was corrected based on the

solution absorbance at UV_{254} and the sample depth. After correcting for shielding, the UV_{254} intensity was 0.14 mW cm^{-2}. Samples were exposed to UV_{254} for 0, 5, 15, and 25 min, which corresponded to UV_{254} doses of 0, 42, 130, 210 mJ cm^{-2}. Negative controls for the UV_{254} experiments were prepared in the same manner as the experimental samples, but were stirred in dark to capture any background virus inactivation and biomolecule reactions.

Virus inactivation kinetics by free chlorine and UV_{254} were calculated based on the Chick-Watson model:[46]

$$\ln\left(\frac{C}{C_0}\right) = -kD$$

where C is the infectious titer (PFU mL^{-1}), C_0 is the initial infectious titer (PFU mL^{-1}), k is the inactivation rate constant (L mg^{-1} s^{-1} or cm^2 mJ^{-1}), and D is the free chlorine concentration (mg L^{-1}) × contact time (s) or UV dose (mJ cm^{-2}).

3.2.3 RT-qPCR assays.

Following the UV_{254} and free chlorine reactions, the viral genomes were extracted by QIAamp viral RNA mini kits (Qiagen). The Phi6 dsRNA genome consists of three segments designated as small (S), medium (M), and large (L) based on their relative sizes. Three primer sets for the Phi6 genome were designed and tested individually, each targeting a different genome segment. The sum of the three amplicons (~1500 bp) covered approximately 10.5% of the Phi6 genome (Table B-1). The extracted viral genomes were mixed with 10 mM forward primer and 10 mM reverse primer at a ratio of 10:1.5:1.5 (v/v/v) in Tris-EDTA buffer (10 mM Tris-HCl, 0.1 mM EDTA, pH 7.7), and then heated at 99 °C for 5 min, and quickly chilled on ice for 5 min before mixing with RT-qPCR reagents. RT-qPCR reactions were prepared in 96-well plates (Eppendorf) and

conducted in duplicates on a Mastercycler ep RealPlex 2 system (Eppendorf) with Gotaq OneStep RT-qPCR kits (Promega). The 20-μL RT-qPCR reactions consisted of 10 μL 2× qPCR master mix, 0.4 μL 50× RT mix, 5.2 μL template-primer mixture, 4 μL 5 M Betaine (Sigma-Aldrich), and 0.4 μL nuclease-free water. The RT reaction was conducted at 40 °C for 15 min, followed by an initial PCR activation step at 95 °C for 10 min. The PCR reaction included 40 cycles of DNA denaturation at 95 °C for 15 s, primer annealing at 59 °C for 30 s, and extension at 72 °C for 40 s. Melting curves were conducted by increasing the temperature from 60 °C to 95 °C over 10 min. RNA standards used for the RT-qPCR calibration curves consisted of Phi6 genomes extracted from the purified stock and quantified with a Qubit Fluorometer 2.0 (ThermoFisher Scientific). The amplification efficiencies (mean ± standard deviation) of RT-qPCR reactions targeting S, M, and L genome segment were 0.82 ± 0.10, 0.81 ± 0.05, and 0.81 ± 0.07, respectively. The mean R^2 were ≥ 0.99. The reaction kinetics of RT-qPCR target regions were modeled with first-order reactions:

$$\ln\left(\frac{N_i}{N_{0,i}}\right) = -k_{g,i}D$$

The reactions of the whole genome were predicted by extrapolating RT-qPCR results from the ~1500 bp covered by the three target regions:[47]

$$\log_{10}\left(\frac{N}{N_0}\right) = \left(\frac{\sum_{i=S,M,L} L_i}{\sum_{i=S,M,L} L_{amp.i}}\right) \sum_{i=S,M,L} \log_{10}\left(\frac{N_i}{N_{0,i}}\right)$$

where N_i is the concentration of the RT-qPCR target region *i* (copies mL^{-1}, *i* = S, M, and L genome segment), $N_{0,i}$ is the mean concentration of the RT-qPCR target region *i* in controls (copies mL^{-1}), $k_{g,i}$ is the reaction rate constant of the RT-qPCR target region *i* (L mg^{-1} s^{-1} or cm^2 mJ^{-1}), *D* is the free chlorine concentration (mg L^{-1}) × contact time (s) or UV dose (mJ cm^{-2}),

$\log_{10}\left(\frac{N}{N_0}\right)$ is the $\log_{10}$ decay of the whole Phi6 genome, L_i is the size of the entire genome segment i (bp), and $L_{amp.i}$ is the size of the RT-qPCR amplicon i (bp). In this extrapolation, we assumed a "single-hit inactivation model" and that the damage measured in the 10.5% of the genome by RT-qPCR was representative of damage in the whole genome.[47]

3.2.4 Peptide LC-MS/MS and quantification.

Following free chlorine or UV_{254} treatment, virus samples were combined with equal amounts of ^{15}N-labeled Phi6 internal standards (see Appendix B for ^{15}N-metabolic labeled Phi6), and the mixture was digested with trypsin (Worthington) or chymotrypsin (Worthington) at 37 °C overnight (see Appendix B for protein digestion). The digests were then analyzed by liquid chromatography-tandem mass spectrometry (LC-MS/MS). Specifically, 20 μL aliquots of the virus protein digests were loaded on an Accucore aQ column (50 × 2.1 mm, 2.6 μm particle size, ThermoFisher Scientific) attached to an Accucore aQ Defender guard column (ThermoFisher Scientific) at a flow rate of 200 μL min^{-1}. The mobile phase was first maintained at 94% solution A (Milli-Q water with 0.1% formic acid) and 6% solution B (LC-MS grade methanol with 0.1% formic acid) for 3 min, and the ratio then increased linearly to 80% B over 30 min, at which point it was maintained at 80% B for 7 min, and then equilibrated at 6% B for 5 min. Full mass spectrometry (MS) scans and data-dependent tandem mass spectrometry (dd-MS^2) scans were conducted with a Q Exactive Orbitrap high resolution mass spectrometer (ThermoFisher Scientific) in positive ion mode (Table B-2). Raw mass spectrometric results were searched against a customized Phi6 protein database with Mascot Distiller (2.6.2.0) on a local Mascot server. The following search parameters were employed for peptide identification: cysteine

carbamidomethylations (+C_2H_4ON) as a fixed modification due to the reactions of iodoacetamide with intact cysteine thiol groups during the protein digestion. When searching for potential oxidation products, we set variable modifications based on oxidation products that were reported previously with LC-MS/MS systems,[48] namely methionine oxidations (+O, +2O), cysteine oxidations (+O, +2O, +3O), and chlorotyrosines (+Cl-H, +2Cl-2H). All searches were set with a 10 ppm mass tolerance for MS scans, and a 0.3 Da mass tolerance for MS^2 scans. False discovery rates of less than 1% and significant P-values of less than 0.05 were employed in each search. Peak areas of all detected peptides and their corresponding ^{15}N-labelled peptides were integrated in TraceFinder 3.2 (ThermoFisher Scientific), and the relative abundance of each peptide was calculated by the peak areas of the ^{14}N-peptide and ^{15}N-labelled peptide:[49]

$$P_j = \frac{PA_{14N-pep.,j}}{PA_{15\text{N}-\text{labeled } pep.,j}}$$

Where P_j is the relative abundance of peptide j; $PA_{14N-pep.,j}$ is the peak area of the ^{14}N-peptide j; $PA_{15\text{N}-\text{labeled } pep.,j}$ is the peak area of the corresponding ^{15}N-labelled peptide j.

Calibration curves of peptides were analyzed to determine limits of quantification (LOQ) and limits of detection (LOD) (see Appendix B for determination of peptide LOQ and LOD). If the relative abundance of a peptide replicate value was below its LOQ but above its LOD, this value was replaced by an expected number between the LOQ and LOD based on the assumption of normal distribution.[50] Peptide reactions were modeled with first-order reaction kinetics:

$$\ln\left(\frac{P_j}{P_{0,j}}\right) = -k_{p,j}D$$

where P_j is the relative abundance of peptide j, $P_{0,j}$ is the mean relative abundance of peptide j in control samples, $k_{p,j}$ is the reaction rate constant of peptide j (L mg^{-1} s^{-1} or cm^2 mJ^{-1}), and D is the free chlorine concentration (mg L^{-1}) × contact time (s) or UV dose (mJ cm^{-2}).

3.2.5 Lipid LC-MS/MS and quantification

Phi6 lipids were extracted following a methyl-tert-butyl ether (MTBE) protocol (see Appendix B, lipid extraction).[51] Lipid extracts (20 μL) were injected on an Accucore aQ column (50 × 2.1 mm, 2.6 μm particle size) attached to an Accucore aQ Defender guard column at a flow rate of 200 μL min^{-1}. The column temperature was maintained at 55 °C. Mobile phases C (60% LC-MS grade acetonitrile and 40% Milli-Q water with 0.1% formic acid) and D (90% LC-MS grade isopropanol and 10% LC-MS grade acetonitrile with 0.1% formic acid) were used for lipid separations. The gradient started at 25% D for 3 min, then linearly increased to 70% D over 15 min, and then to 97% D over 3 min. It was held at 97% D for 4 min, and then decreased to 25% D over 5 min. Full MS and dd-MS^2 scans were operated in negative ion mode (Table B-2). Lipids were identified with LipidXplorer software[52] based on a Phi6 lipid database reported previously,[39] and peak areas were measured with TraceFinder 3.2 (ThermoFisher Scientific). Eight of the most abundant phosphatidylethanolamine (PE) and phosphatidylglycerol (PG) compounds in the Phi6 lipid database were quantified (Figure B-4). Their relative abundances (L/L_0) in the samples were calculated using calibration curves developed from Phi6 lipid extracts (Figure B-4).

3.2.6 Statistical analyses

Rate constants were calculated by pooling all experimental data together and modeling the combined data with linear regressions. Analysis of covariance (ANCOVA) was applied to test whether rate constants were significantly different from zero, and whether two rate constants were significantly different from each other. The corresponding null hypotheses were that the rate

constants were equal to zero or that the two rate constants were identical. Student's unpaired t-tests were used to assess if mean virus inactivation levels (C/C_0) at two chlorine contact times were significantly different. The null hypotheses were that the mean C/C_0 values were the same. A null hypothesis was rejected if the P-value was less than 0.05. Statistical analyses were conducted in GraphPad Prism 7 software.

3.3 Results and discussion

3.3.1 Phi6 inactivation by free chlorine and UV_{254}

Free chlorine inactivation. Phi6 was rapidly inactivated by free chlorine (Figure 3.1), and a continuous quench-flow system was necessary to characterize disinfection while maintaining pseudo-first order conditions. The inactivation displayed significant tailing, which in other viruses has been ascribed to virus aggregation,[53] adsorption to particles,[53,54] and accumulation of oxidation products on the surface of viral particles.[55] In order to minimize the presence of aggregated virus particles, virus stocks were always filtered through 0.22 μm membranes (Phi6 virion is ~85 nm in diameter). Interestingly, the inactivation plateau occurred at lower doses when Phi6 stocks were stored at 4 °C after purification, suggesting that the enveloped viruses aggregated during storage (Figure B-5). Consistent inactivation curves were only possible when Phi6 stocks were purified, filtered through 0.22 μm membranes, and then stored at -80 °C until use. Even then, inactivation nearly levelled off after 4-$\log_{10}$ inactivation by free chlorine (Figure 3.1). We modelled the first 2-$\log_{10}$ inactivation, and obtained an inactivation rate constant equal to 4.6 ± 0.5 (mean ± standard error) L mg^{-1} s^{-1}. For comparison, this rate constant is approximately 30× larger than that of ssRNA MS2 under the same reaction conditions (0.17 L mg^{-1} s^{-1}).[56]

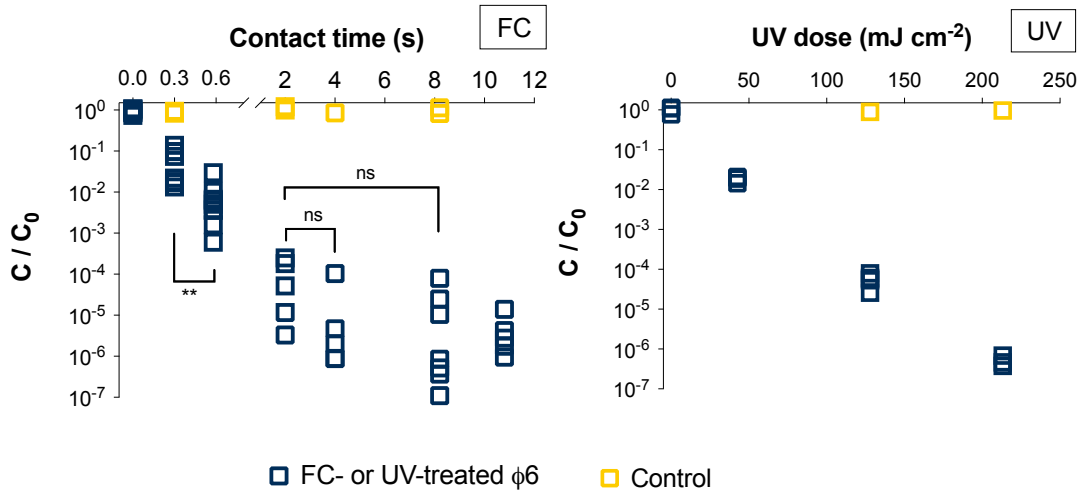

Figure 3.1 Inactivation of Phi6 by 2 mg L^{-1} free chlorine (FC) and UV_{254} (UV). Data includes n ≥ 5 replicates for each chlorine contact time and n = 3 replicates for each UV_{254} dose. Student's unpaired t-tests were used to determine statistical differences of Phi6 infectivity (C/C_0) by free chlorine at two contact times. ** indicates $P < 0.01$, and thus that Phi6 infectivity was significantly different at the two time points; ns indicates Phi6 infectivity was not significantly different at the two time points ($P > 0.05$).

UV_{254} inactivation. Inactivation of Phi6 by UV_{254} followed first-order reactions over the entire measured 6-log_{10} inactivation, with an inactivation rate constant of 0.067 ± 0.005 cm^2 mJ^{-1}. Compared to other enveloped viruses reported in the literature, Phi6 is quite resistant to UV_{254}. For example, it is approximately 15 to 30× more resistant to UV_{254} than influenza A virus (~1 cm^2 mJ^{-1})[11,57] and vesicular stomatitis virus (VSV) (~2.3 cm^2 mJ^{-1}).[58] When compared to nonenveloped viruses, which are better characterized in the literature, Phi6 UV_{254} inactivation kinetics were similar to MS2 (~0.06 cm^2 mJ^{-1})[30,56,59] and adenovirus (~0.046 cm^2 mJ^{-1}).[12]

3.3.2 Reactions in Phi6 genome

Free chlorine reactions. When Phi6 was treated with free chlorine up to 6-log_{10} inactivation, the reaction rate constants of the three ~500 bp regions in the genome were significantly different

from zero as detected by RT-qPCR (Figure 3.2A; Table B-3). The reaction rate constants of the three RT-qPCR regions did not differ significantly from one another following free chlorine treatment ($P > 0.05$ for all the three ANCOVA comparisons). We extrapolated the damage measured in the RT-qPCR regions to the entire genome in order to compare genome damage with inactivation.[47] We note that by measuring ~1500 bp with our RT-qPCR analysis (i.e., 10.5% of the entire Phi6 genome), we aimed to minimize the impact that specific bases and base sequences have on the reactivity of small RNA regions.[47] Based on the RT-qPCR extrapolation results, the fraction of viruses with damaged genomes was less than the fraction that was inactivated (Figure 3.2B). These results suggest that in Phi6, genome damage may not drive Phi6 inactivation by free chlorine. For comparison, genome damage did drive free chlorine inactivation in bacteriophage MS2.[56]

To directly compare the nucleic acid reactivity of two viruses with different genome sizes and types, we normalized the genome reaction rate constants of MS2 (0.066 L mg^{-1} s^{-1})[56] and Phi6 (0.26 L mg^{-1} s^{-1}) to the total number of bases in their genomes. This approach assumes that the genomes have the same proportion of reactive bases. In fact, MS2 and Phi6 do have similar proportions of bases that are reactive to free chlorine and UV_{254} (Table B-4). Interestingly, the normalized MS2 ssRNA genome reaction rate constant with free chlorine (1.8×10^{-5} L mg^{-1} s^{-1} $base^{-1}$) is similar to the normalized value measured here for the Phi6 dsRNA genome (9.4×10^{-6} L mg^{-1} s^{-1} $base^{-1}$).

UV_{254} reactions. Statistically significant decreases in the concentrations of RT-qPCR target regions were detected following 6-log_{10} inactivation by UV_{254} (Figure 3.2A; Table B-3), and the reaction rate constants of the three regions were not significantly different from one another ($P > 0.05$ for each ANCOVA comparison). When the RT-qPCR results were extrapolated to the entire genome, the approximated reaction rate constant of the Phi6 genome (0.063 ± 0.012 cm^2 mJ^{-1}) was

not significantly different from the rate constant of Phi6 inactivation (0.067 ± 0.005 cm^2 mJ^{-1}) ($P > 0.05$). This suggests that genome reactions drive UV_{254} inactivation of the enveloped virus Phi6. Although this type of analysis has not been previously reported for enveloped viruses, our finding is consistent with previous research on nonenveloped viruses.[12,30,56,60] A comparison with the per base reaction rate constants measured here with those reported previously suggests that the dsRNA genome of Phi6 (2.4×10^{-6} cm^2 mJ^{-1} $base^{-1}$) is more resistant to UV_{254} than the dsDNA genome of adenovirus (11×10^{-6} cm^2 mJ^{-1} $base^{-1}$)[61] and the ssRNA genome of MS2 (24×10^{-6} cm^2 mJ^{-1} $base^{-1}$).[56] It is worth noting that in the case of adenovirus, the modified bases detected by PCR can be repaired by the host cell;[12] a similar repair mechanism has not been reported for the RNA viruses.

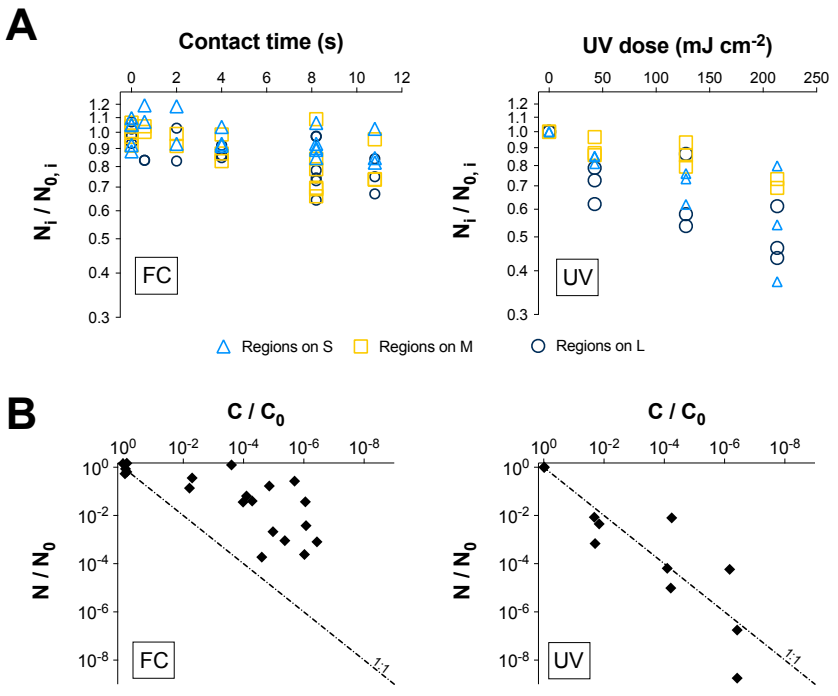

Figure 3.2 Phi6 genome reactions when the viruses were reacted with 2 mg L^{-1} free chlorine (FC) and UV_{254} (UV). A: Reactions in three ~500 bp regions ($N_i/N_{0,i}$) as measured by RT-qPCR with respect to chlorine contact time and UV_{254} doses. Data includes $n \geq 2$ replicates for each chlorine contact time and $n = 3$ replicates for each UV_{254} dose; B: Reactions in the entire Phi6 genome

(N/N_0). This data was extrapolated from the three RT-qPCR regions presented in A, and is presented with respect to virus infectivity (C/C_0) as measured by plaque assays.

We note that using RT-qPCR to estimate genome damage misses a fraction of the RNA modifications that can be detected by mass spectrometry.[44] Work on the photolysis of MS2 by UV_{254}, however, demonstrated that a single-hit inactivation model was appropriate for damage detected with RT-qPCR; in other words, every modification in MS2 RNA that causes virus inactivation can be detected by RT-qPCR.[47] Our ongoing work aims to better characterize the chemistry and biological impact of RNA and DNA modifications detected by reverse transcriptases, polymerases, and mass spectrometry.

3.3.3 Reactions in Phi6 proteins

The Phi6 virion contains 11 distinct proteins that are assembled into three layers, including viral membrane proteins (P3, P6, P9, P10, P13), nucleocapsid proteins (P5, P8), and polymerase complex proteins (P1, P2, P4, P7) (Figure B-6).[38] The functions of these proteins in the Phi6 life cycle have been reviewed in previous literature and are briefly described in the SI (Figure B-6).[38] Our LC-MS/MS method was capable of detecting a total of 184 pairs of ^{14}N- and ^{15}N-labelled Phi6 peptides. Protein coverage was over 60% for all proteins except for P6 and P2 (Figure B-7). The repeated poor coverage of P6 and P2 was likely due to the low number of P6 and P2 protein copies in the viral particles (Figure B-7).

Free chlorine reactions. We tracked Phi6 protein degradation over the first 2-$\log_{10}$ Phi6 inactivation in order to model the peptide reactions with first-order kinetics. Free chlorine reacted with all Phi6 peptides with reaction rate constants ranging from 0.41 to 6.3 L mg^{-1} s^{-1} (Figure 3.3;

Table B-6). As expected, the most reactive peptides contained Met or Cys residues (Table B-6). Despite the similar reactivity of Met and Cys in the free amino acid form (Table B-5), the most reactive Cys-containing peptide C257-F267 in Phi6 P4 (2.8 ± 0.3 L mg^{-1} s^{-1}) reacted slower than the most reactive Met-containing peptide D448-R463 (6.3 ± 0.9 L mg^{-1} s^{-1}) in Phi6 P1 (Table B-6). Furthermore, the rate constants of peptides containing Met varied. For example, in the Phi6 P1, the rate constant of M198-K208 (1.1 ± 0.1 L mg^{-1} s^{-1}) was approximately 3 × smaller than that of peptide L53-Y66 (3.1 ± 0.5 L mg^{-1} s^{-1}) and 4 × smaller than that of peptide M209-K215 (4.5 ± 0.7 L mg^{-1} s^{-1}), despite the three peptides having spatially adjacent Met residues (Figure B-8). The variation in reactivity of peptides containing Met and Cys is likely related to the accessibility of free chlorine to the amino acids.[30] Indeed, the Cryo-EM model (PDB ID: 5muu) of Phi6 suggests that in the P1 complex, the dimethyl sulfide of M198 in M198-K208 is protected by surrounding amino acid residues, whereas the M65 in L53-Y66 and M209 in M209-K215 have higher solvent-accessible surface areas (SASA, Figure B-8). It is also worth noting that oxidized Met residues were the only products in Phi6 proteins detected following 2-$\log_{10}$ inactivation by free chlorine (Figure B-9).

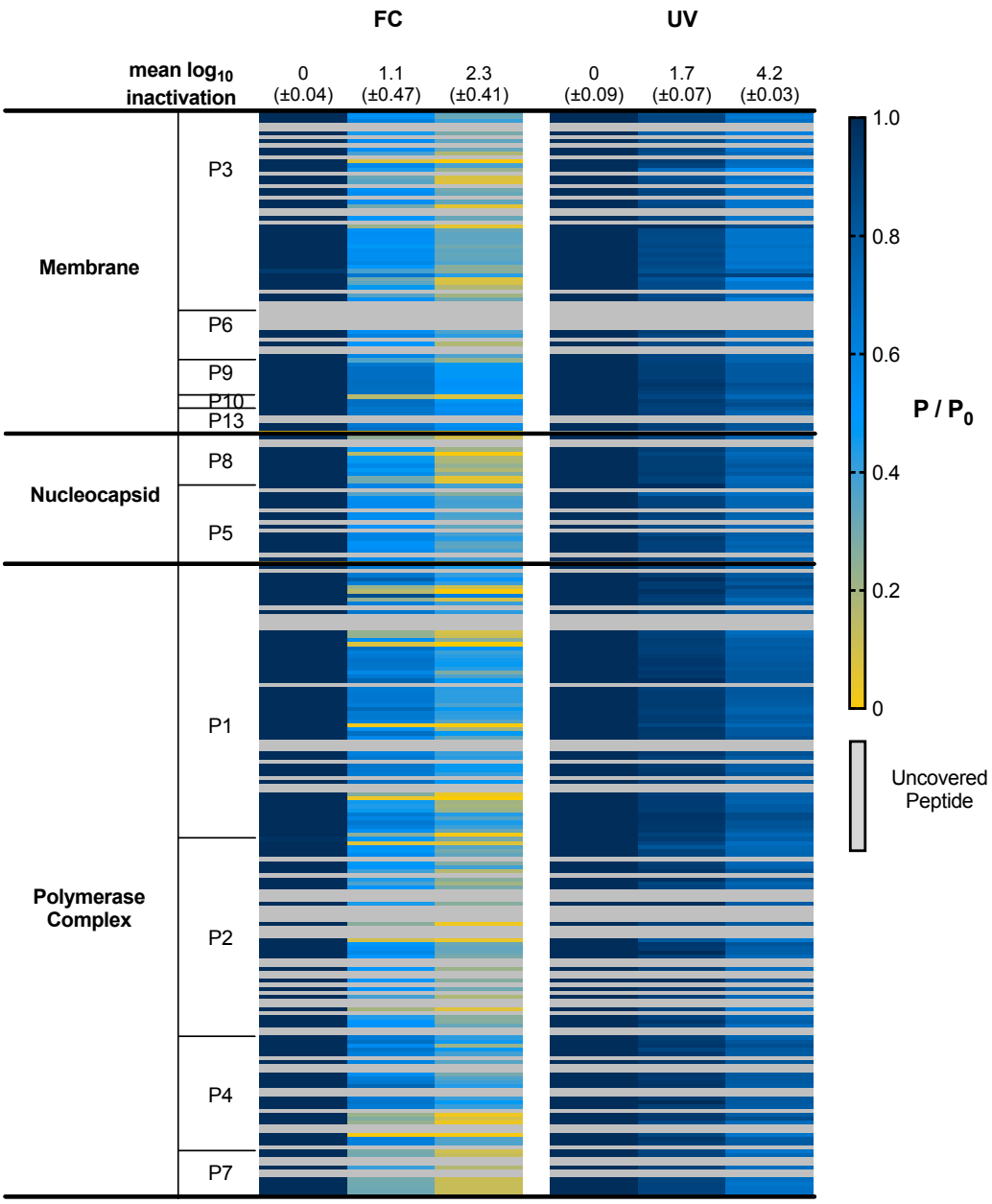

Figure 3.3 Heatplot of Phi6 protein peptide abundances following Phi6 exposure to free chlorine (FC) and UV_{254} (UV). Each row in the heatplot represents one peptide. Peptides were arranged based on their sequential order in proteins, and the undetected peptides are shown in grey. Peptide concentrations (P/P_0) in this heatplot were averaged from 3 independent experiments. Detailed information of peptide sequences, reaction rate constants and standard errors are provided in Table B-6.

We initially hypothesized that the increased susceptibility of Phi6 to free chlorine inactivation compared to nonenveloped viruses, such as MS2, was due to reactions in the membrane proteins. These proteins play critical roles in the early steps of virus infection, and are located on the outermost layer of the viral particle (Figure B-6). In fact, our results showed that in Phi6, some membrane proteins (e.g., P6, P9, P10, P13) reacted slower than the nucleocapsid proteins (e.g., P8) and polymerase complex proteins (e.g., P1, P2, P4) (Figure 3.3; Table B-6). This suggests that free chlorine molecules readily penetrate the lipid membrane and react with proteins in the nucleocapsid and polymerase complex. Similar findings were reported in bacteria, where the non-dissociated HOCl molecules could penetrate the negatively-charged bacterial membrane to react with intracellular structures.[62]

The 8 most reactive peptides found in Phi6 proteins P3, P8, P1, P2, and P4 had rate constants that were comparable to the Phi6 inactivation rate constant (Figure 3.4; Table B-6), forming Met oxidations as the main products (Figure B-9). Consequently, one or several of these protein reactions may drive Phi6 inactivation by free chlorine. Given the protein reactivity and the Phi6 life cycle, Phi6 inactivation may be due to the direct interruption of the ability to bind host cell (P3) or to penetrate plasma membrane (P8).[63,64] Alternatively, damage to proteins P2, P4, and P7 may indirectly inactivate Phi6 by causing changes in the vial structure.[48,64,65]

Peptides in Phi6 proteins were more reactive with free chlorine than peptides in the nonenveloped MS2 proteins. The two most reactive peptides D448-R463 (6.3 ± 0.9 L mg^{-1} s^{-1}) and I678-R697 (5.9 ± 1.0 L mg^{-1} s^{-1}) in Phi6 were approximately 150× more reactive than the fastest reacting peptide S373-R388 in the MS2 A protein (0.033 L mg^{-1} s^{-1}).[56] The marked discrepancies in reactivity of Phi6 and MS2 peptides may be due to the relative solvent accessibilities of their reactive amino acids.[30] The average SASAs of the M456 and M680 residue in the Phi6 peptide are

95 Å^2 and 77 Å^2, respectively, as calculated by YASARA software.[66] Unfortunately, the SASA cannot be estimated for the Met in the most reactive MS2 peptide due to the fact that the crystal structure of the MS2 A protein has not been resolved.

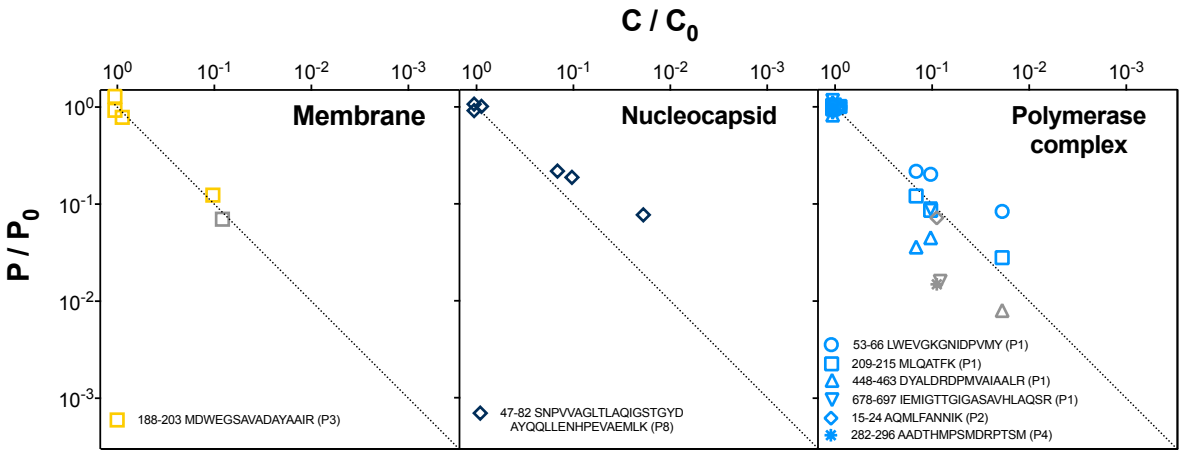

Figure 3.4 Decay of the 8 most reactive Phi6 peptides (P/P_0) by free chlorine with respect to virus infectivity (C/C_0). Data below the LC-MS/MS limit of quantification is shown in grey.

UV_{254} reactions. All Phi6 peptides reacted following UV_{254} exposure, but much less than they reacted with free chlorine at the same levels of inactivation. Peptide concentrations decreased by less than 50% following 4.2-$\log_{10}$ Phi6 inactivation (Figure 3.3), with rate constants ranging from 0.0009 to 0.0048 cm^2 mJ^{-1} (Table B-6). Similar reaction rate constants were reported for peptides in bacteriophage MS2, fr, and GA proteins with UV_{254}.[30,56] Certain peptides in membrane protein P3 and RNA polymerase P2 reacted with faster kinetics, likely due to the presence of one or more UV-reactive amino acids in their sequences, including Trp (W), Tyr (Y), or Phe (F) (Table B-6).[67] Indirect photoreactions with nucleic acids may also play a role in the enhanced photoreactivity of certain viral peptides as reported in MS2.[68]

3.3.4 Reactions in Phi6 lipids

Phi6 lipid membranes consist of glycerophospholipids, including phosphatidylethanolamine (PE), phosphatidylglycerol (PG), and cardiolipin (CL) compounds at a molar ratio of 58:38:4.[39] Here, we measured the relative abundances of the eight most prevalent PE and PG compounds in Phi6 membranes.

Free chlorine reactions. The PE and PG relative concentrations did not decrease significantly over 9.1-$\log_{10}$ Phi6 inactivation by free chlorine (Figure B-10; $P > 0.05$ for all tests). A number of products were detected in the LC-MS spectra, including monochloramine products of PE (16:0/16:1) and PE (18:1/16:1) (Figure 3.5). The peak intensities of PE monochloramine products increased with increasing chlorine contact time, although at the highest inactivation level (i.e., 9.1-$\log_{10}$ Phi6 inactivation), the product peak intensities were still three orders of magnitude smaller than the parent PE peaks (Figure 3.5). The low PE monochloramine product concentration within the Phi6 inactivation timeframe was not surprising given that the reported rate constant for this reaction (1.8×10^4 $M^{-1}s^{-1}$) is three orders of magnitude lower than the rate constants for free chlorine reacting with Met and Cys residues.[69] Other lipid products were detected following free chlorine treatment, with peak intensities no greater than 1% of the parent compound peak intensities (Figure 3.5). The chemical compositions and structures of these products did not correspond to commonly reported lipid oxidation products, such as lipid hydroperoxides and chlorohydrins.[70,71]

UV_{254} reactions. Statistically significant reductions in the relative concentrations of the eight major lipid compounds were not detected following UV_{254} doses resulting in 8.5-$\log_{10}$ Phi6 inactivation (Figure B-10; $P > 0.05$ for all tests). Likewise, no major products were detected in the LC-MS spectra of samples following UV_{254} treatment (Figure 3.5). Previous research on UV_{254}

reactions with the membrane of VSV suggest that the lipid envelope do not protect VSV from inactivation.[72]

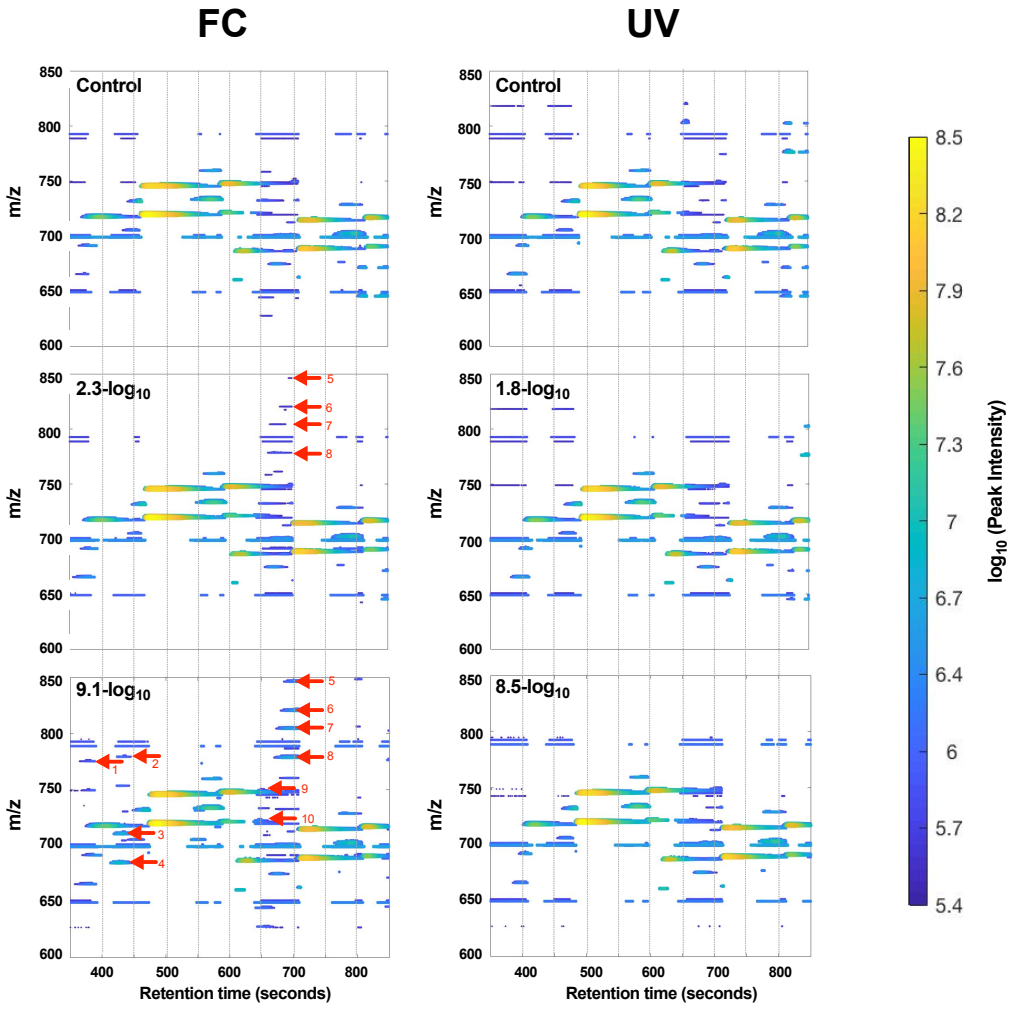

Figure 3.5 Phi6 lipids data collected by LC-MS before and after free chlorine (FC) and UV_{254} (UV) treatments. Arrows identify specific lipid products $[M-H]^-$ following free chlorine treatment, including the following accurate masses (1) 775.513; (2) 779.464; (3) 710.477; (4) 684.461; (5) 846.588; (6) 820.572; (7) 804.541; (8) 778.525; (9) 748.469 (monochloramine of PE(16:0/16:1)); (10) 722.454 (monochloramine of PE(18:1/16:1)).

The lipid compositions of eukaryote enveloped viruses are more diverse than those of bacteriophage Phi6. Influenza virus membranes, for example, contain not only PE and PG, but also cholesterol and phosphatidylserine (PS).[40] The kinetics of these lipids with HOCl, however, are not markedly faster than the lipids in the Phi6 membrane.[73,74] In summary, based on our Phi6 lipid results and what has been reported for other lipids found in virus membranes, we anticipate that reactions in membrane lipids do not drive enveloped virus inactivation by free chlorine or UV_{254}.

3.3.5 Environmental implications

Enveloped viruses are often assumed to be more susceptible than nonenveloped viruses to inactivation in the environment, but mechanistic descriptions of their differing inactivation mechanisms are lacking in the literature. Our preliminary work with enveloped virus Phi6 sheds light on how a model enveloped virus reacts with chemical oxidants and UV radiation. We found that Phi6 was 30× more susceptible to free chlorine inactivation than the commonly studied nonenveloped virus MS2. Our work suggests that unlike MS2, the overall Phi6 particle reactivity with free chlorine is driven more by protein reactions than by genome and lipid reactions. Free chlorine reactions in the most reactive Phi6 peptides were orders of magnitude faster than reactions in the most reactive MS2 peptides, specifically for Phi6 peptides that contain solvent-accessible Met and Cys residues. Consequently, the relatively high number of solvent-accessible Met and Cys residues in the Phi6 proteins may be responsible for its fast inactivation kinetics with free chlorine. In contrast to chlorine, UV_{254} inactivates Phi6 primarily by reacting with the genome. This is consistent with previous research on nonenveloped viruses. It is therefore unlikely that

enveloped viruses are more susceptible than nonenveloped viruses to direct photolysis via sunlight or UV disinfection processes.

Looking beyond this initial comparison of enveloped Phi6 with nonenveloped MS2, this work raises a number of hypotheses about virus reactivity and inactivation that can be tested with additional viruses. For example, future work should explore whether proteins in enveloped viruses are generally more susceptible to oxidants than proteins in nonenveloped viruses, and if this is the reason that enveloped viruses tend to be more susceptible to inactivation by chemical oxidants. Related to this, research should explore the link between the presence of solvent-accessible reactive amino acids in viral proteins with virus inactivation by oxidants. UVC inactivation should be tested with additional enveloped viruses that contain various genome sizes and genome types. Possible enveloped viruses to study in the future include vesicular stomatitis virus and avian influenza viruses. These are animal viruses with particle diameters and genome types that differ from Phi6 and can be propagated to stocks with high titers. This last point is important for cases in which researchers wish to apply the LC-MS/MS methods described in this study. Finally, enveloped viruses in open air may undergo reactions and inactivation mechanisms similar to viruses in water. Future studies should aim to compare aqueous virus reactivity with aerosolized virus reactivity.

Enveloped viruses are structurally diverse, ranging in size, envelope composition, genome type, and shape. These variations are likely reflected in a range of reactivities and inactivation mechanisms. That being said, the structure and composition of the Phi6 are not especially unique amongst the enveloped viruses. We are therefore confident that this study on Phi6 reactivity with free chlorine and UV_{254} will be a valuable benchmark for future studies on enveloped virus fate in disinfection processes.

3.4 References

(1) Pica, N.; Bouvier, N. M. Environmental factors affecting the transmission of respiratory viruses. *Curr. Opin. Virol.* **2012**, *2* (1), 90–95.

(2) Wigginton, K. R.; Ye, Y.; Ellenberg, R. M. Emerging investigators series: The source and fate of pandemic viruses in the urban water cycle. *Environ. Sci.: Water Res. Technol.* **2015**, *1*, 735–746.

(3) Osterholm, M. T.; Moore, K. A.; Kelley, N. S.; Brosseau, L. M.; Wong, G.; Murphy, F. A.; Peters, C. J.; LeDuc, J. W.; Russell, P. K.; Van Herp, M.; et al. Transmission of Ebola viruses: What we know and what we do not know. *mBio* **2015**, *6* (2), 1–9.

(4) Memarzadeh, F. Literature review of the effect of temperature and humidity on viruses. *ASHRAE Trans.* **2012**, *118*, 1049–1060.

(5) Welliver, R. C. Temperature, humidity, and ultraviolet B radiation predict community respiratory syncytial virus activity. *Pediatr. Infect. Dis. J.* **2007**, *26*, S29–S35.

(6) Casanova, L. M.; Jeon, S.; Rutala, W. A.; Weber, D. J.; Sobsey, M. D. Effects of air temperature and relative humidity on coronavirus survival on surfaces. *Appl. Environ. Microbiol.* **2010**, *76* (9), 2712–2717.

(7) Songer, J. R. Influence of relative humidity on the survival of some airborne viruses. *Appl. Microbiol.* **1967**, *15* (1), 35–42.

(8) Weber, T. P.; Stilianakis, N. I. A note on the inactivation of influenza A viruses by solar radiation, relative humidity and temperature. *Photochem. Photobiol.* **2008**, *84* (6), 1601–1602.

(9) Yang, W.; Elankumaran, S.; Marr, L. C. Relationship between humidity and influenza A viability in droplets and implications for influenza's seasonality. *PLoS ONE* **2012**, *7* (10), e46789.

(10) Chumpolbanchorn, K.; Suemanotham, N.; Siripara, N.; Puyati, B.; Chaichoune, K. The effect of temperature and UV light on infectivity of avian influenza virus (H5N1, Thai field strain) in chicken fecal manure. *Southeast Asian J. Trop. Med. Public Health* **2006**, *37* (1), 102–105.

(11) Sagripanti, J. L.; Lytle, C. D. Inactivation of influenza virus by solar radiation. *Photochem. Photobiol.* **2007**, *83* (5), 1278–1282.

(12) Bosshard, F.; Bosshard, F.; Armand, F.; Armand, F.; Hamelin, R.; Hamelin, R.; Kohn, T. Mechanisms of human adenovirus inactivation by sunlight and UVC light as examined by quantitative PCR and quantitative proteomics. *Appl. Environ. Microbiol.* **2012**, *79* (4), 1325–1332.

(13) Ehrlich, R.; Miller, S. Effect of NO_2 on airborne Venezuelan equine encephalomyelitis virus. *Appl. Microbiol.* **1972**, *23* (3), 481–484.

(14) Tseng, C. C.; Li, C. S. Ozone for inactivation of aerosolized bacteriophages. *Aerosol Sci. Technol.* **2006**, *40*, 683–689.

(15) Wigginton, K. R.; Kohn, T. Virus disinfection mechanisms: The role of virus composition, structure, and function. *Curr. Opin. Virol.* **2012**, *2* (1), 84–89.

(16) Ye, Y.; Ellenberg, R. M.; Graham, K. E.; Wigginton, K. R. Survivability, partitioning, and recovery of enveloped viruses in untreated municipal wastewater. *Environ. Sci. Technol.* **2016**, *50*, 5077–5085.

(17) Casanova, L. M.; Weaver, S. R. Inactivation of an enveloped surrogate virus in human sewage. *Environ. Sci. Technol. Lett.* **2015**, *2*, 76–78.

(18) Bibby, K.; Fischer, R.; Casson, L.; Stachler, E. Persistence of Ebola virus in sterilized wastewater. *Environ. Sci. Technol. Lett.* **2015**, *2*, 245–249.
(19) Gallandat, K.; Lantagne, D. Selection of a Biosafety Level 1 (BSL-1) surrogate to evaluate surface disinfection efficacy in Ebola outbreaks: Comparison of four bacteriophages. *PLoS ONE* **2017**, *12* (5), 1–10.
(20) Rabenau, H. F.; Cinatl, J.; Morgenstern, B.; Bauer, G.; Preiser, W.; Doerr, H. W. Stability and inactivation of SARS coronavirus. *Med. Microbiol. Immunol.* **2005**, *194* (1-2), 1–6.
(21) Chan, K. H.; Poon, L. L. L. M.; Cheng, V. C. C.; Guan, Y.; Hung, I. F. N.; Kong, J.; Yam, L. Y. C.; Seto, W. H.; Yuen, K. Y.; Peiris, J. S. M. Detection of SARS coronavirus in patients with suspected SARS. *Emerg. Infect. Dis.* **2004**, *10* (2), 294–299.
(22) Yu, I. T. S.; Li, Y.; Wong, T. W.; Tam, W.; Chan, A. T.; Lee, J. H. W.; Leung, D. Y. C.; Ho, T. Evidence of airborne transmissionof the severe acute respiratory syndrome virus. *N. Engl. J. Med.* **2004**, *350*, 1731–1739.
(23) Tellier, R. Review of aerosol transmission of influenza A virus. *Emerg. Infect. Dis.* **2006**, *12* (11), 1657–1662.
(24) Bean, B.; Moore, B. M.; Sterner, B.; Peterson, L. R.; Gerding, D. N.; Balfour, H. H. Survival of influenza viruses on environmental surfaces. *J. Infect. Dis.* **1982**, *146* (1), 47–51.
(25) Webster, R. G. Influenza: an emerging disease. *Emerg. Infect. Dis.* **1998**, *4* (3), 436–441.
(26) Stallknecht, D. E.; Goekjian, V. H.; Wilcox, B. R.; Poulson, R. L.; Brown, J. D. Avian influenza virus in aquatic habitats: what do we need to learn? *Avian Dis.* **2010**, *54* (s1), 461–465.
(27) Albina, E. Epidemiology of porcine reproductive and respiratory syndrome (PRRS): An overview. *Veterinary microbiol.* **1997**, *55*, 309–316.
(28) Piercy, T. J.; Smither, S. J.; Steward, J. A.; Eastaugh, L.; Lever, M. S. The survival of filoviruses in liquids, on solid substrates and in a dynamic aerosol. *J. Appl. Microbiol.* **2010**, *109* (5), 1531–1539.
(29) Bibby, K.; Aquino de Carvalho, N.; Rule Wigginton, K. Research needs for wastewater handling in virus outbreak response. *Environ. Sci. Technol.* **2017**, *51*, 2534–2535.
(30) Sigstam, T.; Gannon, G.; Cascella, M.; Pecson, B. M.; Wigginton, K. R.; Kohn, T. Subtle differences in virus composition affect disinfection kinetics and mechanisms. *Appl. Environ. Microbiol.* **2013**, *79* (11), 3455–3467.
(31) Gall, A. M.; Shisler, J. L.; Mariñas, B. J. Characterizing bacteriophage PR772 as a potential surrogate for adenovirus in water disinfection: A comparative analysis of inactivation kinetics and replication cycle inhibition by free chlorine. *Environ. Sci. Technol.* **2016**, *50* (5), 2522–2529.
(32) Lee, M. T.; Pruden, A.; science, L. M. E.; 2016. Partitioning of viruses in wastewater systems and potential for aerosolization. *J. Chem. Eng.* **2016**, *3* (5), 210–215.
(33) Lin, K.; Marr, L. C. Aerosolization of Ebola virus surrogates in wastewater systems. *Environ. Sci. Technol.* **2017**, *51* (5), 2669–2675.
(34) Wolfe, M. K.; Gallandat, K.; Daniels, K.; Desmarais, A. M.; Scheinman, P.; Lantagne, D. Handwashing and Ebola virus disease outbreaks: A randomized comparison of soap, hand sanitizer, and 0.05% chlorine solutions on the inactivation and removal of model organisms Phi6 and E. coli from hands and persistence in rinse water. *PLoS ONE* **2017**, *12* (2), e0172734.

(35) Aquino de Carvalho, N.; Stachler, E. N.; Cimabue, N.; Bibby, K. Evaluation of Phi6 persistence and suitability as an enveloped virus surrogate. *Environ. Sci. Technol.* **2017**, *51* (15), 8692–8700.
(36) Gallandat, K.; Wolfe, M. K.; Lantagne, D. Surface cleaning and disinfection: Efficacy assessment of four chlorine types using escherichia coli and the Ebola surrogate Phi6. *Environ. Sci. Technol.* **2017**, *51* (8), 4624–4631.
(37) Cytoviridae. *Virus Taxonomy: Ninth Report of the International Committee on Taxonomy of Viruses*; King, A. M. Q., Adams, M. J., Carstens, E. B., Lefkowitz, E. J., Eds.; Elsevier: Oxford, 2011; pp 515–518.
(38) Poranen, M. M.; Tuma, R.; Bamford, D. H. Assembly of double-stranded RNA bacteriophages. *Adv. Virus Res.* **2005**, *64*, 15–43.
(39) Laurinavičius, S.; Käkelä, R.; Bamford, D. H.; Somerharju, P. The origin of phospholipids of the enveloped bacteriophage Phi6. *Virology* **2004**, *326* (1), 182–190.
(40) Gerl, M. J.; Sampaio, J. L.; Urban, S.; Kalvodova, L.; Verbavatz, J.-M.; Binnington, B.; Lindemann, D.; Lingwood, C. A.; Shevchenko, A.; Schroeder, C.; et al. Quantitative analysis of the lipidomes of the influenza virus envelope and MDCK cell apical membrane. *J. Cell Biol.* **2012**, *196* (2), 213–221.
(41) Bamford, D. H.; Ojala, P. M.; Frilander, M.; Walin, L.; Bamford, J. K. H. Isolation, purification, and function of assembly intermediates and subviral particles of bacteriophages PRD1 and Phi6. *Methods Mol. Genet.* **1995**, *6*, 455–474.
(42) Dodd, M. C.; Vu, N. D.; Ammann, A.; Le, V. C.; Kissner, R.; Pham, H. V.; Cao, T. H.; Berg, M.; Gunten, von, U. Kinetics and mechanistic aspects of As(III) oxidation by aqueous chlorine, chloramines, and ozone: Relevance to drinking water treatment. *Environ. Sci. Technol.* **2006**, *40* (10), 3285–3292.
(43) *Standard Methods for Examination of Water & Wastewater*, 20 ed.; Clescerl, L. S., Greenberg, A. E., Eaton, A. D., Eds.; American Public Health Assocaition: Washington, DC, 1999.
(44) Qiao, Z.; Wigginton, K. R. Direct and indirect photochemical reactions in viral RNA measured with RT-qPCR and mass spectrometry. *Environ. Sci. Technol.* **2016**, *50* (24), 13371–13379.
(45) Rahn, R. O. Potassium iodide as a chemical actinometer for 254 nm radiation: Use of iodate as an electron scavenger. *Photochem. Photobiol.* **1997**, *66* (4), 450–455.
(46) Gyürék, L. L.; Finch, G. R. Modeling water treatment chemical disinfection kinetics. *J. Environ. Eng.* **1998**, *124* (9), 783–793.
(47) Pecson, B. M.; Ackermann, M.; Kohn, T. Framework for using quantitative PCR as a nonculture based method to estimate virus infectivity. *Environ. Sci. Technol.* **2011**, *45* (6), 2257–2263.
(48) Choe, J. K.; Richards, D. H.; Wilson, C. J.; Mitch, W. A. Degradation of amino acids and structure in model proteins and bacteriophage MS2 by chlorine, bromine, and ozone. *Environ. Sci. Technol.* **2015**, *49* (22), 13331–13339.
(49) Goshe, M. B.; Smith, R. D. Stable isotope-coded proteomic mass spectrometry. *Curr. Opin. Biotechnol.* **2003**, *14*, 101–109.
(50) Gleit, A. Estimation for small normal data sets with detection limits. *Environ. Sci. Technol.* **1985**, *19* (12), 1201–1206.

(51) Matyash, V.; Liebisch, G.; Kurzchalia, T. V.; Shevchenko, A.; Schwudke, D. Lipid extraction by methyl-tert-butyl ether for high-throughput lipidomics. *J. Lipid Res.* **2008**, *49* (5), 1137–1146.

(52) Herzog, R.; Schwudke, D.; Schuhmann, K.; Sampaio, J. L.; Bornstein, S. R.; Schroeder, M.; Andrej Shevchenko. A novel informatics concept for high-throughput shotgun lipidomics based on the molecular fragmentation query language. *Genome Biol.* **2011**, *12*, 1–25.

(53) Kahler, A. M.; Cromeans, T. L.; Metcalfe, M. G.; Humphrey, C. D.; Hill, V. R. Aggregation of adenovirus 2 in source water and impacts on disinfection by chlorine. *Food Environ. Virol.* **2016**, *8* (2), 148–155.

(54) Gerba, C. P.; Betancourt, W. Q. Viral aggregation: Impact on virus behavior in the environment. *Environ. Sci. Technol.* **2017**, *51* (13), 7318–7325.

(55) Sigstam, T.; Rohatschek, A.; Zhong, Q.; Brennecke, M.; Kohn, T. On the cause of the tailing phenomenon during virus disinfection by chlorine dioxide. *Water Res.* **2014**, *48*, 82–89.

(56) Wigginton, K. R.; Pecson, B. M.; Sigstam, T.; Bosshard, F.; Kohn, T. Virus inactivation mechanisms: Impact of disinfectants on virus function and structural integrity. *Environ. Sci. Technol.* **2012**, *46* (21), 12069–12078.

(57) Powell, W. F.; Setlow, R. B. The effect of monochromatic ultraviolet radiation on the interfering property of influenza virus. *Water Res.* **1956**, *2*, 337–343.

(58) Bay, P. H.; Reichmann, M. E. UV inactivation of the biological activity of defective interfering particles generated by vesicular stomatitis virus. *J. Virol.* **1979**, *32* (3), 876–884.

(59) Battigelli, D. A.; Sobesey, M. D.; Lobe, D. C. The inactivation of hepatitis A virus and other model viruses by UV irradiation. *Water Sci. Technol.* **1993**, *27*, 339–342.

(60) Simonet, J.; Gantzer, C. Inactivation of poliovirus 1 and F-specific RNA phages and degradation of their genomes by UV irradiation at 254 nanometers. *Appl. Environ. Microbiol.* **2006**, *72* (12), 7671–7677.

(61) Beck, S. E.; Rodriguez, R. A.; Linden, K. G.; Hargy, T. M.; Larason, T. C.; Wright, H. B. Wavelength dependent UV inactivation and DNA damage of adenovirus as measured by cell culture infectivity and long range quantitative PCR. *Environ. Sci. Technol.* **2013**, *48* (1), 591–598.

(62) Dodd, M. C. Potential impacts of disinfection processes on elimination and deactivation of antibiotic resistance genes during water and wastewater treatment. *J. Environ. Monit.* **2012**, *14*, 1754–1771.

(63) Lewis, A. K.; Dunleavy, K. M.; Senkow, T. L.; Her, C.; Horn, B. T.; Jersett, M. A.; Mahling, R.; McCarthy, M. R.; Perell, G. T.; Valley, C. C.; et al. Oxidation increases the strength of the methionine-aromatic interaction. *Nat. Chem. Biol.* **2016**, *12* (10), 860–866.

(64) Ogata, N. Inactivation of influenza virus haemagglutinin by chlorine dioxide: oxidation of the conserved tryptophan 153 residue in the receptor-binding site. *J. Gen. Virol.* **2012**, *93*, 2558–2563.

(65) Liu, D.; Ren, D.; Huang, H.; Dankberg, J.; Rosenfeld, R.; Cocco, M. J.; Li, L.; Brems, D. N.; Remmele, R. L. Structure and stability changes of human IgG1 Fc as a consequence of methionine oxidation. *Biochemistry* **2008**, *47* (18), 5088–5100.

(66) Krieger, E.; Vriend, G. New ways to boost molecular dynamics simulations. *J. Comput. Chem.* **2015**, *36* (13), 996–1007.

(67) Mihalyi, E. Numerical values of the absorbances of the aromatic amino acids in acid, neutral, and alkaline solutions. *J. Chem. Eng.* **1968**, *13*, 179–182.
(68) Wigginton, K. R.; Menin, L.; Sigstam, T.; Gannon, G.; Cascella, M.; Hamidane, H. B.; Tsybin, Y. O.; Waridel, P.; Kohn, T. UV radiation induces genome-mediated, site-specific cleavage in viral proteins. *ChemBioChem* **2012**, *13* (6), 837–845.
(69) Pattison, D. I.; Davies, M. J. Reactions of myeloperoxidase-derived oxidants with biological substrates: Gaining chemical insight into human inflammatory diseases. *Curr. Med. Chem.* **2006**, *13*, 3271–3290.
(70) Spickett, C. M. Chlorinated lipids and fatty acids: An emerging role in pathology. *Pharmacol. Ther.* **2007**, *115* (3), 400–409.
(71) Frankel, E. N. Lipid oxidation: Mechanisms, products and biological significance. *J. Am. Oil. Chem. Soc.* **1984**, *61* (12), 1908–1917.
(72) Anderson, R.; Daya, M.; Reeve, J. An evaluation of the contribution of membrane lipids to protection against ultraviolet radiation. *Adv. Virus Res.* **1987**, *905*, 227–230.
(73) Ghanbari, H. A.; Wheeler, W. B.; Kirk, J. R. Reactions of aqueous chlorine and chlorine dioxide with lipids: Chlorine incorporation. *J. Food Sci.* **1982**, *47*, 482–485.
(74) Carr, A. C.; van den Berg, J. J. M.; Winterbourn, C. C. Chlorination of cholesterol in cell membranes by hypochlorous acid. *Arch. Biochem. Biophys.* **1996**, *332* (1), 63–69.

Chapter 4 Development of an integrated cell culture-mass spectrometry method for monitoring infectious viruses in environmental samples

Yinyin Ye[1], Krista R. Wigginton[1]

[1] Department of Civil and Environmental Engineering, University of Michigan, Ann Arbor, Michigan, USA

4.1 Introduction

Human pathogenic viruses in water are responsible for a number of waterborne human diseases. Compared to other waterborne pathogens (e.g., bacteria, protozoa), virus detection in water is especially challenging due to their small dimensions and low abundances. Sensitive methods have been developed to detect viral nucleic acid sequences, including polymerase chain reaction (PCR) and genome sequencing. These methods alone, however, are not able to differentiate infectious and noninfectious viruses. Culture-based methods, including plaque assays, detect only infective viruses. In culture-based methods, virus replication in their host cells can result in the formation of cytopathic effects (CPEs). These CPEs are often the endpoints used for detection and quantification. However, the formation of clear CPEs requires time, sometimes up to weeks. Furthermore, environmental samples can cause CPEs in the absence of viruses when materials in the samples are toxic to the cells.[1,2] Yet another issue with culture-based methods is that several different viruses can often infect the same cultured cell system. It is therefore often impossible to identify the viruses responsible for the cytopathic effects.

To address the issue of molecular methods detecting noninfective viruses, and the issue of culture-based methods not identifying specific viruses, methods that integrate cell cultures with polymerase chain reaction (integrated cell culture-PCR; ICC-PCR) were developed. This approach has been used to detect many different viruses in environmental samples,[3-6] including enteroviruses in wastewater samples. As few as one infectious virus can be detected by ICC-PCR earlier than the formation of clear CPEs.[6] The other advantage of ICC-PCR over culture-based method alone is that multiple viruses can be detected with a number of primer sets. Hwa Kyung Lett *et al*. [7] used virus specific primers to monitor adenoviruses, enteroviruses, and reoviruses in water samples with ICC-PCR methods.

Although ICC-PCR methods addressed some of the issues of culture methods and PCR methods alone, it still requires primer design and PCR assay optimization. In most ICC-PCR applications, two rounds of PCR amplifications are optimized to improve assay sensitivity and confirm positive results.[8] If virus strain-level identification is necessary, strain-specific primer sets are required, and it may need further characterization by sequencing of PCR products.[9] Another challenge associated with PCR methods is that viruses rapidly evolve, and this can occasionally cause pre-designed PCR primers to fail due to the newly evolved sequences.[10]

Recently-developed mass spectrometry (MS) techniques may be capable of virus detection while alleviating some of the limitations of other techniques.[11] MS instruments can scan peptide ions present in a sample and fragment peptide ions, ultimately making de novo peptide sequencing possible.[12,13] Genetic information carried on proteins can then be used for microorganism identification. For instance, in a shotgun proteomics method for bacterial identification, bacterial proteins were digested into peptides, and the peptide sequences were analyzed on a liquid chromatography tandem mass spectrometry system. The detected peptides were then compared

with sequences in protein database to identify bacteria.[14,15] The most obvious advantage of MS methods over PCR methods is the lack of necessary primer design and method optimization. Moreover, MS is able to detect single amino acid mutations based on the peptide fragments.[16] Methods that integrate cell culture and mass spectrometry (ICC-MS) have been applied for detecting viruses in clinical samples.[17-19] Here, the detected peptide sequences could correctly distinguish viruses at the strain-level.[19] To date, however, ICC-MS methods have not been applied for detecting viruses in environmental samples. Environmental matrices are often more complex than clinical samples, and virus concentrations are typically much lower.

Here, we report on an ICC-MS method for detecting infectious human viruses in environmental water samples. Sample preparation methods and MS detection protocols were developed and optimized with a model virus culture system (i.e., murine hepatitis virus and its host L2 cells). The effects of virus concentrations and the potential toxicity of wastewater samples on the culture system were evaluated. Two monkey kidney cell cultures (i.e., Vero and BSC-1 cells) were then employed to demonstrate the ICC-MS method could detect infectious viruses in samples collected throughout a full-scale wastewater treatment plant. Our results suggest that the ICC-MS method is able to detect multiple infectious viruses in wastewater, and identifies viruses at the strain-level rapidly. The ICC-MS method can be easily adopted for detecting other viruses in water samples.

4.2 Materials and methods

4.2.1 Wastewater samples and concentration

Municipal wastewater primary influent, effluent pre-UV disinfection, and final effluent samples were collected from autosamplers at the Ann Arbor Wastewater Treatment Plant between June and September in 2018. Samples were collected in sterile containers and transported on ice

to the laboratory at the University of Michigan, Ann Arbor. Wastewater samples were concentrated with ultrafiltration methods, which have achieved higher recoveries of both enveloped and nonenveloped viruses than other virus concentration methods.[20, 21] In brief, wastewater samples were concentrated 50 × in volume with an REXEED 25S dialysis filter (Asahi Kasei Medical) or a Pellicon XL 30 kDa ultrafilter (Millipore). The concentrates were filter sterilized with 0.22 μm poly(ether sulfone) (PES) membranes (Millipore) to remove bacteria contamination that can be potentially introduced to cell culture. The final concentrated wastewater samples were aliquoted and stored at -80 °C before use.

4.2.2 Viruses and cell lines

Murine hepatitis virus (MHV) strain A59 and its host L2 cell lines (Table C-1) were used as a model system for detection by an integrated cell culture/mass spectrometry (ICC-MS) method. L2 cells were maintained in Dulbecco's Modified Eagle Medium (DMEM, Life Technologies 11960) supplemented with 10% newborn bovine serum (Life Technologies), 2 mM of L-glutamine (Life Technologies), 1% (v/v) of penicillin/streptomycin (Life Technologies) at 37 °C, 5% CO_2. MHV was propagated in DBT cell lines according to a previously published method. Briefly, DBT cells were grown to 80% confluency, and infected by MHV at a multiplicity of infection (MOI) of 0.1 plaque forming units (PFU) per DBT cell. Infected cells were incubated in DMEM (Life Technologies 11960) with 2% newborn bovine serum at 37 °C and 5% CO_2 for 48 h. After incubation, cells were frozen and then thawed. Cell debris was removed by centrifuging the sample at 3,000 × g for 5 min. The supernatant was collected and filtered through a 0.22 μm PES membrane. The final MHV stocks (~10^6 PFU mL^{-1}) were aliquoted and stored at -80 °C.

Monkey kidney cells include Vero cells and BSC-1 cells (Table C-1) were used as generic cell lines for culturing human viruses in wastewater concentrates. Vero and BSC-1 cells were grown in DMEM (Life Technologies 12430) with 10% newborn bovine serum, 1% (v/v) penicillin/streptomycin at 37 °C and 5% CO_2.

4.2.3 Virus infection and culturing

Initial proof-of-concept experiments were conducted in the MHV-L2 culture systems. For these, MHV stock was added to DMEM with 2% newborn bovine serum to reach final concentrations of 300, 30, and 3 PFU mL^{-1}. At the time of infection, cells were first washed with ice-cold PBS (Life Technologies 10010). 1.2 mL of each concentration was then inoculated into cells grown to ~80-90% confluency in culture plates (~23 cm^2). Consequently, the total inoculated MHV was 360 PFU, 36 PFU, and 3.6 PFU per 23 cm^2, and the ratio of the infectious MHV particles to cells was approximately 0.001, 0.0001 and 0.00001, respectively. The inoculated samples were incubated with cells for 1 h at 37 °C, with manually rocking every 15 min. The inoculum was then removed, and fresh DMEM containing 2% newborn bovine serum was added to sustain minimum cell growth. After culturing, protein samples were extracted (see Protein extraction) between 12 to 42 hours post infection at intervals of 6 hours.

To test the impact of wastewater components on the performance of the ICC-MS method, MHV stock was spiked into wastewater concentrates to reach the same final concentrations of 300, 30, and 3 PFU mL^{-1}. The control experiments in the MHV-L2 culture systems were then conducted in the same procedures of cell infection. Proteins were extracted at 18 and 24 hours post infection from the cells inoculated with 360 PFU, 30 and 36 hours post infection from the cells inoculated with 36 PFU, and 42 and 48 hours post infection from the cells inoculated with 3.6 PFU.

For experiments to detect viruses in wastewater samples, wastewater concentrates without further purification were directly added to cell monolayers of monkey cell culture systems, using the same procedures of virus inoculation. Cytopathic effects (CPE) were observed daily. Vero and BSC-1 cells were replenished with fresh DMEM containing 2% newborn bovine serum at the 7 days post infection, and incubated for a total of 14 days. Negative controls were inoculated with virus-free PBS rather than wastewater extract.

4.2.4 Protein extraction

Proteins were collected from the cell monolayer at various times post inoculation with the MHV viruses or the wastewater extracts. Briefly, liquid culture media in the culture systems was removed, and cells were washed with ice-cold PBS. 100 μL of Triton X-114 buffer (20 mM Tris-HCl, 150 mM NaCl, 0.5% Triton X-114, pH 8) was added to lyse cells on ice. Cell lysates vortexed and centrifuged at 3000 × g for 5 min at 4 °C to pellet nuclei. The supernatant was collected for phase separation to harvest hydrophilic proteins in the aqueous phase and amphiphilic proteins (i.e., integral proteins) in the detergent phase according to a previously published method.[22] The hydrophilic portion of the proteins was precipitated with 25% (v/v) trichloroacetic acid by centrifuging at 14 000 × g for 10 min at 4 °C and then washed twice with cold (-20 °C) acetone. Protein pellets were saved at -80 °C until they were protease digested.

4.2.5 Protein digestion and LC-MS/MS analysis

Protein pellets were dissolved in a reducing buffer (8 M urea, 100 mM dithiothreitol, 50 mM Tris-HCl, pH 8), and denatured by boiling for 3 min. The undissolved fraction was removed by

centrifuging at 14, 000 × g for 5 min. The supernatant was transferred to a Microcon 10 kDa centrifugal filter unit (Millipore), and proteins were protease treated based on a filter-aided sample preparation protocol.[23] After overnight digestion with trypsin (Worthington), peptides were analyzed on a liquid chromatography-tandem mass spectrometry (LC-MS/MS) system. Specifically, peptides were separated in a Dionex UltiMate 3000 LC system (ThermoFisher Scientific) equipped with an Accucore aQ column (50 nm × 2.1 mm, 2.6 μm particle size, ThermoFisher Scientific) protected by an Accucore aQ Defender guard column (ThermoFisher Scientific). 20 μL samples were loaded onto the system at a flow rate of 200 μL min^{-1}. The solvent gradient began at 94% solution A (Milli-Q water with 0.1% formic acid) and 6% solution B (LC-MS grade acetonitrile with 0.1% formic acid) for 3 min. Solution B was then linearly increased to 40% over 30 min, followed by a linear increase to 80% over 2 min, and then maintained at 80% B for 5 min. B was then decreased to 6% and maintained there for 5 min to equilibrate the column. Eluted peptides were analyzed with a Q Exactive Orbitrap high-resolution mass spectrometer (ThermoFisher Scientific) in positive ion mode. Settings for the full mass spectrometry (MS) scans and data-dependent tandem mass spectrometry (dd-MS^2) scans are provided in Table C-2.

4.2.6 MS data analysis

Raw MS data was analyzed with MASCOT Distiller software (2.6.1.0) connected to a local server. Protein database of *Homo sapiens* (174238 sequences, released on September 14th, 2018) and *Mus musculus* (83937 sequences, released on September 14th, 2018) in the FASTA format were downloaded from the UniProtKB. The viral protein database was downloaded from the UniProtKB taxonomic divisions as uniport_sprot_viruses.dat (28453 sequences, modified on September 12th, 2018), and converted to FASTA format with InSilicoSpectro::Databanks modules.

All databases were uploaded to the MASCOT local server. MS results related to the L2 culture system were searched against the *Mus musculus* database and the SwissProt virus database. MS results related to Vero and BSC-1 culture systems were searched against the *Homo sapiens* database and the SwissProt virus database. Carbamidomethylation of cysteine residues was selected as a fixed modification. N-terminal acetylation and methionine oxidation were set as variable modifications. The peptide mass tolerance was set at less than 10 ppm and the fragment mass tolerance was set at less than 0.3 Da. The false discovery rate (FDR) was calculated with a decoy database, and an FDR of less than 0.01 was set for all searches. The significance of peptide sequence (p-values) was defined as less than 0.01, and the peptide expectation (E) value was set at less than 0.001. Protein identification was considered positive when at least two distinct peptides from that protein were detected.

The sequence coverage of a target protein was calculated based on the detected peptide sequences that were assigned to the protein and the length of the protein reported in database:

$$\text{Protein sequence coverage } (\times 100\%) = \frac{\#\ of\ amino\ acids\ detected\ in\ peptides}{Total\ \#\ of\ amino\ acids\ in\ the\ full\ length\ of\ protein\ sequence}.$$

4.3 Results and discussion

4.3.1 Identification of MHV by LC-MS/MS in culture media

Proteins associated with host cells were the most identified in all samples (Data not shown). MHV nucleoproteins were positively detected at 18 hours post infection (hpi) when cells were inoculated with 360 PFU of MHV, at 24 hpi when cells were inoculated with 36 PFU, and at 36 hpi when inoculated with 3.6 PFU (Figure 4.1). Higher sequence coverage of MHV nucleoproteins was observed as the culturing period extended (Figure 4.1; Table C-3). Approximately 30%

coverage was observed for the inoculation of 360 PFU at 27 hpi and 36 PFU at 38 hpi (Figure 4.1). For the 3.6 PFU inoculation, only 12% of nucleoproteins were detected at 42 hpi. At this low MHV inoculation, if cells infection is assumed to follow Poisson probability distribution,[24] majority of cells may not have received an infectious MHV particle (>99.999%), thus explaining why the overall viral protein synthesis was slower. In addition to nucleoproteins, coronavirus spike glycoproteins were also detected at greater hpi in one sample (Table C-3). However, the protein sequence coverage of spike glycoproteins was lower compared to that of nucleoproteins. No viral proteins were detected in negative controls where cells were inoculated with virus-free PBS. These control experiments with the MHV model demonstrated that the ICC-MS method could detect viruses and that the time required for detection depends on the number of infectious viruses in the sample.

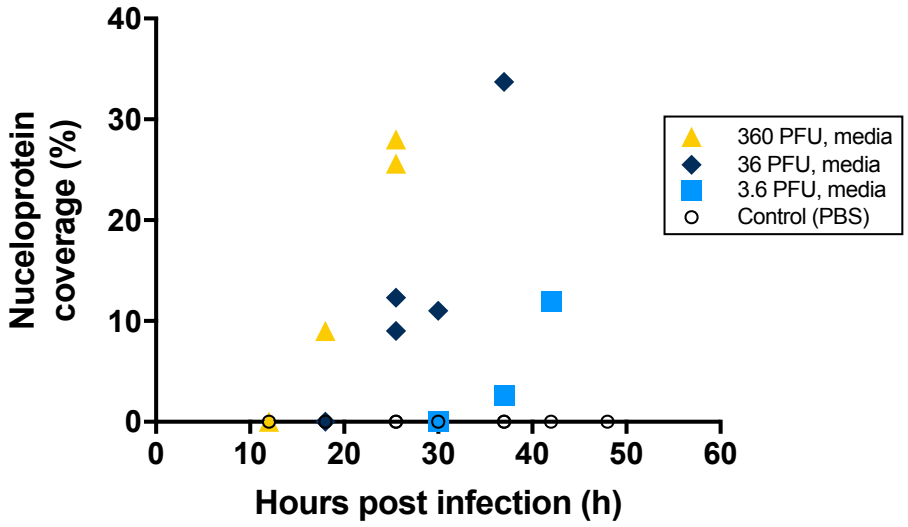

Figure 4.1 Sequence coverage of MHV nucleoproteins detected by LC-MS/MS with respect to hours post infection. MHV was suspended in growth culture media. Negative controls consisted of cells infected with virus-free PBS.

Interestingly, the detected peptide sequences of MHV nucleoproteins made it possible to identify the MHV virus at the strain level. Specifically, the peptide SFVPGQENAGGR with an acetylation modification at the N-terminus was detected early, and this peptide is unique to MHV strain A59 (P03416) and MHV strain 3 (P18447) (Table C-3; Figure C-1). The nucleoproteins of other MHV strains possess peptide SFVPGQENASGR (Figure C-1) at the same position with an S residue at position 11 rather than a G residue. At higher MHV nucleoprotein coverage (i.e., at greater hpi), another unique peptide, namely LGTSDPQFPILAELAPTVGAFFFGSK, helped differentiate strain A59 and strain 3 from other strains (Table C-3; Figure C-1). However, the polymorphisms in nucleoproteins may limit the strain identification to some extent. The detected peptides were not able to distinguish strain A59 from strain 3. This is because the nucleoprotein sequences of these two strains have a similarity of 99.8%, and only vary by one amino acid residue at position 17.

4.3.2 Identification of MHV in concentrated wastewater samples

To test the impact of wastewater samples on the ICC-MS method, we suspended MHV in concentrated influent and effluent wastewater samples and conducted follow-up experiments. We hypothesized that if the wastewater inhibits protein synthesis, fewer viruses will be propagated in the culture system. Infectious MHV propagated and released into the liquid media was first tracked post inoculation by plaque assays. MHV propagation curves were similar when the cells were inoculated with MHV in concentrated wastewater or with MHV in growth media (Figure C-2). This suggests that virus infection was not affected by components in the concentrated wastewater samples.

The cell systems inoculated with MHV in wastewater concentrates were also analyzed with the ICC-MS method. Consistent with the results when MHV in media was added to cells, nucleoproteins of MHV strains A59 and 3 were positively identified in all samples except for the sample collected at 42 hpi of 3.6 PFU inoculation in wastewater influent (Table C-4). Approximately 30% to 40% coverage of MHV nucleoproteins was observed for the inoculation of 360 PFU at 24 hpi, 36 PFU at 36 hpi, and 3.6 PFU at 48 hpi (Figure 4.2). The sequence coverage for MHV in wastewater concentrates was also comparable to the experiments conducted in culture media. These results demonstrate that protein synthesis was not inhibited when the cells were exposed to the concentrated wastewaters.

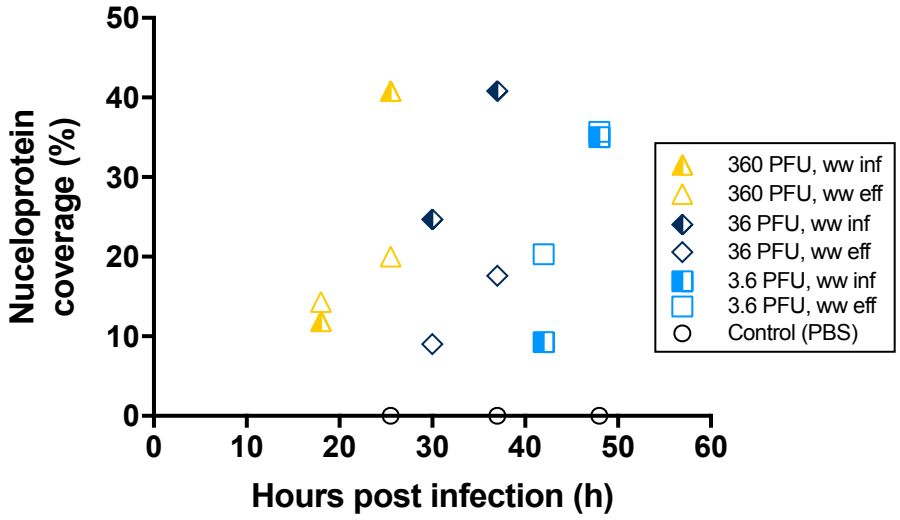

Figure 4.2 MHV nucleoprotein coverage detected by LC-MS/MS at hours post infection. MHV was suspended in concentrated wastewater influent (ww inf) and concentrated wastewater effluent (ww eff). Negative controls were fake infected with virus-free PBS.

Previous work suggests that wastewater can impact cell cultures.[1] It is possible that we avoided these issues by filtering our wastewater samples through filters with 0.22 µm pores. We did

observe bacterial contamination when the wastewater was pre-filtered through 0.45 μm pores rather than 0.22 μm pores (data not shown). Previous studies have conducted organic solvent extractions to remove wastewater toxicity (e.g., Freon, chloroform), but we avoided these steps due to their impact on enveloped viruses.[25,26]

The experiments with MHV in wastewater suggest that the ICC-MS can detect infectious viruses in wastewater samples. Here, we used the nucleoproteins for identification due to the consistent detection and high sequence coverage compared to other viral proteins (i.e., spike glycoproteins) identified in our experiments. In MHV, nucleoproteins are the most abundant proteins.[27] The peptides from the most abundant viral proteins are more likely to be captured earlier by MS. Work on MS-based detection of influenza A viruses in clinical samples reported the correct strains with nucleoprotein peptides when the protein sequence coverage was 30-40%.[19] Evolutionary analyses on the abundant viral capsid proteins of iridoviruses suggests that major capsid proteins are highly conserved but also diverse enough to distinguish close isolates.[28] These findings suggest that the abundant proteins such as nucleoproteins and major capsid proteins are suitable for virus identification.

4.3.3 Identification of infectious viruses in wastewater samples by ICC-MS/MS method

Two monkey kidney cell lines (Vero and BSC-1) were used to detect infectious viruses in the concentrated wastewater samples by the ICC-MS method. Vero and BSC-1 cells have been used to isolate polioviruses, coxsackieviruses, echoviruses, reoviruses, and adenoviruses from sewage samples in a previous study.[25] Here, sewage samples were inoculated to cell cultures and incubated 10 days for the observation of cytopathic effects. Supernatants were collected from the cells with positive cytopathic effects and passaged for another two rounds of 10-day culturing for the

confirmation of positive cytopathic effects. Viruses were finally identified based on immuno-based clinical assays.[25]

We applied the same inoculation procedures as we did in the MHV proof-of-concept experiments to infect Vero and BSC-1 cells with concentrated wastewater samples. Throughout the 14-day culture period, cells did not show clear cytopathic effects, and no cells were observed detaching from the culture plates. The same protein extraction method that was developed in the MHV culture system was applied to extract proteins from Vero and BSC-1 cells at 14 days post infection (dpi). Control cells were inoculated with virus-free PBS.

Virus detection in the influent samples

In both Vero and BSC-1 culture systems, proteins associated with *homo sapiens* are the most identified (data not shown). In addition, in the Vero cell extracts, a number of reovirus proteins were detected (Table 4.1). Reovirus proteins mu-1 and sigma-3 had consistently high sequence coverage (30%-40%) from the cells inoculated with influent samples, followed by sigma-2, sigma-NS and mu-NS proteins of approximately 20% sequence overage. The coverage of lambda-1 and mu-2 varied significantly in two influent samples. Proteins lambda-2, and lambda-3 had sequence coverage less than 10%. Contrary to the Vero samples, no viral proteins were detected in the BSC-1 cell extracts.

A reovirus particle contains 8 distinct virion proteins that assemble into an outer protein capsid containing mu-1, sigma-1, sigma-3, lambda-2 proteins and an inner protein capsid containing proteins lambda-1, lambda-3, sigma-2, mu-2.[29] Three nonstructural proteins are involved in the virus replication cycle,[30-32] namely sigma-NS, mu-NS, and sigma-1s. The consistently high sequence coverage of mu-1 and sigma-3 proteins in our study suggests that these two proteins were

the most abundant in the cell culture system. Indeed, mu-1 and sigma-3 proteins are the major outer capsid proteins in reoviruses, with 600 copies in one reovirus particle (Table C-5). Based on the results in MHV control experiments, we would use the mu-1 and sigma-3 proteins for the strain-level identification of reoviruses. Protein mu-1 and sigma-3 of both type 1 and type 3 strains were identified, suggesting the coexistence of infectious reovirus type 1 and type 3 in the influent samples. Reovirus type 2 was detected in the influent samples based on peptides in protein sigma-3 (coverage = 16 % in average), but peptides from protein mu-1 were not detected. This may be because the protein mu-1 sequences of the three reovirus strains have higher similarities than the three sigma-3 sequences (Figure C-3; Figure C-4); consequently, the chances of detecting unique peptides from protein mu-1 are lower. These results suggest that reovirus type 1, type 2, and type 3 are present in the influent wastewater samples.

Virus detection in the effluent samples

In contrast to the influent samples, only three reovirus proteins were detected in the cells inoculated with the effluent pre-UV treatment (Table 4.1). Sigma-3 proteins of reovirus type 2 and type 3 were detected with sequence coverage of 7% and 15%, respectively. Mu-1 protein of reovirus type 1 was detected with sequence coverage of 6%. Although this assay is not yet quantitative, these results suggest a lower concentration of infectious reoviruses in the effluent samples than in the influent samples. Reovirus proteins were not detected in the cells infected with final effluent, suggesting that the concentrations of infectious reoviruses decreased further through the UV disinfection treatment. These negative results can be interpreted that infectious reoviruses in the final effluent was too low to capture in 1.2 mL of the wastewater concentrate samples that were used for inoculation. In this concentrate sample, 1.2 mL of the concentrate corresponded to

60 mL of the effluent, which suggests that the infectious concentrations of reoviruses in the final effluent are no higher than 16.7 infectious particles/L if single infectious reovirus can be detected by the ICC-MS method after 14-day culturing.

Contrary to the Vero culture system, negative results were observed for all effluent samples in the BSC-1 culture system. BSC-1 cells have been more applied for polioviruses surveillance in water;[33] polioviruses, however, are unlikely to be present in Ann Arbor wastewater samples. This result highlights the importance of the cell types used for an ICC-MS method, because only the viruses that can grow in the cell lines will be detectable by mass spectrometry. Our ongoing work is exploring the application of other cell lines in this method.

By applying the ICC-MS method, we detected infectious reovirus type 1, type 2, and type 3 in the primary influent samples, and we found peptides from reovirus type 1, type 2, and type 3 in the effluent pre-UV samples. This suggests that infectious reoviruses persist after primary and secondary treatment. As mentioned above, no infectious reoviruses were detected in the 60 mL of disinfected effluent.

Table 4.1 Proteins detected in extracts from Vero cells. Vero cells were inoculated with different wastewater samples, and incubated for 14 days.

Primary influent 1, 50× concentrate			
Accession number	**Protein description**	**Sequence coverage (%)**	**Protein score**
P11077	mu-1, Reovirus type 1 (strain Lang)	32	1287
P11078	mu-1, Reovirus type 3 (strain Dearing)	28	918
P03527	sigma-3, Reovirus type 3 (strain Dearing)	24	695
P30211	sigma-3, Reovirus type 2 (strain D5/Jones)	13	503
P07939	sigma-3, Reovirus type 1 (strain Lang)	25	489
P03525	sigma-2, Reovirus type 3 (strain Dearing)	25	204
P11314	sigma-2, Reovirus type 1 (strain Lang)	26	193
P07940	sigma-NS, Reovirus type 1 (strain Lang)	19	418
P03526	sigma-NS, Reovirus type 3 (strain Dearing)	17	384
P12419	mu-NS, Reovirus type 3 (strain Dearing)	17	601

Q9PY83	mu-NS, Reovirus type 1 (strain Lang)	13	428
Q9WAB2	lambda-1, Reovirus type 1 (strain Lang)	7	453
P15024	lambda-1, Reovirus type 3 (strain Dearing)	7	453
P11079	lambda-2, Reovirus type 3 (strain Dearing)	3	128
Q00335	mu-2, Reovirus type 1 (strain Lang)	3	90
P12418	mu-2, Reovirus type 3 (strain Dearing)	3	90
Primary influent 2, 50× concentrate			
Accession number	**Protein description**	**Sequence coverage (%)**	**Protein score**
P11077	mu-1, Reovirus type 1 (strain Lang)	40	1765
P11078	mu-1, Reovirus type 3 (strain Dearing)	36	1400
P03527	sigma-3, Reovirus type 3 (strain Dearing)	43	1234
P07939	sigma-3, Reovirus type 1 (strain Lang)	38	1029
P30211	sigma-3, Reovirus type 2 (strain D5/Jones)	27	862
Q9WAB2	lambda-1, Reovirus type 1 (strain Lang)	29	1975
P12419	mu-NS, Reovirus type 3 (strain Dearing)	24	1165
Q9PY83	mu-NS, Reovirus type 1 (strain Lang)	19	931
P12418	mu-2, Reovirus type 3 (strain Dearing)	17	619
P03526	sigma-NS, Reovirus type 3 (strain Dearing)	22	720
P07940	sigma-NS, Reovirus type 1 (strain Lang)	24	684
P03525	sigma-2, Reovirus type 3 (strain Dearing)	17	323
P11314	sigma-2, Reovirus type 1 (strain Lang)	19	318
Q91RA6	lambda-2, Reovirus type 1 (strain Lang)	9	516
P11079	lambda-2, Reovirus type 3 (strain Dearing)	7	330
P0CK32	lambda-3, Reovirus type 1 (strain Lang)	3	105
Effluent pre-UV, 50× concentrate			
Accession number	**Protein description**	**Sequence coverage (%)**	**Protein score**
P03527	sigma-3, Reovirus type 3 (strain Dearing)	15	199
P30211	sigma-3, Reovirus type 2 (strain D5/Jones)	7	118
P11077	mu-1, Reovirus type 1 (strain Lang)	6	160
Final effluent, 50× concentrate			
No viral protein hit			
Negative control, inoculated with virus-free PBS			
No viral protein hit			

4.3.4 Environmental implications

Results from this proof-of-concept work on the development of an ICC-MS method suggests that it holds promise for the detection of infectious viruses in environmental water samples. The ICC-MS method identifies viruses more directly than ICC-PCR methods, as it avoids the need of primer design and assay development for each strain detected. In our study, the sample preparation and MS detection protocols that have been developed with a mouse virus and its host cells can be

easily adopted for other virus detection in different culture systems. Moreover, the MS technique can readily identify multiple virus strains, given their sequences are present in the database. We were able to detect three reovirus strains in wastewater with Vero cells that displayed no apparent cytopathic effects, and demonstrated the virus removal/inactivation through a full-scale wastewater treatment. Compared to sequencing methods, which can also identify viruses without designing specific primers, the ICC-MS method has the advantage of needing much less data processing. In our study, the MS data analysis took less than an hour, while metagenomic sequencing data may take several days or weeks to process. Furthermore, since metagenomic methods sequence all of the DNA in a sample, much of the data recovered is not relevant. Consequently, numerous copies of a specific gene need to be present for the organism of interest to be detected. Here, we were able to detect MHV in our wastewater samples when as few as 3 infectious particles were present.

Further research will be required before this method can be broadly applied. Specifically, the ICC-MS method will need to be optimized for different cell lines so that a range of viruses can be detected. Ideally, cell lines that can detect several human viruses at once would be selected for environmental monitoring. The impact of multiple virus infection will need to be assessed as it is possible that only the fastest replicating viruses will be identified. Finally, it is worth pointing out that at this point the method is qualitative or semi-quantitative. We believe the method could be readily modified to become quantitative by developing a most-probable-number type method. Here, sequential dilutions of the wastewater are assessed simultaneously, and statistics performed on the positive/negative replicates can provide a value of the infective viruses present in the sample.

4.4 References

(1) Schmidt, N. J.; Ho, H. H.; Riggs, J. L.; Lennette, E. H. Comparative sensitivity of various cell culture systems for isolation of viruses from wastewater and fecal samples. *Appl. Environ. Microbiol.* **1978**, *36* (3), 480–486.

(2) Farré, M.; Barceló, D. Toxicity testing of wastewater and sewage sludge by biosensors, bioassays and chemical analysis. *Trends Analyt. Chem.* **2003**, *22* (5), 299–310.

(3) Reynolds, K. A.; Gerba, C. P.; Abbaszadegan, M.; Pepper, I. L. ICC/PCR detection of enteroviruses and hepatitis A virus in environmental samples. *Can. J. Microbiol.* **2001**, *47*, 153–157.

(4) Gallagher, E. M.; Margolin, A. B. Development of an integrated cell culture—Real-time RT-PCR assay for detection of reovirus in biosolids. *J. Virol. Methods* **2007**, *139* (2), 195–202.

(5) Rigotto, C.; Victoria, M.; Moresco, V.; Kolesnikovas, C. K.; Corrêa, A. A.; Souza, D. S. M.; Miagostovich, M. P.; Simões, C. M. O.; Barardi, C. R. M. Assessment of adenovirus, hepatitis A virus and rotavirus presence in environmental samples in Florianopolis, South Brazil. *J. Appl. Microbiol.* **2010**, *109* (6), 1979–1987.

(6) Reynolds, K. A.; Gerba, C. P.; Pepper, I. L. Detection of infectious enteroviruses by an integrated cell culture-PCR procedure. *Appl. Environ. Microbiol.* **1996**, *62* (4), 1424–1427.

(7) Lee, H. K.; Lee, H. K.; Jeong, Y. S.; Jeong, Y. S. Comparison of total culturable virus assay and multiplex integrated cell culture-PCR for reliability of waterborne virus detection. *Appl. Environ. Microbiol.* **2004**, *70* (6), 3632–3636.

(8) Green, J.; Henshilwood, K.; Gallimore, C. I.; Brown, D. W.; Lees, D. N. A nested reverse transcriptase PCR assay for detection of small round-structured viruses in environmentally contaminated molluscan shellfish. *Appl. Environ. Microbiol.* **1998**, *64* (3), 858–863.

(9) Kojima, S.; Kageyama, T.; Fukushi, S.; Hoshino, F. B.; Shinohara, M.; Uchida, K.; Natori, K.; Takeda, N.; Katayama, K. Genogroup-specific PCR primers for detection of Norwalk-like viruses. *J. Virol. Methods* **2002**, *100* (1-2), 107–114.

(10) Johansson, H.; Bzhalava, D.; Ekström, J.; Hultin, E.; Dillner, J.; Forslund, O. Metagenomic sequencing of "HPV-negative" condylomas detects novel putative HPV types. *Virology* **2013**, *440* (1), 1–7.

(11) Aebersold, R.; Mann, M. Mass spectrometry-based proteomics. *Nature* **2003**, *422* (6928), 198–207.

(12) Dančík, V.; Addona, T. A.; Clauser, K. R.; Vath, J. E.; Pevzner, P. A. De Novo Peptide Sequencing via Tandem Mass Spectrometry. *J. Comput. Biol.* **1999**, *6* (3-4), 327–342.

(13) Syka, J. E. P.; Coon, J. J.; Schroeder, M. J.; Shabanowitz, J.; Hunt, D. F. Peptide and protein sequence analysis by electron transfer dissociation mass spectrometry. *Proc. Natl. Acad. Sci.* **2004**, *101* (26), 9528–9533.

(14) Kooken, J.; Fox, K.; Fox, A.; Wunschel, D. Assessment of marker proteins identified in whole cell extracts for bacterial speciation using liquid chromatography electrospray ionization tandem mass spectrometry. *Mol. Cell Probes* **2014**, *28* (1), 34–40.

(15) Tracz, D. M.; McCorrister, S. J.; Chong, P. M.; Lee, D. M.; Corbett, C. R.; Westmacott, G. R. A simple shotgun proteomics method for rapid bacterial identification. *Journal of Microbiological Methods* **2013**, *94*, 54–57.

(16) Ray Bakhtiar, A.; John J Thomas; Gary Siuzdak. Mass spectrometry in viral proteomics. *Acc. Chem. Res.* **2000**, *33* (3), 179–187.

(17) Calderaro, A.; Arcangeletti, M. C.; Rodighiero, I.; Buttrini, M.; Montecchini, S.; Simone, R. V.; Medici, M. C.; Chezzi, C.; De Conto, F. Identification of different respiratory viruses, after a cell culture step, by matrix assisted laser desorption/ionization time of flight mass spectrometry (MALDI-TOF MS). *Sci. Rep.* **2016**, *6* (1), 36082.

(18) Nguyen, A. P.; Downard, K. M. Proteotyping of the parainfluenza virus with high-resolution mass spectrometry. *Anal. Chem.* **2013**, *85*, 1097–1105.

(19) Majchrzykiewicz-Koehorst, J. A.; Heikens, E.; Trip, H.; Hulst, A. G.; de Jong, A. L.; Viveen, M. C.; Sedee, N. J. A.; van der Plas, J.; Coenjaerts, F. E. J.; Paauw, A. Rapid and generic identification of influenza A and other respiratory viruses with mass spectrometry. *J. Virol. Methods* **2015**, *213*, 75–83.

(20) Ye, Y.; Ellenberg, R. M.; Graham, K. E.; Wigginton, K. R. Survivability, partitioning, and recovery of enveloped viruses in untreated municipal wastewater. *Environ. Sci. Technol.* **2016**, *50*, 5077–5085.

(21) Hill, V. R.; Polaczyk, A. L.; Hahn, D.; Jothikumarr, N.; Cromeans, T. L.; Roberts, J. M.; Amburgey, J. E. Development of a rapid method for simultaneous recovery of diverse microbes in drinking water by ultrafiltration with sodium polyphosphate and surfactants. *Appl. Environ. Microbiol.* **2005**, *71* (11), 6878–6884.

(22) Bordier, C. Phase separation of integral membrane proteins in triton X-114 solution. *J. Biol. Chem.* **1981**, *256*, 1604–1607.

(23) Wiśniewski, J. R.; Zougman, A.; Nagaraj, N.; Mann, M. Universal sample preparation method for proteome analysis. *Nat. Meth.* **2009**, *6* (5), 359–362.

(24) Dixit, N. M.; Perelson, A. S. Multiplicity of human immunodeficiency virus infections in lymphoid tissue. *J. Virol.* **2004**, *78* (16), 8942–8945.

(25) Payment, P.; Ayache, R.; Trudel, M. A survey of enteric viruses in domestic sewage. *Can. J. Microbiol.* **2011**, *29* (1), 111–119.

(26) Lewis, M. A.; Nath, M. W.; Johnson, J. C. A multiple extraction–centrifugation method for the recovery of viruses from waste water treatment plant effluents and sludges. *Can. J. Microbiol.* **2011**, *29* (12), 1661–1670.

(27) Ye, Y.; Hauns, K.; Langland, J. O.; Jacobs, B. L.; Hogue, B. G. Mouse hepatitis coronavirus A59 nucleocapsid protein is a type I interferon antagonist. *J. Virol.* **2007**, *81* (6), 2554–2563.

(28) Tidona, C. A.; Schnitzler, P.; Kehm, R.; Darai, G. Is the major capsid protein of iridoviruses a suitable target for the study of viral evolution? *Virus Genes* **1998**, *16* (1), 59–66.

(29) Dryden, K. A.; Wang, G.; Yeager, M.; Nibert, M. L.; Coombs, K. M.; Furlong, D. B.; Fields, B. N.; Baker, T. S. Early steps in reovirus infection are associated with dramatic changes in supramolecular structure and protein conformation: analysis of virions and subviral particles by cryoelectron microscopy and image reconstruction. *J. Cell Biol.* **1993**, *122* (5), 1023–1041.

(30) Gomatos, P. J.; Prakash, O.; Stamatos, N. M. Small reovirus particle composed solely of sigma NS with specificity for binding different nucleic acids. *J. Virol.* **1981**, *39* (1), 115–124.
(31) Boehme, K. W.; Guglielmi, K. M.; Dermody, T. S. Reovirus nonstructural protein σ1s is required for establishment of viremia and systemic dissemination. *Proc. Natl. Acad. Sci.* **2009**, *106* (47), 19986–19991.
(32) Shelton, I. H.; Kasupski, G. J., Jr; Oblin, C.; Hand, R. DNA binding of a nonstructural reovirus protein. *Can. J. Biochem.* **1980**, *59* (2), 122–130.
(33) Gerba, C. P.; Sobsey, M. D.; Wallis, C.; Melnick, J. L. Adsorption of poliovirus onto activated carbon in wastewater. *J. Chem. Eng.* **1975**, *9* (8), 727–731.

Chapter 5 Significance and implications

5.1 Overview

This dissertation research seeks to advance our current state of knowledge on the detection and fate of nonenveloped viruses in water environments. The outcomes help fill the knowledge gaps of treating enveloped viruses in wastewater and monitoring infectious viruses in water samples. This dissertation begins to explore the survivability and partitioning of model enveloped viruses in municipal wastewater (Chapter 2). Lab-scale experiments and computational simulations were used to quantitatively characterize the inactivation of model viruses in liquid and solids fractions of wastewater and the partitioning of model viruses to wastewater solids. The knowledge obtained from the experiments facilitated the optimization of an ultrafiltration method for concentrating infectious enveloped viruses from wastewater with high recovery rates (Chapter 2). Chapter 3 focuses on the inactivation of enveloped viruses with common disinfectants. Considering the difficulties with studying the inactivation kinetics of highly pathogenic enveloped viruses and viruses that are nonculturable, we developed a framework to understand the inactivation of enveloped viruses on a molecular basis. Virus infectivity, reactions in lipids and proteins, and reactions in nucleic acids following the treatment by common disinfectants were tracked by cell culture assays, quantitative mass spectrometry, and molecular polymerase chain reaction (PCR) techniques. Finally, Chapter 4 reports an integrated cell culture-mass spectrometry (ICC-MS) method for detecting infectious viruses. This ICC-MS method was developed and optimized with an enveloped murine coronavirus and its culture system, and was then validated

by applying it to detect infectious viruses in wastewater samples collected throughout a full-scale municipal wastewater treatment plant. Major findings from this dissertation research and their implications for water quality control and viral disease control are discussed in detail below.

5.2 Implications for operations of wastewater treatment plants

Our findings from the survivability of enveloped viruses underscore that enveloped viruses can persist in wastewater, especially at cooler temperatures.[1-3] Considering that outbreaks of certain enveloped virus diseases peak during the winter, higher concentrations of infectious enveloped viruses may be present in wastewater during winter. Further studies on enveloped virus removal throughout wastewater treatment plants should focus more on removal during conditions of cooler temperatures.

Enveloped viruses tended to partition to a greater extent to wastewater solids than nonenveloped viruses. Consequently, a larger fraction of enveloped viruses is expected to be removed by primary treatment settling. The models developed here were built based on the partitioning experiments at 4 °C. Wastewater temperatures, however, can range from 3 °C to 27 °C.[4] We would expect higher levels of enveloped virus sorption to solids in wastewater at higher temperatures. Another limitation to our sorption study is that when viruses are shed, any can be within fecal solids, whereas we spiked purified model enveloped viruses into the wastewater and observed their partitioning between solids and liquids. The fraction of enveloped viruses that are associated with solids at equilibrium may therefore be underestimated in our study. Given these two points, the fraction of enveloped viruses that are removed in the primary settling tank in real systems is likely to be greater than the fraction estimated in our study.

Our models also indicate that the inactivation kinetics of enveloped viruses in the liquid fraction of wastewater is similar to the inactivation kinetics of enveloped viruses sorbed on the solid surfaces, suggesting that infectious enveloped viruses may persist in sediments. The presence of enveloped virus genes in the sludge of anaerobic reactors have been reported previously.[5] More research regarding the fate of enveloped viruses in solids needs further investigation.

5.3 Implications for predict enveloped virus reactivity with disinfectants

To understand virus susceptibility to disinfectants, culture-based infectivity assays have been used widely to track the loss of virus infectivity following disinfection treatments. However, some enveloped viruses are too dangerous to work with, and many viruses are not culturable. A molecular-based understanding of virus inactivation could help in predicting virus reactivity with disinfectants. The framework developed in our study identifies the molecular features in a model enveloped virus that drive virus inactivation by common disinfectants. Our results demonstrate that the presence of reactive amino acids in viral proteins that are easily accessible by solvents correlate with high virus reactivity with free chlorine. Genome reactions, on the other hand, drive virus inactivation by UV_{254}. The molecular-based understanding of virus inactivation explains the discrepancies of inactivation kinetics among viruses. For example, we were able to identify that the higher resistance of nonenveloped virus MS2 to free chlorine compared to the enveloped virus Phi6 is due to the different reactivities of their proteins. The most reactive peptide in MS2 is 150× less reactive to free chlorine than the most reactive peptide in Phi6. Before generalizations about enveloped virus mechanisms versus non-enveloped virus mechanisms are possible, similar investigations with other model enveloped and nonenveloped viruses must be conducted.

5.4 Implications for virus environmental surveillance

Human viruses are generally at very low concentrations in water environments. It is therefore challenging to monitor their presence and infectivity in water. In this dissertation, we optimized an ultrafiltration method for concentrating infectious viruses from water samples with high recovery rates for both enveloped and nonenveloped viruses. To follow up the concentration method, we developed a new virus detection method that integrates cell culture and mass spectrometry (ICC-MS) for detecting infectious viruses in the concentrated water samples. This ICC-MS method has a number of advantages over other currently available virus detection methods; most notably, the sample preparation and mass spectrometry protocols can be easily adopted for detecting multiple viruses at once, as long as they are propagated in the same culture system. This would not be possible for PCR-based detection methods, which require primer design and PCR assay optimization for different viruses. The ICC-MS detects the most abundant viral proteins that carry conservative but diverse genetic information suitable for virus identification. Data processing by comparing the detected peptide sequences with the sequences available in viral protein database takes less than one hour. This is an advantage over viral genome sequencing, for which data processing may take several days or weeks and requires a supercomputer.

5.5 References

(1) Casanova, L. M.; Jeon, S.; Rutala, W. A.; Weber, D. J.; Sobsey, M. D. Effects of air temperature and relative humidity on coronavirus survival on surfaces. *Appl. Environ. Microbiol.* **2010**, *76* (9), 2712–2717.

(2) Casanova, L. M.; Weaver, S. R. Inactivation of an enveloped surrogate virus in human sewage. *Environ. Sci. Technol. Lett.* **2015**, *2*, 76–78.

(3) Pica, N.; Bouvier, N. M. Environmental factors affecting the transmission of respiratory viruses. *Curr. Opin. Virol.* **2012**, *2* (1), 90–95.

Appendices

Appendix A. Supplementary Information for Chapter 2

Optimization of Ultrafiltration Method. A higher MHV recovery was achieved when the wastewater solids removal step was carried out with filtration through 0.22 μm PES membranes rather than centrifugation at 30,000 × g for 10 min (P = 0.0046; Figure A-3A). Employing 10 kDa ultra-filters for the concentration step resulted in higher and more consistent MHV recoveries compared to 100-kDa ultra-filters (Figure A-3B). In comparison, the specific solids-removal techniques and the 10 kDa versus 100 kDa filter sizes did not impact the MS2 recoveries. Following ultra-filter regeneration, the mean recovery of MHV decreased and the mean recovery of MS2 increased, although neither change was significant (P = 0.2444; Figure S3B).

Recovery of MHV from Wastewater Solids. When solids were collected from the wastewater with centrifugation at 30,000 × g for 10 min., the extraction solution consisting of pH 9.5 glycine buffer resulted in the highest recovery of MHV (3.7% of spiked MHV; Figure A-3C) from the wastewater solids; this recovery was low considering that nearly a quarter of spiked MHV were reversibly adsorbed to solids after incubating for one-hour, and therefore should have been recoverable. The limited recovery may be due to viruses losing infectivity as they are detached from the soil surface, as reported elsewhere.[1] MS2 recoveries were ~2% for all of the tested

extraction solutions; this was not surprising based on the low percentage (6%) of MS2 associated with the wastewater solids at equilibrium.

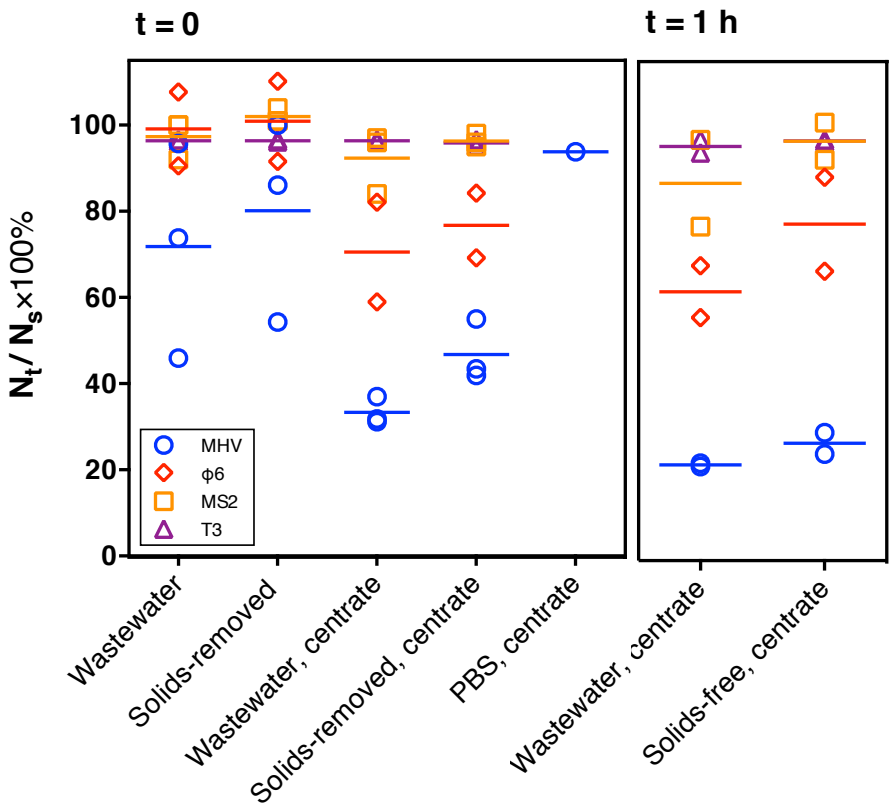

Figure A-1 Virus recovery immediately after viruses were spiked into samples at 4 °C (t = 0) and after 1-hour incubation at 4 °C. Here, $\boldsymbol{N_t}$ (PFU) represents the amount of infective viruses measured at time T; $\boldsymbol{N_s}$ (PFU) is the amount of infective viruses in the spiked aliquots. Bars indicate the mean recovery for each tested viruses.

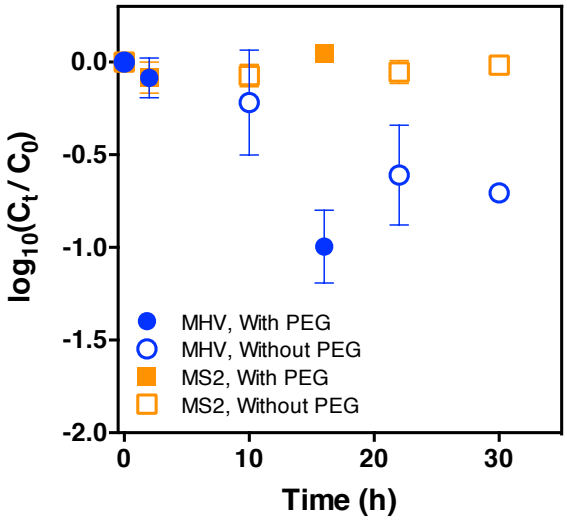

Figure A-2 Virus inactivation in 4 °C wastewater with and without the presence of PEG. Error bars represent the ranges of replicates from wastewater samples collected on different days (n = 2).

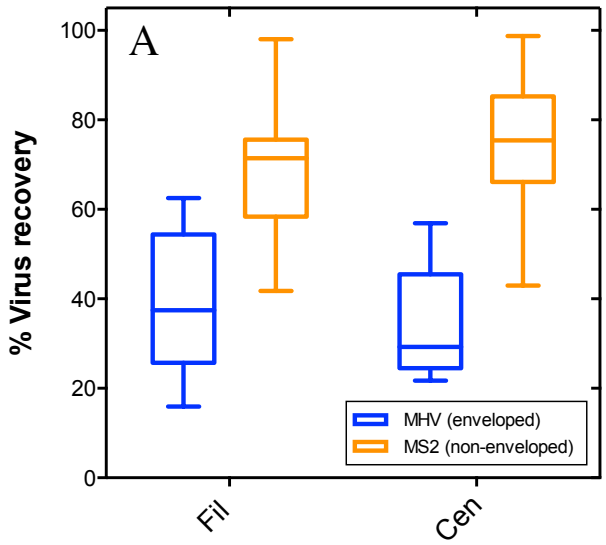
A
% Virus recovery
100
80
60
40
20
0
MHV (enveloped)
MS2 (non-enveloped)
Fil
Cen

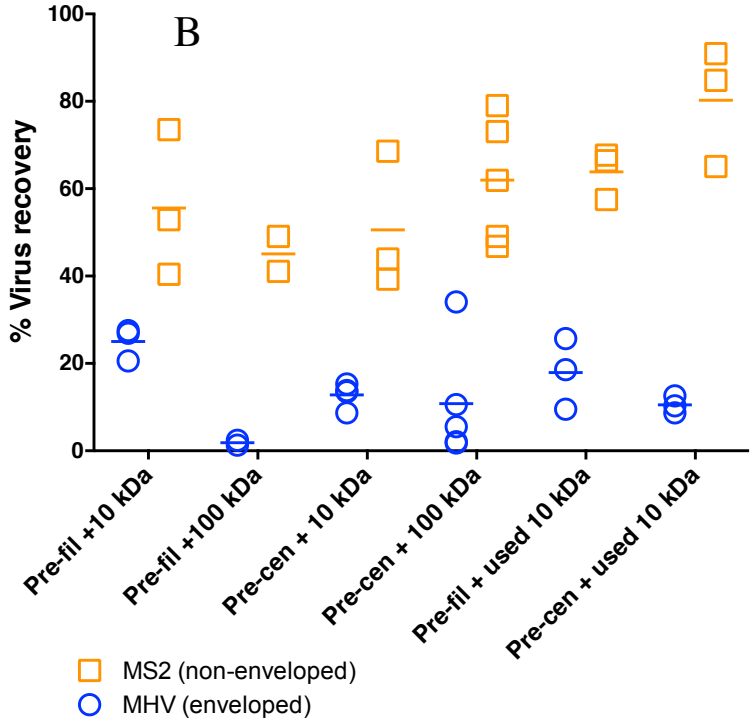
B
% Virus recovery
100
80
60
40
20
0
Pre-fil +10 kDa
Pre-fil +100 kDa
Pre-cen + 10 kDa
Pre-cen + 100 kDa
Pre-fil + used 10 kDa
Pre-cen + used 10 kDa
MS2 (non-enveloped)
MHV (enveloped)

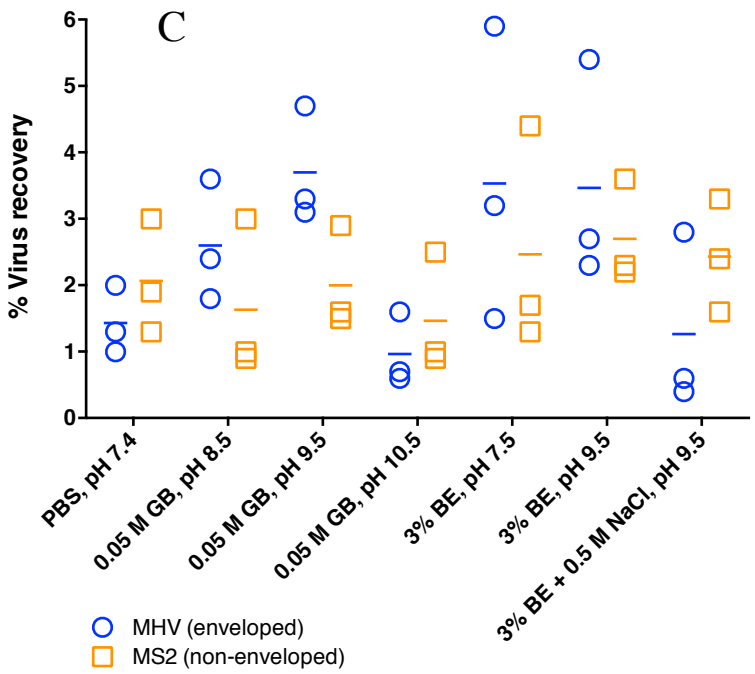

Figure A-3 Method optimization for enveloped virus (MHV) and nonenveloped virus (MS2) in liquid and solid phases: (A) Virus recoveries in liquid fraction of wastewater following solids removal by centrifuging at 30,000 × g for 10 min at 4 °C (Cen), or by centrifugation at 2,500 × g for 5 min at 4 °C followed by 0.22 μm filtration (Fil); (B) Ultrafiltration method tested with pre-filtration and pre-centrifugation, with filter cut-off sizes of 100 kDa and 10 kDa, and with filter reuse. (C) Virus recoveries from wastewater solids collected from wastewater samples by centrifuging at 30,000 × g for 10 min at 4 °C. Tested elution buffers include PBS (pH 7.4), 0.05 M glycine buffer (0.05 M GB, pH 8.5, pH 9.5, and pH 10.5), 3% beef extract (3% BE, pH 7.5 and pH 9.5), and 3% beef extract with 0.5 M sodium chloride (3% BE + 0.5 M NaCl, pH 9.5). Bars represent the average infective virus recoveries of the replicate experiments (n≥3).

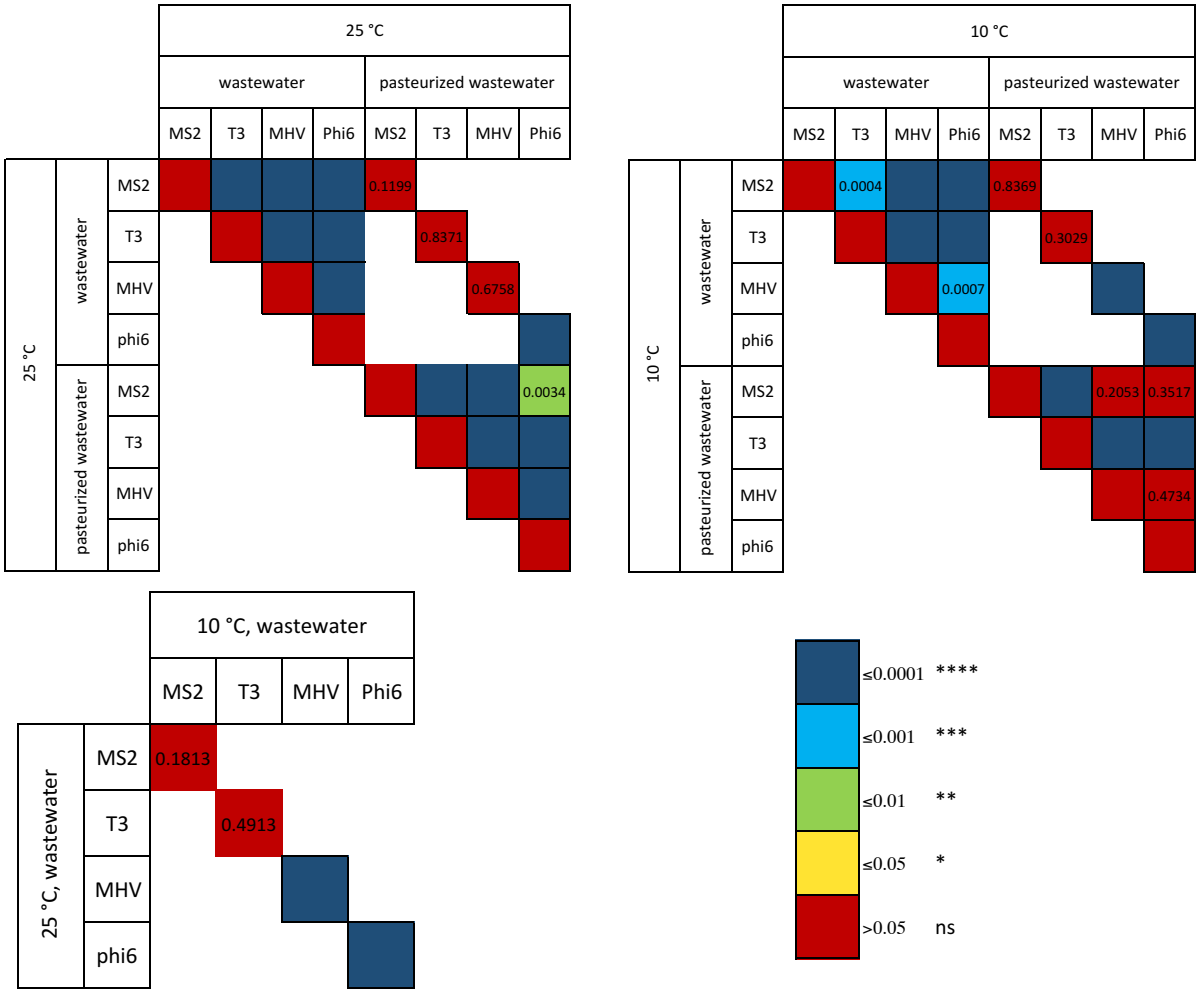

Figure A-4 Statistical significance analysis of virus inactivation kinetics under different conditions.

Table A-1 Wastewater parameters

TSS (mg L^{-1}) [a]	235 ± 97
VSS (mg L^{-1}) [a]	205 ± 85
VSS/TSS [a]	0.87 ± 0.13
pH [a]	7.63 ± 0.25
Total COD (mg COD L^{-1}) [b]	300—768
Background bacteriophage concentrations tested with *E. coli* ATCC 15597 (PFU mL^{-1}) [b]	800—1000

[a]Results from 34 wastewater samples.

[b]Ranges of 3 wastewater samples.

Table A-2 TSS and VSS removal by centrifugation at 30,000 × g for 10 min.

	TSS (VSS) of wastewater samples (mg L^{-1})	**TSS (VSS) after centrifugation (mg L^{-1})**	**TSS (VSS) Removal (%)**
1	327 (297)	50.0 (43.3)	85 (85)
2	213 (183)	15.0 (10.0)	95 (95)
3	237 (193)	16.7 (16.7)	93 (91)

Table A-3 Inactivation rates of enveloped and nonenveloped virus surrogates in unpasteurized and pasteurized wastewater.

		Temp.	First order rate constant (h^{-1}) (avg±s.d.)	Estimated T_{90} (h) (avg±s.d.)	R^2 (avg)
Wastewater	MHV (enveloped)	25 °C	0.142 ± 0.015	13 ± 1	0.88
		10 °C	0.059 ± 0.006	36 ± 5	0.95
	Phi6 (enveloped)	25 °C	0.317 ± 0.022	7 ± 0.4	0.99
		10 °C	0.091 ± 0.010	28 ± 2	0.96
	MS2 (nonenveloped)	25 °C	0.022 ± 0.006	121 ± 36	0.85
		10 °C	0.014 ± 0.003	175 ± 33	0.78
	T3 (nonenveloped)	25 °C	n.a.	n.a.	n.a.
		10 °C			
Pasteurized wastewater	MHV (enveloped)	25 °C	0.120 ± 0.037	19 ± 8	0.97
		10 °C	0.021 ± 0.012	149 ± 103	0.84
	Phi6 (enveloped)	25 °C	0.044 ± 0.004	53 ± 8	0.95
		10 °C	0.017 ± 0.005	146 ± 43	0.86
	MS2 (nonenveloped)	25 °C	0.020 ± 0.007	121 ± 55	0.95
		10 °C	0.013 ± 0.006	212 ± 88	0.73
	T3 (nonenveloped)	25 °C	n.a.	n.a.	n.a.
		10 °C			

Table A-4 Simulation results for virus sorption and inactivation kinetics in wastewater at 4 °C.

Virus	k_1 (h^{-1})[a]	k_2 (h^{-1})[b]	k_3 (h^{-1})[c]	Viruses adsorbed at equilibrium (%)	T (90% equilibrium, h)	T (99% equilibrium, h)
MHV (enveloped)	0.048	2.8	0.048	26.3	0.3	0.4
Phi6 (enveloped)	0.026	0.33	0.026	22	1.5	2.9
MS2 (nonenveloped)	0.0013	0.13	0.037	6.0	1.1	2.5
T3 (nonenveloped)[d]	n.a.	n.a.	n.a.	n.a.	n.a.	n.a.

[a] k_1 is the virus inactivation rate constant in the liquid fraction of wastewater, equal to the virus inactivation rate constant in solids-removed wastewater;

[b] k_2 is the rate constant for reversible adsorption from the liquid to solid phase;

[c] k_3 is the virus inactivation rate constant on solid surfaces. In our model, the rate constant for reversibly adsorbed viruses transitioning to irreversible adsorption (k_4) was assumed to equal zero.

[d] No significant decline of the T3 infectivity was observed in wastewater and solids-free samples within the experimental time-scale.

References

(1) Taylor, D. H.; Bellamy, A. R.; Wilson, A. T. Interaction of bacteriophage R17 and reovirus type III with the clay mineral allophane. *Water Res*. **1980**, *14* (4), 339–346.

Appendix B. Supplementary Information for Chapter 3

Protein digestion. The virus samples (2.4 mL, ~10^{11} PFU) were concentrated with 100 kDa Amicon Ultra-0.5 centrifugal filters (Millipore), washed three times with 50 mM Tris-HCl buffer (pH 8) and eventually collected at a final volume of approximately 40 μL. Protein concentrations were measured in a Qubit Fluorometer 2.0 with Protein Assay Kits (ThermoFisher Scientific). Total protein concentrations of 28.6 ± 2.2 μg per 10^{11} PFU were consistently measured in the concentrated virus samples. Each of the 40 μL concentrate was equally split into two portions, and the two 20 μL samples were digested with trypsin and chymotrypsin, respectively. In brief, the virus concentrates were denatured by submerging the sealed centrifuge tube in boiling water for 5-6 min. Following the denaturing step, iodoacetamide was added to a final concentration of 10 mM in order to prevent the formation of disulfide bonds, and the sample was incubated in the dark at 37 °C for 1 h. Unreacted iodoacetamide was deactivated by adding L-cysteine to a final concentration of 16.7 mM and incubating the solution in the dark at room temperature for 30 min. Finally, calcium chloride was added to a final concentration of 1 mM and trypsin or chymotrypsin was added to achieve a protein-to-enzyme ratio of 50:1. Samples were gently vortexed and then incubated at 37 °C overnight. After incubation, samples were injected directly onto the LC-MS/MS system without further purification.

^{15}N-Metabolic labeled Phi6. To prepare a stock of ^{15}N-labeled Phi6, the Phi6 host *P. syringae* was first cultured in ^{15}N-M9 medium (1g L^{-1} $^{15}NH_4Cl$, 48 mM Na_2HPO_4, 22 mM KH_2PO_4, 8.5 mM NaCl, 2 mM $MgSO_4$, 0.1 mM $CaCl_2$, and 0.4% (v/v) glucose, pH 7.4). ^{14}N-Phi6 was then added to ^{15}N-labeled *P. syringae* at an OD_{640} of ~0.1 and at a MOI of 2, and incubated at 26 °C while shaking at 180 rpm. Propagation was stopped 12-17 hours after infection. The Phi6 propagation in ^{15}N-labeled *P. syringae* was repeated for two generations in ^{15}N-M9 medium to obtain a stock with over 99% ^{15}N. The virus concentration and purification techniques used for the ^{15}N-labeled Phi6 were the same as those used for the ^{14}N-Phi6. The final ^{15}N-labeled Phi6 stocks (8×10^{11} PFU mL^{-1}) were filtered through 0.22 μm PES membranes, aliquoted, and stored at -80 °C until use.

Determination of peptide limit of quantification (LOQ) and limit of detection (LOD). The LOQ of each Phi6 peptide measured by LC-MS/MS was determined from its calibration curve. In brief, ^{14}N-Phi6 samples were serially diluted and mixed with equal amounts of ^{15}N-labeled Phi6 to yield PFU ratios of 3:1, 1:1, 0.3:1 and 0.1:1. The mixtures were digested with trypsin and chymotrypsin (see digestion procedure above), and were analyzed with LC-MS/MS. The ratios of peak areas of the ^{14}N-peptides and ^{15}N-labelled peptides (Y) were plotted as a function of PFU ratios (X). The linear regression model and the LOQ, LOD of peptide *j* were expressed as:[1]

$$Y = b_j X + a_j$$

$$LOQ_j = 10S_{a_j}/b_j$$

$$LOD_j = 3S_{a_j}/b_j$$

Where a_j and b_j are the intercept and slope of the linear curve, and S_{a_j} is the standard deviation of the intercept a_j.

Lipid extraction. For lipid analysis, virus samples (2.4 mL, ~10^{11} PFU) were freeze-dried (FreeZone 6, Labconco) to a final volume of 200 μL. Viral lipids were then extracted with methyl-tert-butyl ether (MTBE) as described previoulsy.[2] In brief, the 200 μL samples were mixed with 1.5 mL methanol and 5 mL MTBE, and were shaken at room temperature for 1 h. After the addition of 1.25 mL Milli-Q water, the mixture was centrifuged at 1000 × g for 10 min. The upper organic phase, where the lipids partitioned, was collected and dried under nitrogen gas. The dried lipids were then resuspended in 400 μL of acetonitrile/isopropanol/water (6.5:3:0.5, v/v/v) prior to lipid analysis.

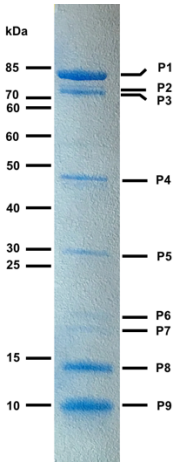

Figure B-1 SDS-PAGE of purified Phi6 stock. Electrophoresis was conducted in 8-16% TGX^{TM} precast gels (Bio-Rad).

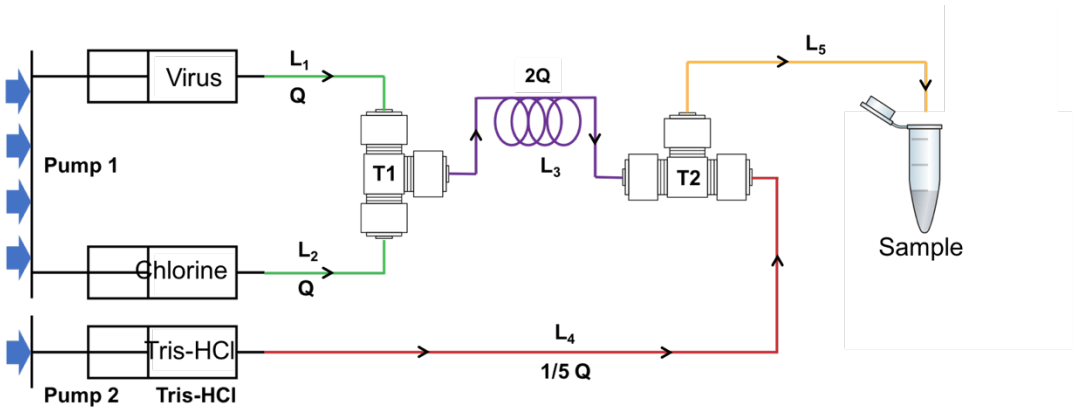

Figure B-2 Lab-scale continuous quench-flow system for free chlorine treatment. The system was modified from a previous study on ozone reactions.[3]

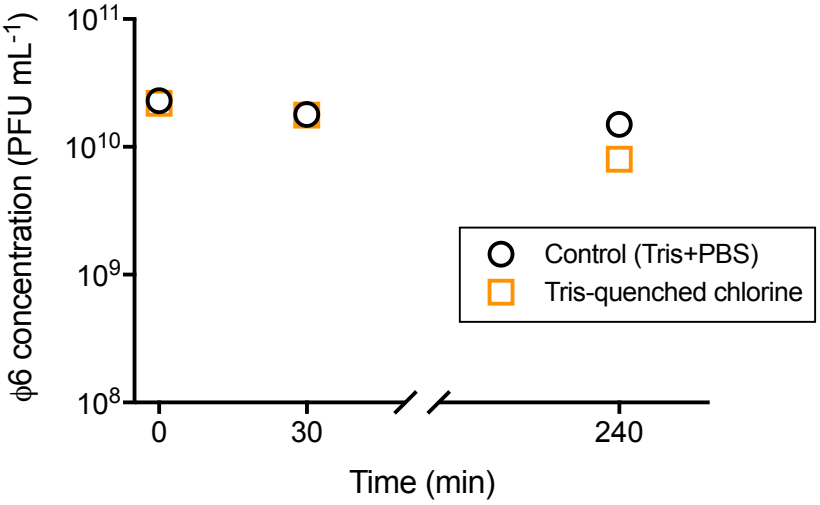

Figure B-3 Effect of Tris-HCl quenching on Phi6 inactivation. Phi6 inactivation was compared when samples sit on ice in 5 mM phosphate buffer (PBS; 10 mM NaCl, pH 7.4) added with Tris-HCl (no chlorine control) and when samples sit on ice in free chlorine solution quenched with Tris-HCl. The Phi6 inactivation was effectively quenched with Tris-HCl for up to 30 min (i.e., the time that samples sit on ice following the addition of Tris-HCl in the experiments).

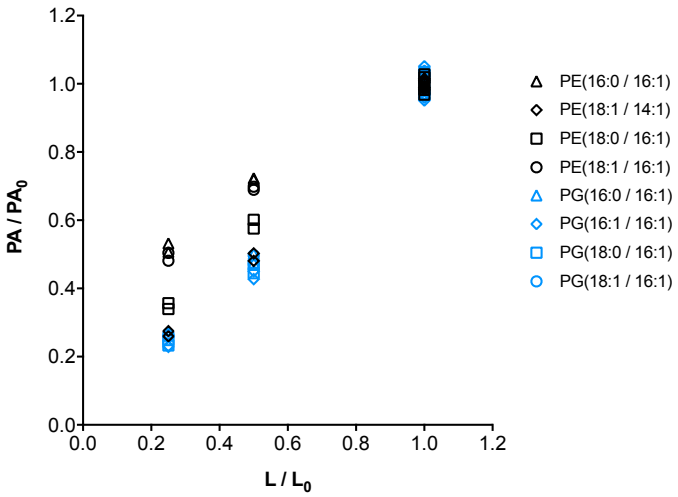

Figure B-4 Calibration curves of eight the most abundant Phi6 lipid compounds. The relative peak areas of lipids (PA/PA_0) were determined by lipid LC-MS/MS method, and the relative lipid concentrations (L/L_0) were prepared from Phi6 lipid extracts that were not exposed to free chlorine or UV_{254}.

PE(16:0/16:1): $Y=0.623X+0.382$ ($R^2=0.990$),

PE(18:1/14:1): $Y=0.986X+0.012$ ($R^2=0.998$),

PE(18:0/16:1): $Y=0.859X+0.144$ ($R^2=0.994$),

PE(18:1/16:1): $Y=0.662X+0.341$ ($R^2=0.995$),

PG(16:1/16:0): $Y=0.989X+0.009$ ($R^2=0.994$),

PG(16:1/16:1): $Y=1.048X-0.054$ ($R^2=0.988$),

PG(16:1/18:0): $Y=1.029X-0.033$ ($R^2=0.994$),

PG(16:1/18:1): $Y=0.993X+0.005$ ($R^2=0.994$).

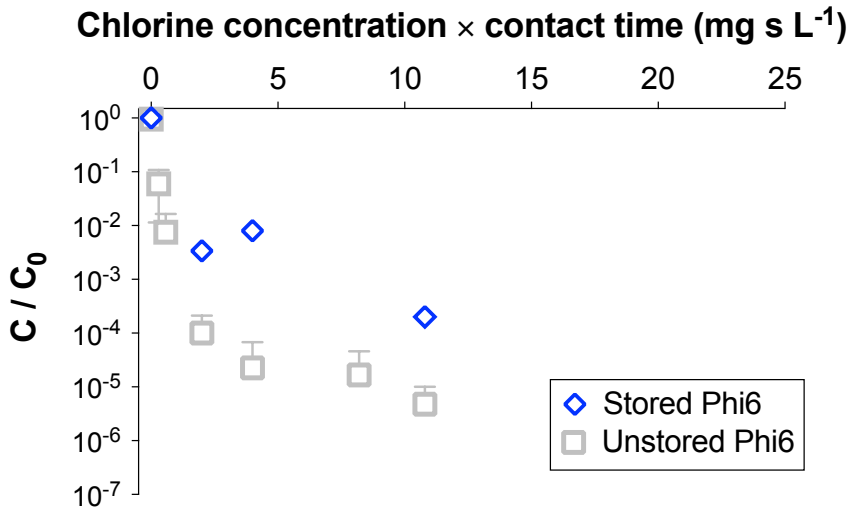

Figure B-5 The impact of storage at 4 °C for 48 hours on Phi6 resistance to free chlorine. Here, the "unstored Phi6" refers to an experiment where the stock was thawed from -80 °C and treated with free chlorine on the same day of the experiments. The "stored Phi6" refers to an experiment in which the stock was thawed from -80 °C and stored at 4 °C for 48 hours before the chlorine treatment was conducted.

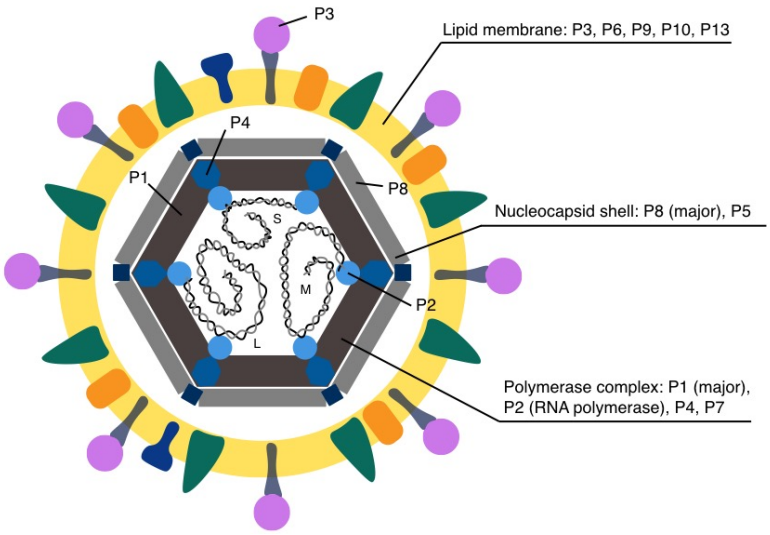

Figure B-6 Schematic of Phi6 structure.[4] For the early infection steps, the Phi6 viral particle binds to the pilus of *Psudomonas syringae* with spike protein P3. Then P6 initiates the virus membrane fusion with the host membrane. P5 is responsible for the penetration of the nucleocpasid and polymerase complex through the peptidoglycan layer. Finally, nucleocapsid protein P8 helps the polymerase complex continuously penetrate the cytoplasmic membrane, delivering the viral genome into the cytoplasm for replication.[4]

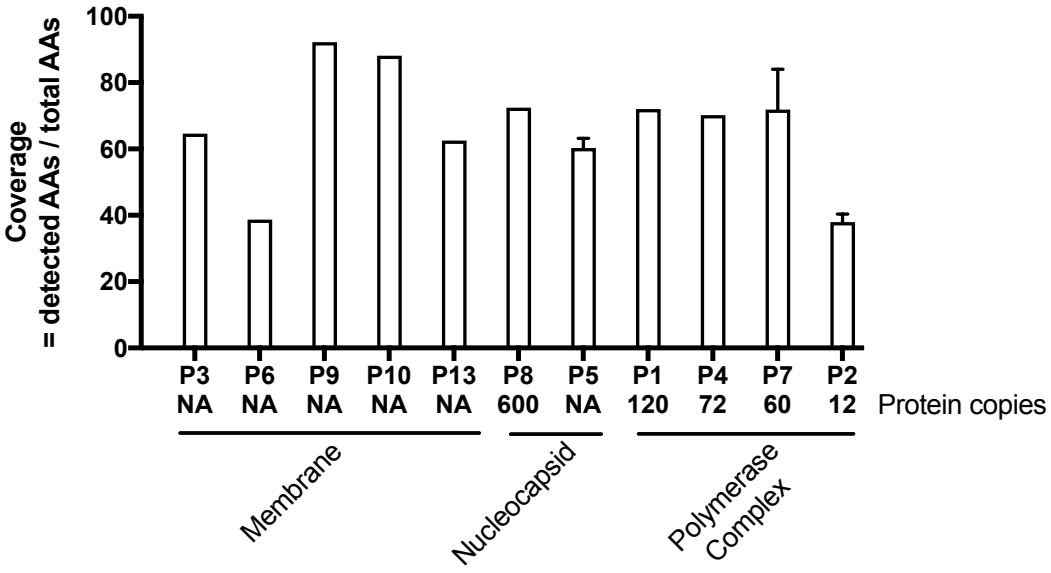

Figure B-7 Phi6 protein coverage captured with the LC-MS/MS method. Error bars represent the standard deviations of protein coverage in free chlorine and UV_{254} experiments, n=18. NA indicates information not available.

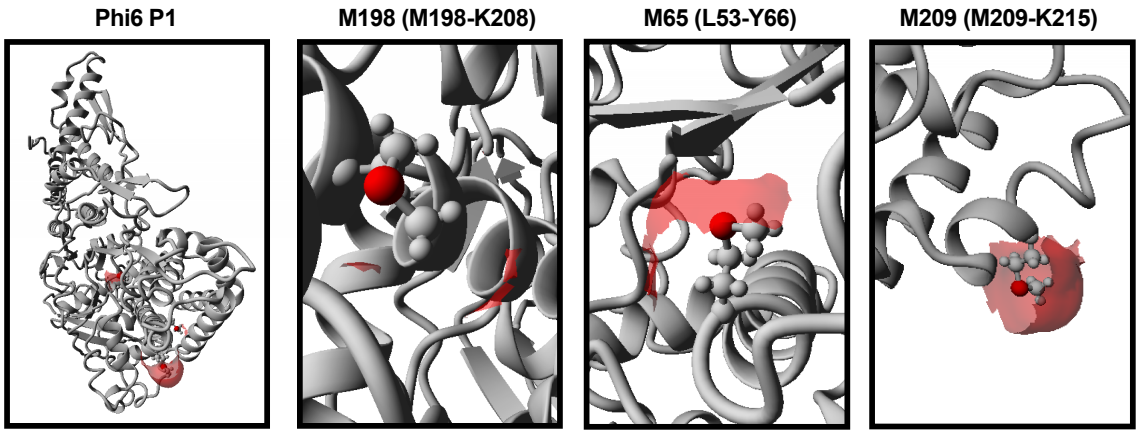

Figure B-8 Cryo-EM structure of Phi6 protein P1 (PDB ID: 5muu) and close-up of residues Met 65, Met 198, Met 209 within P1. Sulfur atoms in Met 65, Met 198, and Met 209 are colored in red. Solvent-accessible surface areas of Met 65, Met 198, and Met 209 are identified with transparent red coloring.

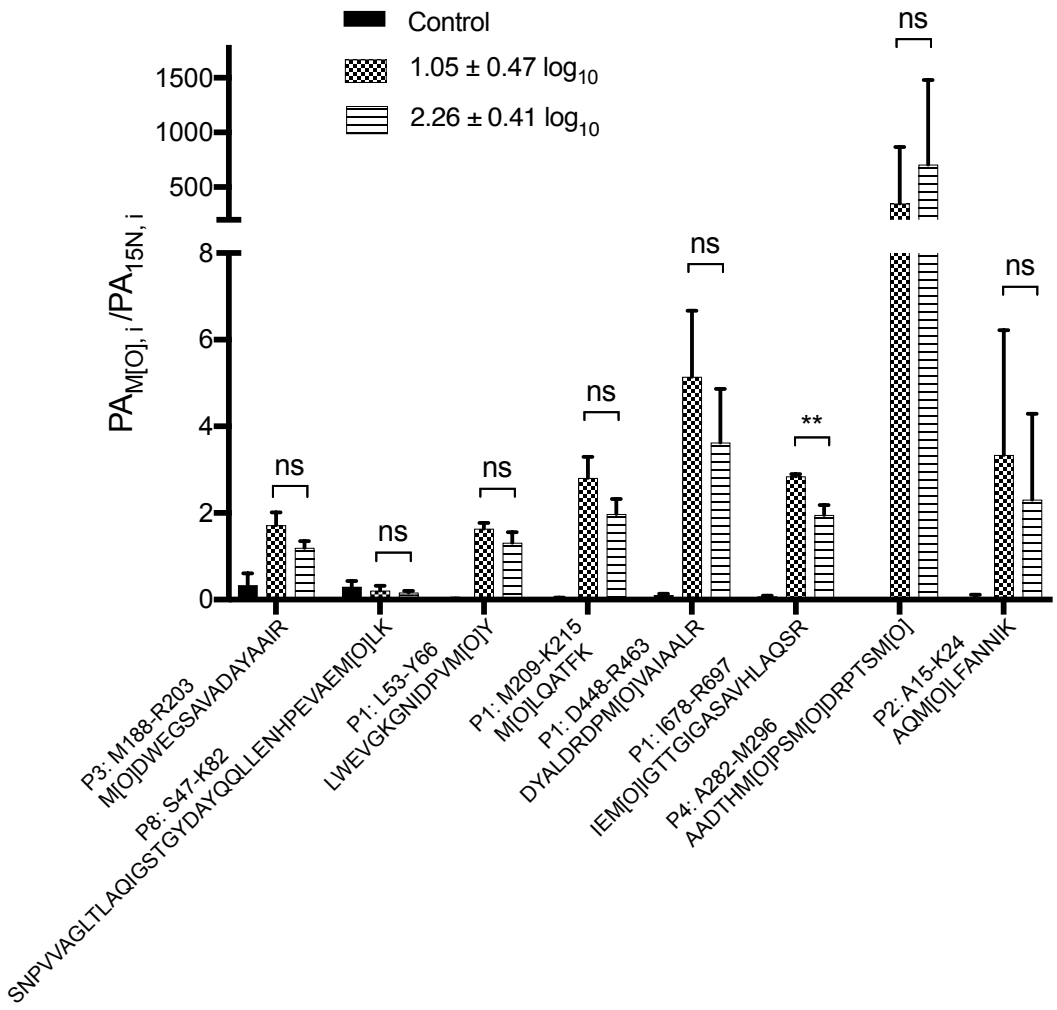

Figure B-9 Relative abundances of Met oxidation products of the fastest reacting peptides following chlorine treatments. The peak areas of the oxidized peptide ions ($PA_{M[O]}$) were normalized to the peak areas of the corresponding ^{15}N-labeled peptide ions (PA_{15N}). Unpaired student's t tests were used to identify statistical difference in the relative abundances of oxidation products at two levels of Phi6 inactivation. ** indicates $P < 0.01$ and ns indicates not significant ($P > 0.05$).

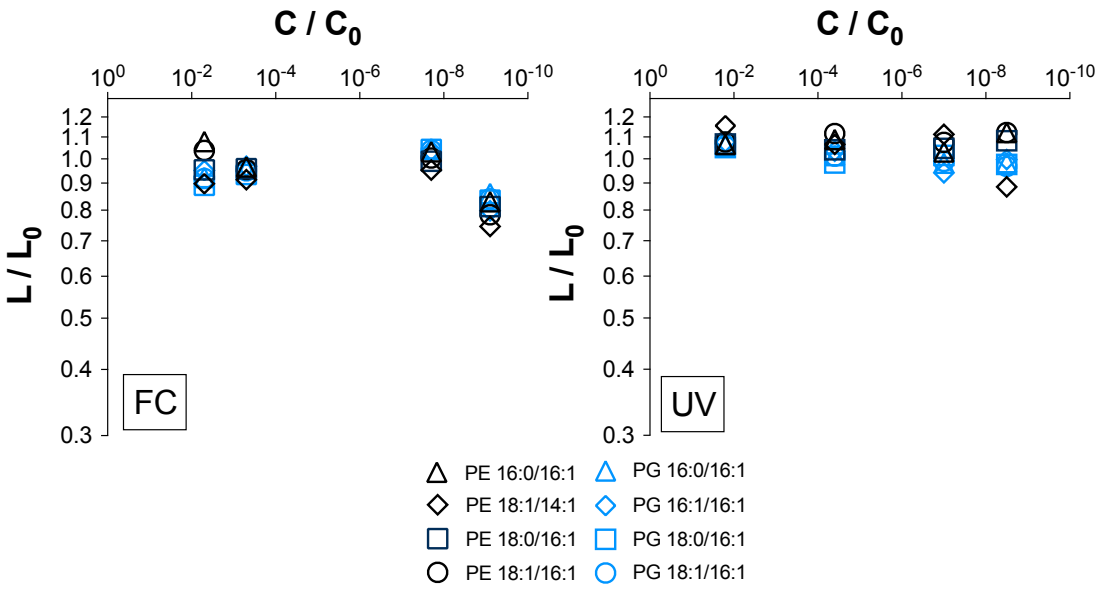

Figure B-10 Relative abundances (L/L_0) of eight major Phi6 lipid compounds with respect to Phi6 inactivation (C/C_0) by free chlorine (FC) and UV_{254} (UV).

Table B-1 Phi6 primers and amplicon sizes.

Primer set ID	Genome segment	Genome segment size (kbp)	Direction	Primer sequence (5'-3')	Nucleotide position	RT-qPCR amplicon size (bp)	Amplicon size relative to genome segment size (%)
S	Segment S	2.95	F R	GCAGACCCAGCTGACTTCTT AAGGCGCTATCCTTGGACAC	1141-1160 1639-1620	499	16.9
M	Segment M	4.06	F R	CCTGAGGAAACGGCTCAACT CATAGCCAACGAACTGCTGC	1307-1326 1778-1759	472	11.6
L	Segment L	6.37	F R	GCCTACCAGCTCCACCAAAT CGTACCCCATGTTGAGCAGT	1510-1529 1993-1974	484	7.6

Table B-2 Q Exactive settings for Phi6 protein and lipid analysis.

	Protein (positive mode)	**Lipid (negative mode)**
Sheath gas flow rate	24	24
Auxiliary gas flow rate	8	8
Sweep gas flow rate	1	1
Spray voltage	3 kV	2.8 kV
Capillary temp.	300 °C	250 °C
S-len RF level	50.0	50
Aux gas heater temp.	275 °C	275 °C
Column temperature	25 °C	55 °C
Full MS settings		
Resolution	70,000	70,000
AGC target	5e5	1e6
Max IT	200 ms	200
Scan range	400-1800 m/z	400-1800 m/z
dd-MS^2 settings		
Resolution	35,000	35,000
AGC target	2e5	2e5
Max IT	100 ms	100 ms
Loop count	20	5
Isolation window	1.6 Da	3 Da
NCE	30	30
Intensity threshold	2e4	2e4
Charge exclusion:	Unassigned, 1	Unassigned, 5-8, >8
Dynamic exclusion	20 sec	30 sec

Table B-3 Reaction rate constants (k_g) of three RT-qPCR regions on S, M, and L segments measured by RT-qPCR and extrapolated rate constants of the entire Phi6 genome following free chlorine and UV_{254} treatments. Errors represent standard errors of the reaction rate constants. ANCOVA analyses were applied to test whether the reaction rate constants were significantly different from zero. The results of ANCOVA analyses were shown in the table.

	Size of RT-qPCR amplicon or Phi6 gnome in base pairs	Free chlorine ($L\ mg^{-1}\ s^{-1}$)	UV_{254} ($cm^2\ mJ^{-1}$)
S segment	499	$0.0070 \pm 0.0027^{*}$	$0.0027 \pm 0.0007^{**}$
M segment	472	$0.0127 \pm 0.0032^{***}$	$0.0014 \pm 0.0003^{***}$
L segment	484	$0.0109 \pm 0.0032^{**}$	$0.0027 \pm 0.0007^{**}$
Genome (extrapolated)	13380	0.26 ± 0.06	0.063 ± 0.012

All rate constants were significantly different from zero, where * indicates $P < 0.05$; ** indicates $P < 0.01$; *** indicates $P < 0.001$.

Table B-4 UV-reactive and chlorine-reactive bases in Phi6 and MS2 genomes, and the fraction these bases make up in the entire genome sequence.

Bases that are reactive with UV_{254} [5]

	Genome size	Bases in genome	U	C	UU	Total reactive bases (U+C+UU) per genome base [a]
Phi6, dsRNA	13.4 kbp	26.8 kb	5914	7471	1120	0.54
MS2, ssRNA	3.6 kb	3.6 kb	901	909	185	0.55

Bases that are reactive with free chlorine[6,7]

	Genome size	Bases in genome	U	C	A	Total reactive bases (U+C+A) per gnome base [b]
Phi6, dsRNA	13.4 kbp	26.8 kb	5922	7471	5922	0.72
MS2, ssRNA	3.6 kb	3.6 kb	901	909	827	0.73

[a] The proportion of UV-reactive bases in Phi6 and MS2 genomes is similar.
[b] The proportion of chlorine-reactive bases in Phi6 and MS2 genomes is similar.

Table B-5 Number of reactive amino acid residues in Phi6 proteins, and literature values for second-order rate constants of individual amino acids reaction with HOCl at pH 7.4, 22 °C.[8]

Protein location	Protein	UniProt Accession	Amino acids (AA) (Second-order reaction rate constant, M^{-1} s^{-1})						Total AAs
			Met[a] (3.8×10^7)	Cys (3.0×10^7)	His (1.0×10^5)	Trp (1.1×10^4)	Lys (5.0×10^3)	Tyr (4.4×10^1)	
Membrane	P3	P11129	17	9	7	17	24	22	648
	P6	P11128	0	0	0	7	10	2	168
	P9	P07581	0	0	1	1	5	1	90
	P10	P11127	0	0	0	0	4	1	42
	P13	P11130	0	0	0	0	3	2	72
Nucleo-capsid	P8	P07579	4	0	1	0	6	6	149
	P5	P07582	0	0	3	2	10	10	220
Polymerase complex	P1	P11126	19	3	18	11	25	23	769
	P2	P11124	24	7	14	12	37	28	665
	P4	P11125	10	3	5	2	13	7	332
	P7	P11123	4	0	5	3	5	3	161

[a] The first Met residue in the protein sequence was not counted.

Table B-6 Detailed information of Phi6 peptides, reaction rate constants following inactivation by UV_{254} and free chlorine.

P_j: the relative abundance of peptide j
$P_{0,j}$: the mean initial relative abundance of peptide j
$K_{P,j}$: first-order rate constant of peptide j
na: not available
Data in red: value below the limit of quantification, and was replaced by an expected number.
The 8 most reactive Met-containing peptides with free chlorine
The most reactive Cys-containing peptides with free chlorine
The 8 most reactive peptides with UV_{254}
Uncovered Peptide

Membrane proteins

Phi6 Peptides									Chlorine, $P_j/P_{0,j}$											UV254, $P_j/P_{0,j}$										
									Rep 1			Rep 2			Rep 3			$K_{Cl,j}$	SE of $K_{Cl,j}$	R^2	Rep 1			Rep 2			Rep 3			$K_{UV,j}$	SE of $K_{UV,j}$	R^2
	pep_seq	Pro_ID	pep_formula	z	m/z_14N	m/z_15N	Retention time	pep_start	pep_end	0 mg s/L	0.6 mg s/L	1.2 mg s/L	0 mg s/L	0.6 mg s/L	1.2 mg s/L	0 mg s/L	0.6 mg s/L	1.2 mg s/L	L/(mg s)			0 mJ/cm2	42 mJ/cm2	130 mJ/cm2	0 mJ/cm2	42 mJ/cm2	130 mJ/cm2	0 mJ/cm2	42 mJ/cm2	130 mJ/cm2	cm2/mJ		
										-0.024 log10	0.99 log10	2.4 log10	0.052 log10	0.84 log10	1.9 log10	-0.024 log10	1.7 log10	2.8 log10				0.11 log10	1.8 log10	4.2 log10	-0.053 log10	1.6 log10	4.2 log10	-0.039 log10	1.7 log10	4.2 log10			
	YQGINEWLGGAK	P3	C61H90N16O18	2	668.338	676.313	18-19.5	3	14	1.066	0.521	0.348	0.999	0.617	0.361	0.935	0.485	0.308	0.90	0.07	0.96	1.112	1.047	0.908	0.894	0.656	0.597	0.994	0.906	0.506	0.0033	0.0013	0.47
	LITANGEIGAIYLSAAPPTDAAR	P3	C99H161N27O34	2	1137.092	1150.550	20.5-22	16	38	1.101	0.565	0.344	0.982	0.587	0.338	0.917	0.440	0.292	0.94	0.08	0.95	1.067	1.054	0.903	0.886	0.666	0.582	1.047	0.958	0.464	0.0037	0.0014	0.48
	LSAAPPTDAARADAKAVDF	P3	C82H131N23O28	3	629.658	637.301	17-20	28	46	1.252	0.575	0.374	0.944	0.725	0.467	0.804	0.541	0.372	0.75	0.11	0.87	1.208	1.095	0.990	0.865	0.721	0.593	0.928	0.844	0.489	0.0032	0.0015	0.38
	TAGWPSAIVDCADATRAKQNY	P3						47	67																							
	QNYLWVGDNVVHIGAK	P3						65	80																							
	LDLWGGTGDAW	P3	C55H75N13O17	2	595.777	602.258	22-24	85	95																							
	ACPMLDLCRAW	P3						102	112																							
	ASASVTTGSLQGY	P3	C52H84N14O21	2	621.304	628.283	14-15.5	117	129	1.124	0.529	0.368	1.004	0.658	0.338	0.872	0.482	0.326	0.89	0.08	0.95	1.150	1.098	0.949	0.857	0.697	0.619	0.993	0.842	0.499	0.0031	0.0014	0.41
	LDVEQQQF	P3						135	142																							
	AKDNLNLY	P3	C42H67N11O14	2	475.751	481.234	13.5-14	143	150	1.098	0.541	0.353	0.982	0.607	0.323	0.919	0.482	0.309	0.93	0.06	0.97	1.107	1.057	0.896	0.893	0.696	0.607	1.001	0.916	0.461	0.0036	0.0014	0.50
	DNLNLYGDNCLDLATSSSAQR	P3	C94H151N29O38S1	3	776.357	785.663	19.2-20	145	165	1.130	0.567	0.256	1.065	0.379	0.119	0.805	0.209	0.161	1.47	0.25	0.84	1.151	1.066	0.960	0.893	0.702	0.630	0.956	0.814	0.566	0.0027	0.0013	0.39
	AFLEQCMGCALPEDCIFGWYVK	P3						166	187																							
	MDWEGSAVADAYAAIR	P3	C75H112N20O25S1	2	863.399	873.368	21-28	188	203	1.289	0.124	na	0.785	0.070	na	0.926	0.070	na	4.07	0.40	0.96	1.181	1.195	0.955	0.800	0.686	0.606	1.019	0.940	0.633	0.0026	0.0014	0.32
	AAIRVQGF	P3	C39H64N12O10	2	431.251	437.232	15-16.5	200	207	1.067	0.560	0.414	1.009	0.642	0.378	0.924	0.514	0.353	0.80	0.06	0.96	1.116	1.089	1.009	0.885	0.701	0.618	0.999	0.920	0.478	0.0032	0.0015	0.38
	VQGFATVMAPWQSVGGAGYVYAR	P3	C111H163N29O30S1	3	805.735	815.375	22.8-33.5	204	226	1.226	0.398	0.255	0.682	0.449	0.305	1.092	0.503	0.128	1.25	0.21	0.84	0.658	0.631	0.606	0.750	0.670	0.621	1.592	0.892	0.326	0.0048	0.0021	0.42
	ARVPQKGAW	P3						225	233																							
	MGVNLLAY	P3	C40H65N9O11S1	1	880.460	889.432	20.7-21.3	234	241				1.113	0.392	0.119	0.887	0.256	0.062	2.04	0.24	0.95	1.110	0.989	1.043	0.882	0.664	0.557	1.008	0.891	0.473	0.0033	0.0016	0.37
	VHGTSGQPAYGIPM	P3	C62H99N17O19S1	2	707.843	716.317	15.1-16.5	242	255	1.192	0.370	0.072	0.970	0.426	0.104	0.838	0.270	0.052	2.17	0.19	0.95	1.124	1.028	0.872	0.884	0.692	0.583	0.992	0.899	0.472	0.0037	0.0013	0.53
	TLSGFTGNMGQVASKWLM	P3						256	273																							
	LMVDPHVVQIL	P3	C64H109N15O16S1	2	688.902	696.379	24-25.5	276	287	1.083	0.510	0.309	0.992	0.611	0.340	0.924	0.469	0.281	0.98	0.07	0.97	1.098	1.070	0.930	0.901	0.702	0.627	1.002	0.895	0.491	0.0032	0.0013	0.46
	IVDPHVVQIL	P3	C53H89N13O14	2	566.840	573.320	20.1-21	280	289	1.080	0.533	0.333	1.003	0.621	0.343	0.917	0.496	0.300	0.94	0.06	0.97	1.131	1.085	0.951	0.886	0.701	0.600	0.983	0.916	0.496	0.0033	0.0014	0.44
	RGTKSDPR	P3						295	302																							
	TTDVYADPK	P3	C44H68N10O17	2	505.245	510.230	8.2-9	303	311	1.085	0.532	0.351	0.995	0.615	0.360	0.920	0.475	0.304	0.90	0.07	0.96	1.130	1.055	0.923	0.875	0.629	0.579	0.995	0.914	0.508	0.0033	0.0014	0.43
	ADPKVPASRISGPM	P3	C61H104N18O19S1	3	475.922	481.904	12-14.5	308	321	1.062	0.314	0.071	0.985	0.382	0.078	0.953	0.219	0.034	2.38	0.21	0.95	1.127	1.046	0.914	0.887	0.696	0.606	0.986	0.939	0.490	0.0034	0.0013	0.48
	INGTVAPPATIPATIPVPL	P3						322	340																							
	APLGGAGGPGAGGF	P3						341	354																							
	QVYPVFTW	P3	C53H70N10O12	2	520.266	525.251	21.5-23	355	362	1.284	0.470	0.326	0.900	0.592	0.355	0.816	0.442	0.310	0.91	0.12	0.90	1.077	1.004	0.905	0.835	0.750	0.639	1.088	0.945	0.459	0.0035	0.0014	0.48
	MTDVTIEGTVTADSNGL	P3						366	384																							
	HVVDDVRNY	P3	C48H73N15O16	2	558.775	566.253	12.3-13.5	385	393	1.216	0.100	na	1.165	0.475	na	0.619	0.100	na	2.90	0.94	0.70	1.248	1.363	1.595	0.787	0.841	0.515	0.965	0.927	0.492	0.0024	0.0026	0.12
	NYVWNGTALAAIEQVNAADGR	P3	C97H148N29O32	3	745.038	754.675	22-24	392	412	1.153	0.545	0.335	1.035	0.629	0.375	0.812	0.414	0.280	0.92	0.12	0.90	1.157	1.143	0.993	0.785	0.585	0.503	1.058	0.928	0.513	0.0034	0.0019	0.33
	VTLTDSER	P3	C37H58N11O16	2	460.738	466.221	8.5-9.7	413	420	1.081	0.534	0.366	0.993	0.613	0.364	0.926	0.477	0.310	0.88	0.07	0.96	1.111	1.054	0.919	0.884	0.642	0.592	1.005	0.931	0.523	0.0032	0.0014	0.44
	AQLASLTVR	P3	C41H75N13O13	2	479.788	486.268	14-15.5	421	429	1.093	0.531	0.364	0.994	0.609	0.361	0.913	0.469	0.315	0.88	0.07	0.95	1.118	1.052	0.927	0.873	0.642	0.587	1.009	0.912	0.518	0.0032	0.0014	0.43
	QQLSVGADPLSK	P3	C53H91N15O19	2	621.838	629.315	14-15.5	435	446	1.083	0.529	0.353	0.994	0.605	0.375	0.923	0.472	0.309	0.89	0.07	0.95	1.123	1.068	0.920	0.887	0.642	0.588	0.990	0.912	0.511	0.0033	0.0014	0.44
	SVGADPLSKTSIW	P3	C61H97N15O20	2	680.859	688.336	19.5-20.5	438	450	1.432	0.457	0.326	0.809	0.552	0.312	0.759	0.421	0.294	0.94	0.15	0.85	1.170	1.087	0.985	0.901	0.664	0.610	0.929	0.932	0.502	0.0031	0.0015	0.37
	ADYDLLSQQIEADTVK	P3	C84H136N20O31	2	961.491	971.461	21-23	456	472	1.095	0.543	0.354	1.017	0.627	0.372	0.889	0.487	0.310	0.88	0.07	0.95	1.093	1.043	0.922	0.894	0.635	0.579	1.014	0.912	0.508	0.0033	0.0014	0.45
	SQQIEADTVKNLPAVTF	P3	C88H144N22O29	2	987.531	998.497	22.4-23.5	462	479	1.077	0.503	0.340	0.962	0.634	0.343	0.961	0.509	0.328	0.91	0.06	0.97	1.116	1.063	0.930	0.852	0.680	0.607	1.032	0.921	0.473	0.0034	0.0015	0.44
	NLPAVTFAQANK	P3	C57H92N16O17	2	637.349	645.324	16-17.5	473	484	1.044	0.524	0.344	1.035	0.639	0.375	0.920	0.481	0.305	0.90	0.07	0.95	1.126	1.045	0.924	0.871	0.636	0.574	1.004	0.915	0.509	0.0033	0.0014	0.44
	AQANKAAGGQSETLW	P3	C65H102N20O23	2	766.379	776.348	13.5-15	480	494	1.064	0.529	0.365	1.009	0.663	0.389	0.927	0.532	0.362	0.82	0.06	0.96	1.099	1.041	0.955	0.903	0.706	0.612	0.997	0.915	0.491	0.0032	0.0014	0.45
	AAGGQSETLWHQMYR	P3	C75H111N23O23S1	3	578.939	586.582	15-17	485	499	1.008	0.491	0.271	0.986	0.568	0.309	1.006	0.431	0.210	1.12	0.09	0.96	1.142	1.080	0.921	0.865	0.647	0.565	0.994	0.911	0.486	0.0035	0.0015	0.44
	VNDIAGDQVTAIQITGTMATGIR	P3	C98H169N29O35S1	3	782.409	792.046	23.7-24.5	500	522	1.110	0.443	0.168				0.780	0.324	0.360	1.11	0.29	0.79	1.083	1.049	0.952	0.921	0.758	0.682	0.996	0.740	0.577	0.0024	0.0011	0.40
	WSATAGGLVVDADEQDAVIAISSGKPVK	P3	C122H198N32O42	3	928.819	939.453	25-28	523	550	1.194	0.702	0.501	1.260	0.850	0.456	0.545	0.441	0.339	0.66	0.22	0.55	1.315	1.326	1.443	0.722	0.799	0.857	0.963	0.670	0.415	0.0015	0.0026	0.04
	NSSDLPTADAVNYLFGITADDMPGIVSSQK	P3	C135H212N34O49S1	3	1042.836	1054.135	28-29	551	580	1.170	0.359	0.057	0.882	0.281	0.126	0.948	0.285	0.057	2.16	0.19	0.95	0.888	0.751	0.606	0.972	0.740	0.636	1.140	1.013	0.511	0.0042	0.0008	0.79
	GITADDMPGIVSSQKEM	P3	C73H123N19O28S2	2	889.919	899.390	18-20	566	582	1.051	0.345	0.092	0.988	0.432	0.113	0.961	0.265	0.074	1.99	0.13	0.97	1.077	1.009	0.879	0.910	0.699	0.617	1.013	0.910	0.503	0.0034	0.0012	0.54
	EMNSEFEEGFLQK	P3	C69H102N16O25S1	2	794.353	802.329	18-19.5	581	593	1.099	0.471	0.177	0.974	0.554	0.211	0.927	0.378	0.140	1.46	0.11	0.96	1.112	1.052	0.906	0.883	0.653	0.590	1.005	0.903	0.489	0.0035	0.0014	0.47
	LWNPR	P3						596	600																							
	LVENVQNAYFLMVYAR	P3	C89H136N22O24S1	3	644.001	651.312	23-24.5	602	617	1.648	0.414	0.311	0.701	0.488	0.287	0.651	0.184	0.032	1.55	0.54	0.54	1.378	1.115	1.141	0.765	0.604	0.547	0.857	0.878	0.524	0.0026	0.0021	0.18
	QFHSLVASSLAMAK	P3	C66H108N18O19S1	3	497.266	503.248	17.75-21.8	621	634	1.211	0.575	0.364	1.191	0.691	0.370	0.598	0.347	0.227	0.93	0.22	0.72	1.161	1.068	0.886	0.840	0.783	0.595	0.999	0.820	0.403	0.0041	0.0015	0.50
	LGVSTR	P3						635	640																							
	ACKESYGC	P3						641	648																							
	SIFSSLFK	P6						1	9																							
	KVIKKVISKVVATLKKIF	P6						9	26																							
	KKIWPLLLIVAIIYF	P6						27	41																							
	APYLAGF	P6						42	48																							
	FTGIGGIF	P6						54	61																							
	SSIATTITPTLTSF	P6	C64H106N14O23	2	720.385	727.363	23.3-24.3	62	75	1.326	0.604	0.455	0.856	0.560	0.356	0.819	0.457	0.330	0.79	0.13	0.83	1.206	1.138	0.961	0.905	0.777	0.649	0.889	0.864	0.583	0.0026	0.0012	0.38
	SGVGSLASTAW	P6	C45H70N12O16	2	518.259	524.240	19.1-19.8	81	91	1.088	0.619	0.464	0.989	0.704	0.411	0.924	0.526	0.401	0.71	0.07	0.94	1.097	1.051	0.929	0.964	0.784	0.669	0.939	0.840	0.600	0.0025	0.0010	0.50
	SGFQSL	P6						92	97																							
	GMGTQLAVVSGAAAL	P6	C57H100N16O19S1	2	673.361	681.337	21.7-22	98	112	1.553	0.747	0.255	0.830	0.457	0.176	0.617	0.295	0.103	1.43	0.30	0.77	1.262	1.068	1.028	0.859	0.734	0.589	0.879	0.887	0.601	0.0025	0.0014	0.31
	IAPEETAQL	P6						113	121																							
	VTEIGTTVGDIAGTIIGGVAKAL	P6						122	144																							
	ALPGWIWIAAGGLAVWALWPSSDSK	P6	C126H186N30O31	3	884.804	894.774	33.1-33.8	143	167	1.323	0.708	0.442	0.938	0.605	0.390	0.739	0.443	0.285	0.81	0.16	0.79	1.317	1.262	1.209	0.870	0.691	0.557	0.813	0.764	0.499	0.0027	0.0021	0.18
	MPFPLVK	P9	C41H66N8O8S1	2	416.243	420.231	18.0-18.6	1	7	1.296	0.642	0.421	0.966	0.225	0.126	0.738	0.247	0.151	1.32	0.35	0.67	1.426	1.342	1.162	0.784	0.636	0.565	0.790	0.733	0.543	0.0023	0.0023	0.13
	PFPLVKGDPTSKAF	P9	C79H115N17O20	2	787.932	796.406	17.8-19.4	2	15	1.165	0.626	0.451	0.939	0.719	0.484	0.896	0.634	0.480	0.63	0.06	0.94	1.064	1.037	0.959	0.974	0.812	0.771	0.962	0.910	0.678	0.0018	0.0007	0.45
	AFTEASER	P9	C38H59N11O15	2	455.717	461.200	7.2-8.2	14	21	1.017	0.682	0.483	1.017	0.767	0.514	0.966	0.654	0.446	0.61	0.04	0.97	1.081	1.064	0.966	0.957	0.801	0.760	0.962	0.911	0.697	0.0017	0.0008	0.41
	STGTQILDVVK	P9	C50H89N13O18	2	580.830	587.310	18.1-18.6	22	32	1.025	0.688	0.485	1.019	0.762	0.517	0.957	0.650	0.442	0.61	0.04	0.97	1.089	1.073	0.968	0.949	0.794	0.753	0.961	0.919	0.703	0.0017	0.0008	0.40
	APIGLFGDDAK	P9	C50H78N12O16	2	552.290	558.272	16.5-17.5	33	43	1.025	0.685	0.484	1.014	0.760	0.510	0.961	0.655	0.447	0.61	0.04	0.97	1.081	1.061	0.965	0.948	0.790	0.749	0.971	0.918	0.699	0.0017	0.0008	0.41
	GDDAKHEF	P9	C39H59N11O15	2	459.701	465.184	5.9-7.0	39	46	1.040	0.703	0.521	1.006	0.762	0.526	0.954	0.672	0.507	0.55	0.03	0.98	1.086	1.064	0.969	0.958	0.834	0.786	0.956	0.908	0.676	0.0017	0.0008	0.41
	VTRGEQAVSVVSW	P9	C65H100N19O21	2	744.894	754.366	17.2-18.5	47	59	1.079	0.706	0.528	0.981	0.740	0.534	0.940	0.670	0.520	0.53	0.03	0.97	1.090	1.097	1.026	0.963	0.859	0.817	0.947	0.903	0.708	0.0014	0.0008	0.29
	AVAAGLIGELIGY	P9	C58H95N13O17	2	623.856	630.336	26.1-26.9	60	72	1.052	0.693	0.520	1.008	0.751	0.536	0.942	0.662	0.506	0.54	0.03	0.97	1.096	1.083	0.995	0.956	0.845	0.782	0.948	0.902	0.693	0.0016	0.0008	0.36
	KAILANIPFLA	P9	C57H95N13O13	2	585.866	592.346	24.4-25.0	80	90	1.021	0.691	0.500	1.011	0.762	0.511	0.968	0.654	0.452	0.60	0.04	0.97	1.098	1.068	0.964	0.935	0.787	0.739	0.967	0.916	0.692	0.0018	0.0008	0.40
	MDNILDPLK	P10	C46H79N11O15S1	2	529.781	535.264	19.6-20.6	1	9	0.901	0.212	0.127	1.114	0.189	0.061	0.986	0.091	0.058	2.14	0.32	0.87	0.957	0.921	0.790	1.012	0.792	0.732	1.032	0.950	0.698	0.0023	0.0004	0.82
	APFSSEAAAK	P10	C43H67N11O15	2	489.748	495.231	8.5-9.4	10	19	1.072	0.718	0.512	0.993	0.761	0.485	0.935	0.621	0.421	0.63	0.06	0.94	1.121	1.125	1.047	0.925	0.781	0.754	0.954	0.917	0.696	0.0015	0.0010	0.25
	IAVYALVGLVGGLLLTK	P10	C87H151N19O21	1	900.074	909.545	34.8-35.8	25	42	1.201	0.900	0.690	0.938	0.680	0.496	0.861	0.551	0.482	0.49	0.13	0.66	1.085	1.078	1.007	0.980	0.837	0.829	0.935	0.857	0.762	0.0011	0.0007	0.25
	ISTLESQLQPLVK	P13	C65H114N16O21	2	728.425	736.400	20.6-21.0	6	18	1.269	0.794	0.687	0.890	0.606	0.483	0.841	0.604	0.434	0.52	0.14	0.68	1.349	1.272	1.199	0.814	0.653	0.629	0.837	0.789	0.604	0.0018	0.0020	0.10
	VKLVATETPGAL	P13	C54H95N13O17	2	599.856	606.336	17.4-18.0	17	28	1.330	0.809	0.712	0.870	0.602	0.500	0.800	0.588	0.451	0.49	0.15	0.60	1.366	1.266	1.087	0.731	0.605	0.489	0.903	0.882	0.682	0.0024	0.0021	0.15
	VAYARGL	P13						29	35																							
	GLSSADRSRLYRLLR	P13						34	48																							
	SLEQAIPK	P13	C39H68N10O13	2	443.256	448.240	13.5-13.9	49	56	1.234	0.778	0.700	0.906	0.607	0.477	0.859	0.574	0.440	0.52	0.13	0.68	1.348	1.303	1.212	0.810	0.660	0.645	0.842	0.797	0.633	0.0016	0.0020	0.18
	LSSAVVSATTLAAR	P13	C57H103N17O20	2	673.886	682.359	17.1-17.6	57	70	1.277	0.852	0.750	0.926	0.662	0.499	0.797	0.564	0.450	0.48	0.15	0.58	1.387	1.325	1.216	0.776	0.672	0.647	0.838	0.768	0.600	0.0017	0.0021	0.08

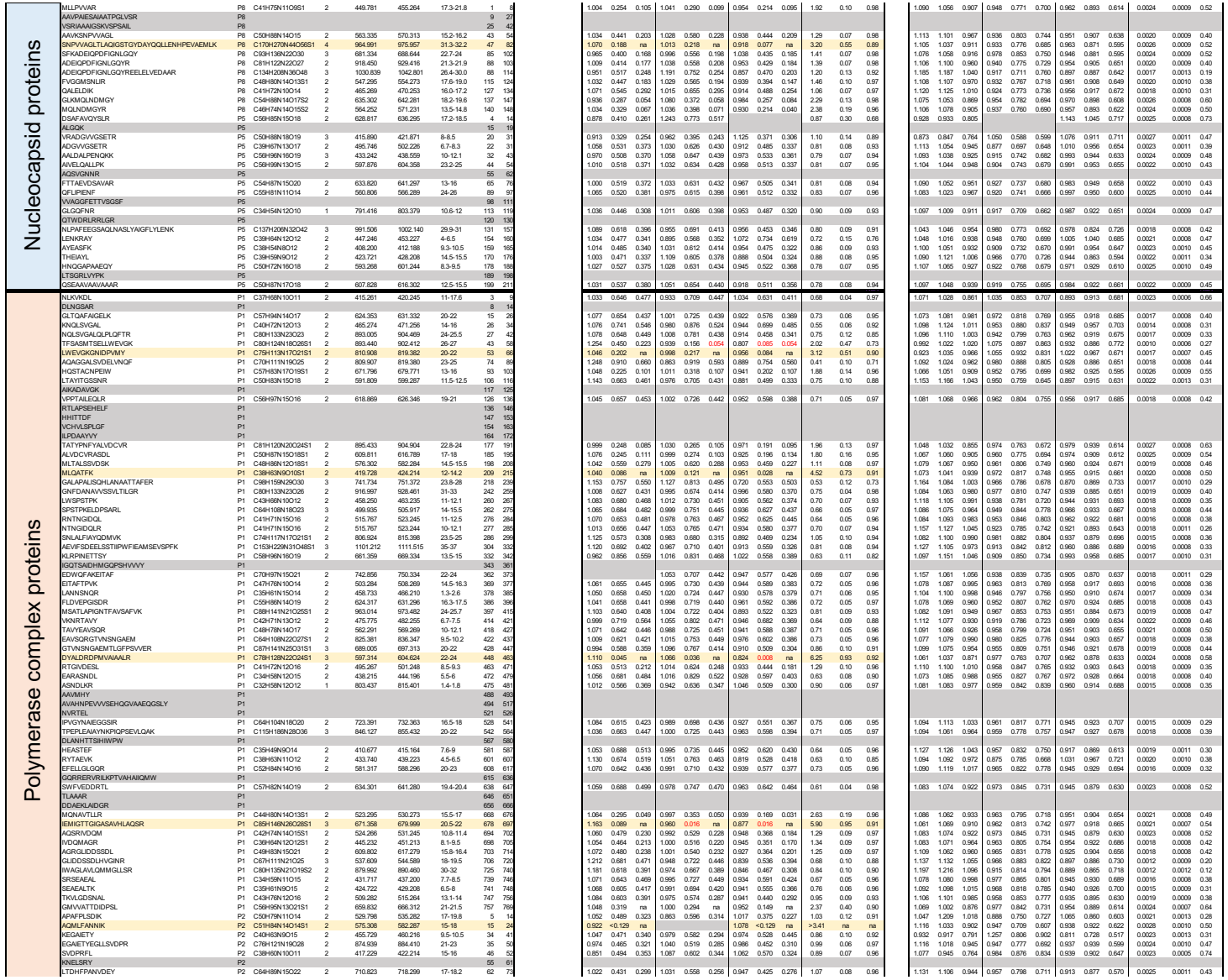
Nucleocapsid proteins
Polymerase complex proteins

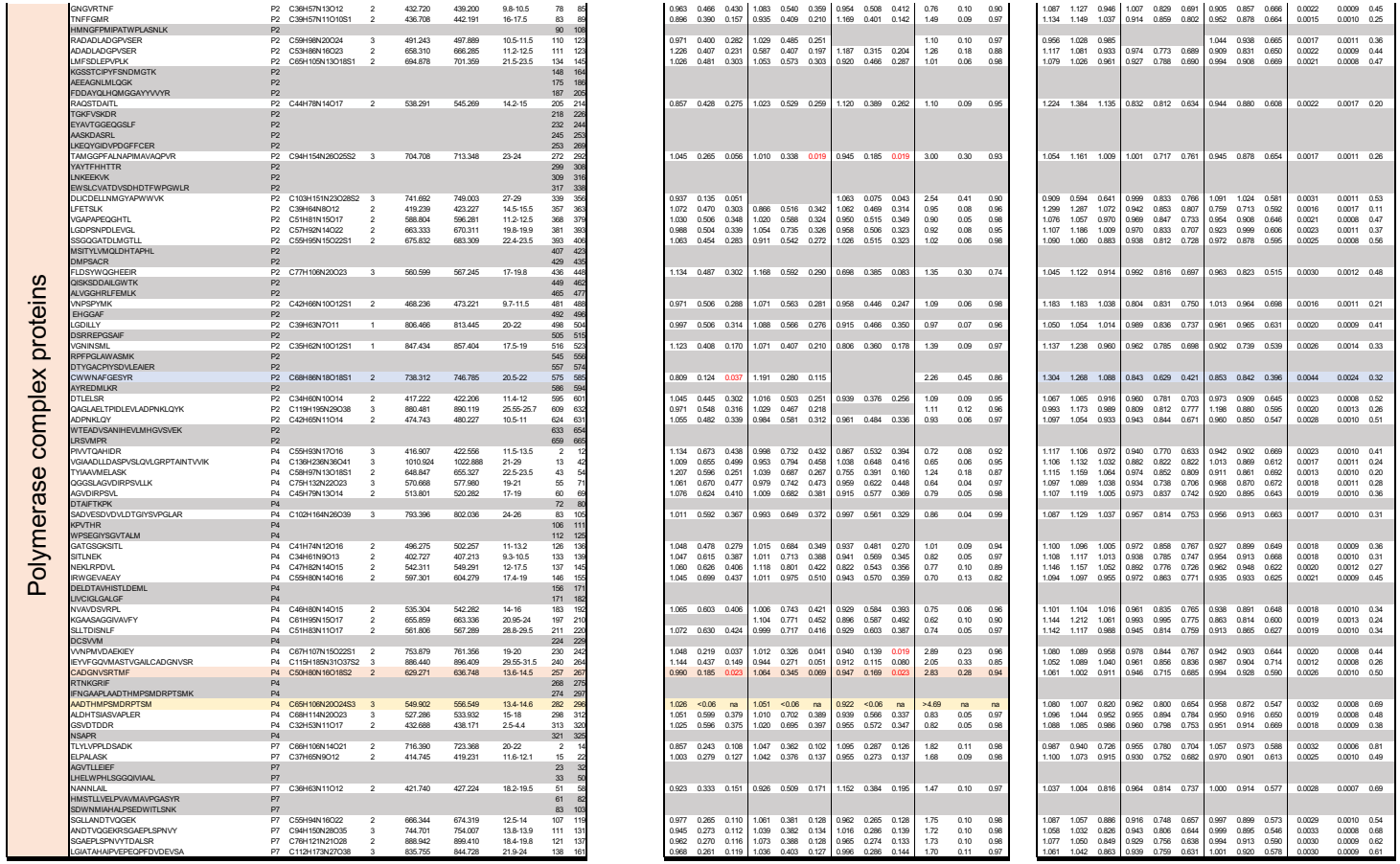
Polymerase complex proteins

References:

(1) Shrivastava, A.; Gupta, V. B. Methods for the determination of limit of detection and limit of quantification of the analytical methods. *Chron. Young Sci.* **2011**, *2* (1), 21–25.

(2) Matyash, V.; Liebisch, G.; Kurzchalia, T. V.; Shevchenko, A.; Schwudke, D. Lipid extraction by methyl-tert-butyl ether for high-throughput lipidomics. *J. Lipid Res.* **2008**, *49* (5), 1137–1146.

(3) Dodd, M. C.; Vu, N. D.; Ammann, A.; Le, V. C.; Kissner, R.; Pham, H. V.; Cao, T. H.; Berg, M.; Gunten, von, U. Kinetics and mechanistic aspects of As(III) oxidation by aqueous chlorine, chloramines, and ozone: Relevance to drinking water treatment. *Environ. Sci. Technol.* **2006**, *40* (10), 3285–3292.

(4) Poranen, M. M.; Tuma, R.; Bamford, D. H. Assembly of double-stranded RNA bacteriophages. *Adv. Virus Res.* **2005**, *64*, 15–43.

(5) Nikogosyan, D. N. Two-quantum UV photochemistry of nucleic acids: Comparison with conventional low-intensity UV photochemistry and radiation chemistry. *Int. J. Radiat. Biol.* **2009**, *57* (2), 233–299.

(6) W H Dennis, J.; Olivieri, V. P.; Kruse, C. W. The reaction of nucleotides with aqueous hypochlorous acid. *Water Res.* **1979**, *13* (4), 357–362.

(7) Prütz, W. A. Interactions of hypochlorous acid with pyrimidine nucleotides, and secondary reactions of chlorinated pyrimidines with GSH, NADH, and other substrates. *Arch. Biochem. Biophys.* **1998**, *349* (1), 183–191.

(8) Pattison, D. I.; Davies, M. J. Absolute rate constants for the reaction of hypochlorous acid with protein side chains and peptide bonds. *Chem. Res. Toxicol.* **2001**, *14*, 1453–1464.

Appendix C. Supplementary Information for Chapter 4

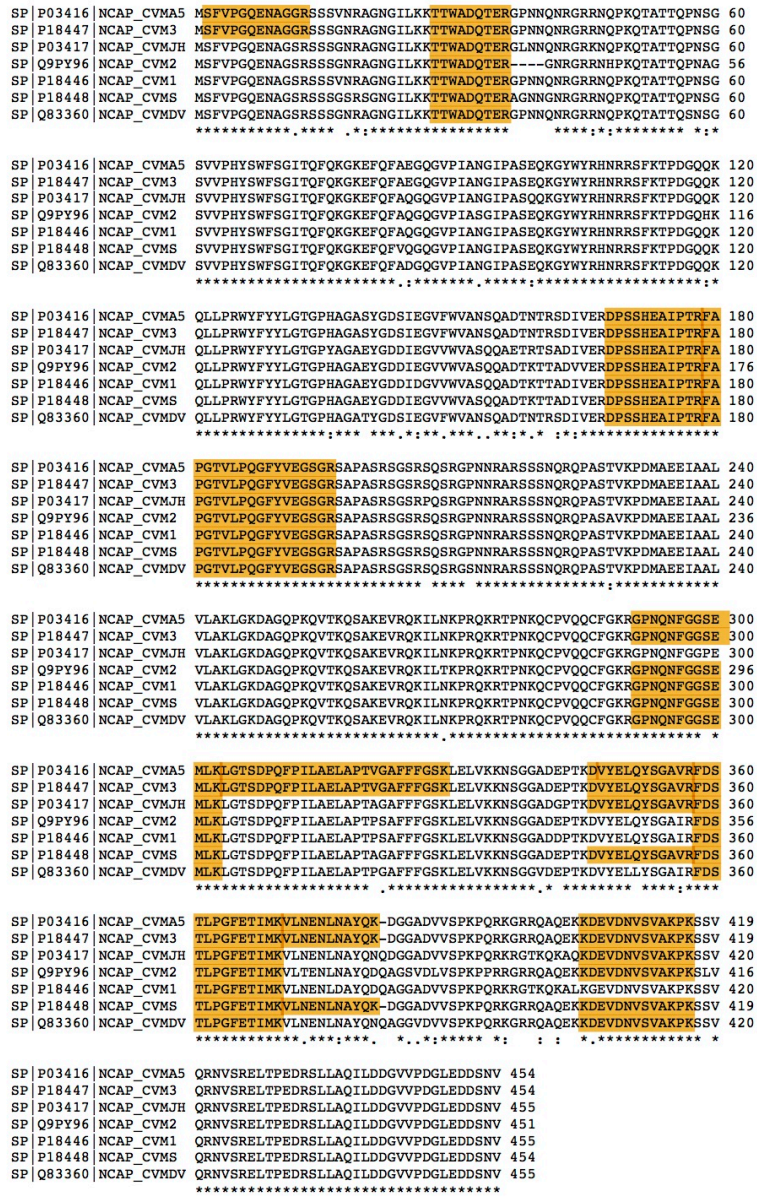

Figure C-1 Multiple sequence alignment of MHV nucleoproteins for seven MHV strains on SwissProt, including MHV-A59 (P03146), MHV-3 (P18447), MHV-JHM (P03417), MHV-2 (Q9PY96), MHV-1 (P18446), and MHV-S (P18448), and MHV-DVIM (Q83360). All detected peptides by LC-MS/MS were highlighted.

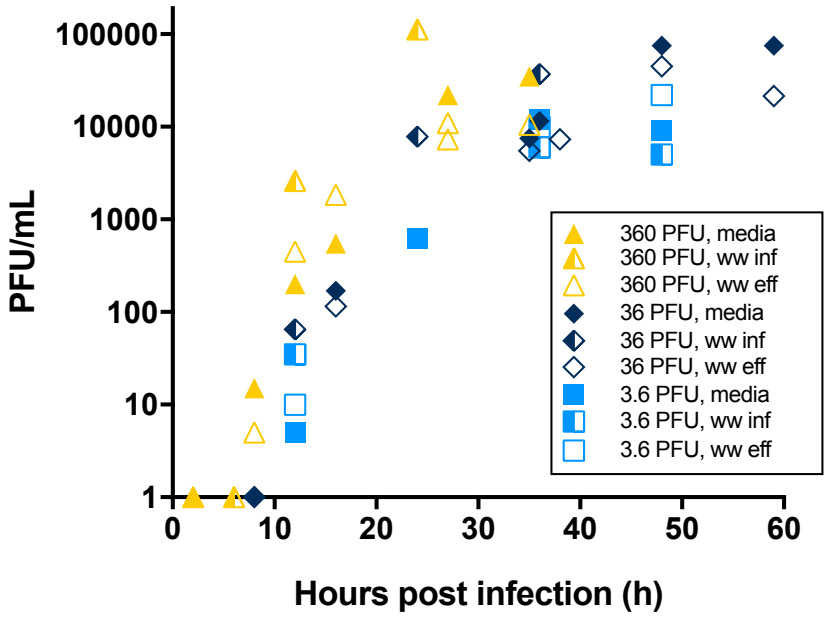

Figure C-2 MHV propagation curves when the L2 culture system inoculated with MHV suspended in various aqueous environments, including media, concentrated wastewater influent (ww inf), and concentrated wastewater effluent (ww eff).

```
SP|P03527|SIGM3_REOVD MEVCLPNGHQVVDLINNAFEGRVSIYSAQEGWDKTISAQPDMMVCGGAVVCMHCLGVVGS 60
SP|P07939|SIGM3_REOVL MEVCLPNGHQIVDLINNAFEGRVSIYSAQEGWDKTISAQPDMMVCGGAVVCMHCLGVVGS 60
SP|P30211|SIGM3_REOVJ MEVCLPNGHQIVDWINNAFEGRVSIYSAQQGWDKTISAQPDMMVCGGAVVCMHCLGVVGS 60
                      **********:** ***************:****************************

SP|P03527|SIGM3_REOVD LQRKLKHLPHHRCNQQIRHQDYVDVQFADRVTAHWKRGMLSFVAQMHEMMNDVSPDDLDR 120
SP|P07939|SIGM3_REOVL LQRKLKHLPHHRCNQQIRHQDYVDVQFADRVTAHWKRGMLSFVAQMHAMMNDVSPEDLDR 120
SP|P30211|SIGM3_REOVJ LQRKLKHLPHHKCNQQLRQQDYVDVQFADRVTAHWKRGMLSFVSQMHAIMNDVTPEELER 120
                      ***********:****:*:*************************** :****:*:::*:*

SP|P03527|SIGM3_REOVD VRTEGGSLVELNWLQVDPNSMFRSIHSSWTDPLQVVDDLDTKLDQYWTALNLMIDSSDLI 180
SP|P07939|SIGM3_REOVL VRTEGGSLVELNWLQVDPNSMFRSIHSSWTDPLQVVDDLDTKLDQYWTALNLMIDSSDLV 180
SP|P30211|SIGM3_REOVJ VRTDGGSLAELNWLQVDPGSMFRSIHSSWTDPLQVVEDLDTQLDRYWTALNLMIDSSDLV 180
                      ***:****.*********.*****************:****:**:***************:

SP|P03527|SIGM3_REOVD PNFMMRDPSHAFNGVKLGGDARQTQFSRTFDSRSSLEWGVMVYDYSELEHDPSKGRAYRK 240
SP|P07939|SIGM3_REOVL PNFMMRDPSHAFNGVRLEGDARQTQFSRTFDSRSSLEWGVMVYDYSELEHDPSKGRAYRK 240
SP|P30211|SIGM3_REOVJ PNFMMRDPSHAFNGVKLEGEARQTQFSRTFDSRSNLEWGVMIYDYSELERDPLKGRAYRK 240
                      ***************:* *:**************.******:*******:** *******

SP|P03527|SIGM3_REOVD ELVTPARDFGHFGLSHYSRATTPILGKMPAVFSGMLTGNCKMYPFIKGTAKLKTVRKLVE 300
SP|P07939|SIGM3_REOVL ELVTPARDFGHFGLSHYSRATTPILGKMPAVFSGMLTGNCKMYPFIKGTAKLKTVRKLVD 300
SP|P30211|SIGM3_REOVJ EVVTPARDFGHFGLSHYSRATTPILGKMPAVFSGMLTGNCKMYPFIKGTAKLRTVKKLVD 300
                      *:************************************************:**:***:

SP|P03527|SIGM3_REOVD AVNHAWGVEKIRYALGPGGMTGWYNRTMQQAPIVLTPAALTMFPDTIKFGDLNYPVMIGD 360
SP|P07939|SIGM3_REOVL SVNHAWGVEKIRYALGPGGMTGWYDRTMQQAPIVLTPAALTMFSDTTKFGDLDYPVMIGD 360
SP|P30211|SIGM3_REOVJ AVNHTWGSEKIRYALGPGGMTGWYNRTMQQAPIVLTPAALTMFPDMTKFGDLQYPIMIGD 360
                      :***:** ***************:****************** *  *****:**:****

SP|P03527|SIGM3_REOVD PMILG 365
SP|P07939|SIGM3_REOVL PMILG 365
SP|P30211|SIGM3_REOVJ PAVLG 365
                      * :**
```

Figure C-3 Multiple sequence alignment of reovirus sigma-3 proteins. Sequence similarity: 88.9%.

```
SP|P11078|MU1_REOVD MGNASSIVQTINVTGDGNVFKPSAETSSTAVPSLSLSPGMLNPGGVPWIAVGDETSVTSP 60
SP|P11077|MU1_REOVL MGNASSIVQTINVTGDGNVFKPSAETSSTAVPSLSLSPGMLNPGGVPWIAIGDETSVTSP 60
SP|P12397|MU1_REOVJ MGNASSIVQTINVTGDGNVFKPSAETSSTAVPSLSLSPGMLNPGGVPWIAIGDETSVTSP 60
                     **************************************************:*********

SP|P11078|MU1_REOVD GALRRMTSKDIPETAIINTDNSSGAVPSESALVPYIDEPLVVVTEHAITNFTKAEMALEF 120
SP|P11077|MU1_REOVL GALRRMTSKDIPETAIINTDNSSGAVPSESALVPYNDEPLVVVTEHAIANFTKAEMALEF 120
SP|P12397|MU1_REOVJ GALRRMTSKDIPETAIINTDNSSGAVPSESALVPYNDEPLVVVTEHAIANFTKAEMALEF 120
                     ********************************** ************:************

SP|P11078|MU1_REOVD NREFLDKMRVLSVSPKYSDLLTYVDCYVGVSARQALNNFQKQVPVITPTRQTMYVDSIQA 180
SP|P11077|MU1_REOVL NREFLDKLRVLSVSPKYSDLLTYVDCYVGVSARQALNNFQKQVPVITPTRQTMYVDSIQA 180
SP|P12397|MU1_REOVJ NREFLDKLRVLSVSPKYSDLLTYVDCYVGVSARQALNNFQKQVPVITPTRQTMYVDSIQA 180
                     *******:**************************************************

SP|P11078|MU1_REOVD ALKALEKWEIDLRVAQTLLPTNVPIGEVSCPMQSVVKLLDDQLPDDSLIRRYPKEAAVAL 240
SP|P11077|MU1_REOVL ALKALEKWEIDLRVAQTLLPTNVPIGEVSCPMQSVVKLLDDQLPDDSLIRRYPKEAAVAL 240
SP|P12397|MU1_REOVJ ALKALEKWEIDLRVAQTLLPTNVPIGEVSCPMQSVVKLLDDQLPDDSLIRRYPKEAAVAL 240
                     ************************************************************

SP|P11078|MU1_REOVD AKRNGGIQWMDVSEGTVMNEAVNAVAASALAPSASAPPLEEKSKLTEQAMDLVTAAEPEI 300
SP|P11077|MU1_REOVL AKRNGGIQWMDVSEGTVMNEAVNAVAASALAPSASAPPLEEKSKLTEQAMDLVTAAEPEI 300
SP|P12397|MU1_REOVJ AKRNGGIQWMDVSEGTVMNEAVNAVAASALAPSASAPPLEEKSKLTEQAMDLVTAAEPEI 300
                     ************************************************************

SP|P11078|MU1_REOVD IASLAPVPAPVFAIPPKPADYNVRTLRIDEATWLRMIPKSMNTPFQIQVTDNTGTNWHLN 360
SP|P11077|MU1_REOVL IASLVPVPAPVFAIPPKPADYNVRTLKIDEATWLRMIPKTMGTPFQIQVTDNTGTNWHLN 360
SP|P12397|MU1_REOVJ IASLVPVPAPVFAIPPKPADYNVRTLKIDEATWLRMIPKTMNTPFQIQVTDNTGTSWHMN 360
                     ****.*********************:************:*.*************.**:*

SP|P11078|MU1_REOVD LRGGTRVVNLDQIAPMRFVLDLGGKSYKETSWDPNGKKVGFIVFQSKIPFELWTAASQIG 420
SP|P11077|MU1_REOVL LRGGTRVVNLDQIAPMRFVLDLGGKSYKETSWDPNGKKVGFIVFQSKIPFELWTAASQIG 420
SP|P12397|MU1_REOVJ LRGGTRVVNLDQIAPMRFVLDLGGKSYKETSWDPNGKKVGFIVFQSKIPFELWTAASQIG 420
                     ************************************************************

SP|P11078|MU1_REOVD QATVVNYVQLYAEDSSFTAQSIIATTSLAYNYEPEQLNKTDPEMNYYLLATFIDSAAITP 480
SP|P11077|MU1_REOVL QATVVNYVQLYAEDSSFTAQSIIATTSLAYNYEPEQLNKTDPEMNYYLLATFIDSAAITP 480
SP|P12397|MU1_REOVJ QATVVNYVQLYAEDSSFTAQSIIATTSLAYNYEPEQLNKTDPEMNYYLLAAFIDSAAIST 480
                     **************************************************:*******:

SP|P11078|MU1_REOVD TNMTQPDVWDALLTMSPLSAGEVTVKGAVVSEVVPADLIGSYTPESLNASLPNDAARCMI 540
SP|P11077|MU1_REOVL TNMTQPDVWDALLTMSPLSAGEVTVKGAVVSEVVPAELIGSYTPESLNASLPNDAARCMI 540
SP|P12397|MU1_REOVJ SNMTQPDVWDALLTMSPLSAGEVTVKGAVVSEVIPADLVGSYTPESLNASLPNDAARCMI 540
                     :*******************************:**:*:********************

SP|P11078|MU1_REOVD DRASKIAEAIKIDDDAGPDEYSPNSVPIQGQLAISQLETGYGVRIFNPKGILSKIASRAM 600
SP|P11077|MU1_REOVL DRASKIAEAIKIDDDAGPDEYSPNSVPIQGQLAISQLETGYGVRIFNPKGILSKIASRAM 600
SP|P12397|MU1_REOVJ DRASKIAEAIKIDDDAGPDEYSPNSVPIQGQLAISQLETGYGVRIFNPKGILSKIASRAM 600
                     ************************************************************

SP|P11078|MU1_REOVD QAFIGDPSTIITQAAPVLSDKNNWIALAQGVKTSLRTKSLSAGVKTAVSKLSSSESIQNW 660
SP|P11077|MU1_REOVL QAFIGDPSTIITQAAPVLSDKNNWIALAQGVKTSLRTKSLSAGVKTAVSKLSSSESIQNW 660
SP|P12397|MU1_REOVJ QAFIGDPSTIITQAAPVLSDKNNWIALAQGVKTSLRTKSLSAGVKTAVSKLSSSESIQSW 660
                     ************************************************************.*

SP|P11078|MU1_REOVD TQGFLDKVSAHFPAPKPDCPTSGDSGESSNRRVKRDSYAGVVKRGYTR 708
SP|P11077|MU1_REOVL TQGFLDKVSTHFPAPKPDCPTNGDGSEPSARRVKRDSYAGVVKRGYTR 708
SP|P12397|MU1_REOVJ TQGFLDKVSTHFPAPKPDCPQSGDSGDGSARRLKRDSYAGVVKRGYTR 708
                     *********:********** .**..: * **:***************
```

Figure C-4 Multiple sequence alignment of reovirus mu-1 proteins. Sequence similarity: 96.2%.

Table C-1 Cell lines and viruses used in this study.

Cell line	Cell type	Source	Example viruses that can be cultured	Citations
L2	Mouse lung epithelial cells	Dr. Julian Leibowitz's lab at Texas A&M Health Science Center College of Medicine	murine hepatitis virus	
DBT	Mouse lung epithelial cells	Dr. Julian Leibowitz's lab at Texas A&M Health Science Center College of Medicine	murine hepatitis virus	
Vero	Monkey kidney epithelial cells	Dr. Michael J. Imperiale's lab, University of Michigan	poliovirus, coxsackie virus, echovirus, reovirus, adenovirus, picornavirus simian virus 40	[1,2]
BSC-1	Monkey kidney epithelial cells	Dr. Michael J. Imperiale's lab, University of Michigan	poliovirus, coxsackie virus, echovirus, reovirus, hepatitis A virus, simian virus 40	[1,3,4]
Virus				
Murine hepatitis virus strain A59		Dr. Julian Leibowitz's lab at Texas A&M Health Science Center College of Medicine		

Table C-2 MS instrument settings for ICC-MS proteomics analysis.

Peptides (positive mode)	
Sheath gas flow rate	24
Auxiliary gas flow rate	8
Sweep gas flow rate	1
Spray voltage	3 kV
Capillary temp.	300 °C
S-len RF level	50.0
Aux gas heater temp.	275 °C
Column temperature	25 °C
Full MS settings	
Resolution	70,000
AGC target	5e5
Max IT	200 ms
Scan range	400-1800 m/z
dd-MS² settings	
Resolution	35,000
AGC target	2e5
Max IT	100 ms
Loop count	20
Isolation window	1.6 Da
NCE	30
Intensity threshold	2e4
Charge exclusion:	Unassigned, 1
Dynamic exclusion	20 sec

Table C-3 Viral peptides detected by LC-MS/MS in MHV control experiments, where MHV was added to culture media. Nucleoproteins of MHV strains A59 and 3 were confidently identified. Peptides that differentiate strains are highlighted. A protein score greater than 76 was considered significant identification.

	Hours post infection	Identified Protein	Detected peptides	Protein sequence coverage	Protein score
300 PFU/mL, 1.2 mL inoculum	12 h		N.A.	N.A.	N.A.
	18 h	Nucleoprotein (MHV-A59, MHV-3)	TTWADQTER DPSSHEAIPTR **SFVPGQENAGGR** FAPGTVLPQGFYVEGSGR	9%	120
	26 h	Nucleoprotein (MHV-A59, MHV-3)	TTWADQTER DPSSHEAIPTR SFVPGQENAGGR VLNENLNAYQK GPNQNFGGSEMLK DVYELQYSGAVR KDEVDNVSVAKPK FAPGTVLPQGFYVEGSGR **LGTSDPQFPILAELAPTVGAFFFGSK**	25%	509
		Spike glycoprotein (Coronavirus)	SAIEDLLFDK	0.7%	76
	26 h	Nucleoprotein (MHV-A59, MHV-3)	DPSSHEAIPTR SFVPGQENAGGR VLNENLNAYQK DGGADVVSPKPQR GPNQNFGGSEMLK DVYELQYSGAVR FDSTLPGFETIMK FAPGTVLPQGFYVEGSGR **LGTSDPQFPILAELAPTVGAFFFGSK**	28%	469
30 PFU/mL, 1.2 mL inoculum	18 h		N.A.	N.A.	N.A.
	24 h	Nucleoprotein (MHV-A59, MHV-3)	TTWADQTER SFVPGQENAGGR FAPGTVLPQGFYVEGSGR **LGTSDPQFPILAELAPTVGAFFFGSK**	12%	77
	30 h	Nucleoprotein (MHV-A59, MHV-3)	DPSSHEAIPTR SFVPGQENAGGR FAPGTVLPQGFYVEGSGR	9%	113
	37 h	Nucleoprotein (MHV-A59, MHV-3)	TTWADQTER DPSSHEAIPTR SFVPGQENAGGR FAPGTVLPQGFYVEGSGR	11%	242
	37 h	Nucleoprotein (MHV-A59, MHV-3)	DPSSHEAIPTR SFVPGQENAGGR DGGADVVSPKPQR GPNQNFGGSEMLK DVYELQYSGAVR KDEVDNVSVAKPK FDSTLPGFETIMK RGPNQNFGGSEMLK FAPGTVLPQGFYVEGSGR QPASTVKPDMAEEIAALVLAK **LGTSDPQFPILAELAPTVGAFFFGSK**	33%	593
3 PFU/mL, 1.2 mL inoculum	30 h		N.A.	N.A.	N.A.
	36 h	Nucleoprotein (MHV-A59, MHV-3)	DPSSHEAIPTR SFVPGQENAGGR	2%	40
	42 h	Nucleoprotein (MHV-A59, MHV-3)	DPSSHEAIPTR SFVPGQENAGGR VLNENLNAYQK GPNQNFGGSEMLK FAPGTVLPQGFYVEGSGR	12%	263

Table C-4 Viral peptides detected by LC-MS/MS in MHV wastewater experiments.

Wastewater influent					
	Hours post infection	**Identified Protein**	**Detected peptides**	**Protein sequence coverage**	**Protein score**
300 PFU/mL, 1.2 mL inoculum	18 h	Nucleoprotein (MHV-A59, MHV-3)	TTWADQTER DPSSHEAIPTR SFVPGQENAGGR GPNQNFGGSEMLK FAPGTVLPQGFYVEGSGR	12%	249
	24 h	Nucleoprotein (MHV-A59, MHV-3)	TTWADQTER DPSSHEAIPTR SFVPGQENAGGR DEVDNVSVAKPK VLNENLNAYQK DGGADVVSPKPQR GPNQNFGGSEMLK DVYELQYSGAVR KDEVDNVSVAKPK FDSTLPGFETIMK FAPGTVLPQGFYVEGSGR QPASTVKPDMAEEIAALVLAK EFQFAEGQGVPIANGIPASEQK LGTSDPQFPILAELAPTVGAFFFGSK	40%	640
		Spike glycoprotein (MHV)	SAIEDLLFDK FGAISASLQEILTR	2%	98
30 PFU/mL, 1.2 mL inoculum	30 h	Nucleoprotein (MHV-A59, MHV-3)	TTWADQTER DPSSHEAIPTR SFVPGQENAGGR VLNENLNAYQK GPNQNFGGSEMLK DVYELQYSGAVR FAPGTVLPQGFYVEGSGR LGTSDPQFPILAELAPTVGAFFFGSK	25%	645
	36 h	Nucleoprotein (MHV-A59, MHV-3)	DPSSHEAIPTR SFVPGQENAGGR DEVDNVSVAKPK VLNENLNAYQK DGGADVVSPKPQR GPNQNFGGSEMLK DVYELQYSGAVR KDEVDNVSVAKPK FDSTLPGFETIMK FAPGTVLPQGFYVEGSGR QPASTVKPDMAEEIAALVLAK EFQFAEGQGVPIANGIPASEQK EFQFAEGQGVPIANGIPASEQK LGTSDPQFPILAELAPTVGAFFFGSK	40%	761
		Spike glycoprotein (MHV)	CFGSISVDK SAIEDLLFDK SVPSPLNWER YDLYGITGQGEILTR FGAISASLQEILTR VANLPACNIEEWLTAR	5%	239
3 PFU/mL, 1.2 mL inoculum	42 h	Nucleoprotein (MHV-A59, MHV-3, MHV-S, RCV-NJ)	DPSSHEAIPTR VLNENLNAYQK GPNQNFGGSEMLK FAPGTVLPQGFYVEGSGR	9%	168
	48 h	Nucleoprotein (MHV-A59, MHV-3)	TTWADQTER DPSSHEAIPTR SFVPGQENAGGR VLNENLNAYQK DGGADVVSPKPQR GPNQNFGGSEMLK DVYELQYSGAVR FAPGTVLPQGFYVEGSGR QPASTVKPDMAEEIAALVLAK EFQFAEGQGVPIANGIPASEQK LGTSDPQFPILAELAPTVGAFFFGSK	35%	642
		Spike glycoprotein (coronavirus)	SAIEDLLFDK	0.7%	88

Table C-4 Continued.

Wastewater effluent					
	Hours post infection	**Identified Protein**	**Detected peptides**	**Protein sequence coverage**	**Protein score**
300 PFU/mL, 1.2 mL inoculum	18 h	Nucleoprotein (MHV-A59, MHV-3)	TTWADQTER DPSSHEAIPTR SFVPGQENAGGR VLNENLNAYQK GPNQNFGGSEMLK FAPGTVLPQGFYVEGSGR	14%	386
	24 h	Nucleoprotein (MHV-A59, MHV-3)	DPSSHEAIPTR SFVPGQENAGGR VLNENLNAYQK DGGADVVSPKPQR GPNQNFGGSEMLK FDSTLPGFETIMK FAPGTVLPQGFYVEGSGR	20%	355
30 PFU/mL, 1.2 mL inoculum	30 h	Nucleoprotein (MHV-A59, MHV-3)	ELTPEDR DPSSHEAIPTR SFVPGQENAGGR FAPGTVLPQGFYVEGSGR	9%	265
	36 h	Nucleoprotein (MHV-A59, MHV-3)	TTWADQTER DPSSHEAIPTR SFVPGQENAGGR DGGADVVSPKPQR GPNQNFGGSEMLK FDSTLPGFETIMK FAPGTVLPQGFYVEGSGR	17%	577
3 PFU/mL, 1.2 mL inoculum	42 h	Nucleoprotein (MHV-A59, MHV-3)	DPSSHEAIPTR VLNENLNAYQK GPNQNFGGSEMLK FDSTLPGFETIMK FAPGTVLPQGFYVEGSGR LGTSDPQFPILAELAPTVGAFFFGSK	20%	210
	48 h	Nucleoprotein (MHV-A59, MHV-3)	ELTPEDR TTWADQTER DPSSHEAIPTR SFVPGQENAGGR DEVDNVSVAKPK DGGADVVSPKPQR GPNQNFGGSEMLK DVYELQYSGAVR KDEVDNVSVAKPK FDSTLPGFETIMK FAPGTVLPQGFYVEGSGR EFQFAEGQGVPIANGIPASEQK LGTSDPQFPILAELAPTVGAFFFGSK	36%	740
		Spike glycoprotein (MHV)	SAIEDLLFDK SVPSPLNWER FGAISASLQEILTR	2%	205

Table C-5 Proteins in reovirus virion.

Location	Protein	Molecule copies in reovirus virion[5]
Outer capsid	mu-1	600
	sigma-3	600
	lambda-2	60
	sigma-1	36-48
Inner capsid (core)	sigma-2	150
	lambda-1	120
	lambda-3	12
	mu-2	12

References:

(1) Payment, P.; Ayache, R.; Trudel, M. A survey of enteric viruses in domestic sewage. *Can. J. Microbiol.* **2011**, *29* (1), 111–119.

(2) Gelb, L. D.; Kohne, D. E.; Martin, M. A. Quantitation of simian virus 40 sequences in African green monkey, mouse and virus-transformed cell genomes. *J. Mol. Biol.* **1971**, *57* (1), 129–145.

(3) Gerba, C. P.; Sobsey, M. D.; Wallis, C.; Melnick, J. L. Adsorption of poliovirus onto activated carbon in wastewater. *J. Chem. Eng.* **1975**, *9* (8), 727–731.

(4) Sompayrac, L. M.; Danna, K. J. Efficient infection of monkey cells with DNA of simian virus 40. *Proc. Natl. Acad. Sci.* **1981**, *78* (12), 7575–7578.

(5) Dryden, K. A.; Wang, G.; Yeager, M.; Nibert, M. L.; Coombs, K. M.; Furlong, D. B.; Fields, B. N.; Baker, T. S. Early steps in reovirus infection are associated with dramatic changes in supramolecular structure and protein conformation: analysis of virions and subviral particles by cryoelectron microscopy and image reconstruction. *J. Cell Biol.* **1993**, *122* (5), 1023–104.